

CHALMERS



Operational Transfer Path Analysis of components of a high-speed train bogie

Master's Thesis in the Master's programme in Sound and Vibration

ROBERT STRÖM

Department of Civil and Environmental Engineering
Division of Applied Acoustics
Vibroacoustics Group
CHALMERS UNIVERSITY OF TECHNOLOGY
Göteborg, Sweden 2014
Master's Thesis 2014:158

Operational Transfer Path Analysis of components of a high-speed train bogie

ROBERT STRÖM

Department of Civil and Environmental Engineering
Division of Applied Acoustics
Vibroacoustics Group
CHALMERS UNIVERSITY OF TECHNOLOGY
Göteborg, Sweden 2014

Operational Transfer Path Analysis of components of a high-speed train bogie

© ROBERT STRÖM, 2014

Master's Thesis 2014:158

Department of Civil and Environmental Engineering
Division of Applied Acoustics
Vibroacoustics Group
Chalmers University of Technology
SE-41296 Göteborg
Sweden

Tel. +46-(0)31 772 1000

Reproservice / Department of Civil and Environmental Engineering
Göteborg, Sweden 2012

Operational Transfer Path Analysis of components of a high-speed train bogie

Master's Thesis in the Master's programme in Sound and Vibration

ROBERT STRÖM

Department of Civil and Environmental Engineering

Division of Applied Acoustics

Vibroacoustics Group

Chalmers University of Technology

Abstract

In this thesis a method to use the Operational Transfer Path Analysis (OTPA) when ranking the different transmission paths through the secondary suspension of a train bogie is developed. The thesis is done for Bombardier Transportation in cooperation with the Division of Applied Acoustics at Chalmers University of Technology.

It is seen that OTPA is a useful method to analyze the contribution due to the different paths through the bogie, however it is important to have a good knowledge about the theory behind it and set up the measurements properly, since a lot of errors can occur when the analysis is not performed correctly.

A computer program performing an OTPA is created and applied to both a simulated measurement of an experimental setup consisting of a plate-beam arrangement and a high-speed train bogie. From the parameter study of the experimental setup it is seen that the method is relatively insensitive to noise in the receiving points, but it is critical to measure all contributing paths. When analyzing the transmission through the train bogie it is seen that the most important paths in the frequency range analysed are the airborne sound, the traction rod and the yaw dampers.

Keywords: Operational Transfer Path Analysis, OTPA, Cross Talk Cancellation, CTC, Railway Noise

Contents

Abstract	iii
Contents	iv
Acknowledgements	vii
List of Abbreviations	ix
1. Introduction	1
1.1. Background	1
1.2. Objective	1
1.3. Scope	2
1.4. Structure of thesis	2
2. Theory	3
2.1. Acoustics of railway vehicles	3
2.1.1. Auxiliary sources	3
2.1.2. Rolling noise and curve squeal	3
2.1.3. Aerodynamic noise	4
2.1.4. Airborne sound	4
2.1.5. Structure-borne sound	5
2.2. The Classical Transfer Path Analysis Method	5
2.2.1. Finding the Frequency Response Function	5
2.2.2. Finding the Operational Forces	6
2.2.3. Applicability and Limitations of classical Transfer Path Analysis	7
2.3. The Operational Transfer Path Analysis	8
2.3.1. Least-Squares Algorithm	9
2.3.2. Cross-Talk Cancellation	10
2.3.3. Response Synthesis	12
2.3.4. Practical implementation of Operational Transfer Path Analysis	13
3. Implementation of OTPA on a beam-plate structure	15
3.1. MATLAB script	15
3.1.1. OTPA-function	15
3.1.2. Plot-function	17
3.2. Implementation and validation of OTPA on a test structure	19
3.2.1. Definition of structure	19

3.2.2. Calculations	22
3.2.3. Results	22
4. Implementation of OTPA on a high-speed train	35
4.1. The high-speed train	35
4.2. Measurements	36
4.3. Results	37
4.3.1. Campbell diagrams	37
4.3.2. Transfer Functions	38
4.3.3. Structure-borne vs. airborne sound	40
4.3.4. Transfer Paths	47
4.3.5. Traction motor fan	54
4.3.6. Validity of results	57
5. Conclusions and suggestions for further work	59
5.1. Summary	59
5.2. Suggestions for further work	60
Bibliography	61
A. MATLAB Script	63
A.1. Main script (<i>analysis.m</i>)	63
A.2. OTPA-function (<i>otpa_function.m</i>)	70
A.3. Plot-function (<i>otpa_plot.m</i>)	72
B. Transfer functions	83

Acknowledgements

This thesis is written in the spring of 2014 as a part of the master's programme in Sound & Vibration at Chalmers University of Technology.

The subject was proposed by the Acoustics and Vibration group at Bombardier Transportation in Västerås and is carried out with guidance from both Bombardier Transportation and the Applied Acoustics division at Chalmers University of Technology.

First and foremost, I would like to thank my supervisor at Bombardier Transportation in Västerås, Dr. Ulf Orrenius who's technical expertise, in particular about sound and vibration in trains, has been invaluable for this thesis. Thanks also to Tommy Sigemo for all help with facts and details of the measurements. Also thank you to the rest of the Acoustics and Vibration group at Bombardier Transportation in Västerås for your help and feedback.

I also would like to thank my supervisor at Chalmers University, Prof. Wolfgang Kropp for all the help, particularly with the understanding of the theory behind OTPA. Thanks also to Mihkel Toome and Dr. Juha Plunt at Müller-BBM Scandinavia in Göteborg for taking the time to answer my questions.

Also thank you to my fellow classmates at the master's programme. It has been a wonderful couple of years that went by way to fast!

Finally, thank you to my beloved wife, Mira, for all your love, patience and support, especially during the last 5 months when I have spent a lot of my time away in Västerås.

Robert Ström
Göteborg, June 2014

List of Abbreviations

CTC	Cross Talk Cancellation
DFT	Discrete Fourier Transform
DoF(s)	Degree(s) of Freedom
FEM	Finite Element Method
FRF	Frequency Response Function
IDFT	Inverse Discrete Fourier Transform
MIMO	Multiple Input/Multiple Output
NVH	Noise, Vibration & Harshness
OTPA	Operational Transfer Path Analysis
PC(s)	Principal Component(s)
PCA	Principal Component Analysis
SVD	Singular Value Decomposition
SNR	Signal to Noise Ratio
TF	Transfer Function
TPA	Transfer Path Analysis

1. Introduction

1.1. Background

The noise and vibrations inside a train car is often a problem for train manufacturers and operators, hence it is desired to find measures to make the trains as quiet and vibration free as possible.

To find measures to damp the interior noise in a train, it is essential know what causes the sound and its transmission paths to the interior. A lot of the noise in a train is originally generated in the rail-wheel contact, gearbox and traction motor. The sound is transmitted through the bogie, structure-borne or airborne, finally radiating into the train cabin generating a sound pressure.

When damping vibrations or sound pressures, the closer you get to the source the better the reduction you will get. It is therefore useful to be able to rank the contribution of each path in a system when deciding upon a measure to reduce the sound.

There exist several ways of ranking the contributing paths of structural and airborne sound to a system, of which probably the most common is the Transfer Path Analysis (TPA). The method used in this thesis is the variation of the classical TPA called Operational Transfer Path Analysis (OTPA). The OTPA does only include operational measurements, which means that the frequency response functions (FRF) do not have to be measured by physically isolating each path as in the TPA. Hence OTPA is often a faster and cheaper way of analyzing the system.

1.2. Objective

Since OTPA is a quite new method it has not yet been widely used in the train industry. It has however potential of being a useful tool when finding ways to reduce noise and vibrations in trains.

The aim of this study is to develop a method for Bombardier Transportation to use the OTPA when ranking the contribution to the overall noise inside the train cabin of each transmission path through the secondary suspension of a train.

Further the aim is to develop an understanding for the applicability of the method, including

pitfalls like effects of a limited dataset and measurement noise.

1.3. Scope

In this thesis the OTPA is implemented in a MATLAB script. An FE model is created and simulated. The results from the simulation is used as input data to the OTPA script. The OTPA model is validated and a couple of parameter studies done. The application of the method is then restricted to an analysis of a high-speed train bogie.

1.4. Structure of thesis

The major differences between TPA and OTPA as well as both pros and cons with both methods are discussed in Chapter 2 together with the theory behind. In this chapter also the acoustics of railway vehicles is described.

In Chapter 3 the OTPA is implemented on simulated vibrations of a simple beam-plate structure. The OTPA is performed with using a script written in MATLAB (attached in Appendix A). The OTPA of the simulated results is mainly done to validate the model, but also a parameter study is done. The parameter study consists of an investigation of the sensitivity to noise (in both reference and receiver points) and missed paths.

The OTPA method is applied to real measurements of a Bombardier high-speed train in Chapter 4.

Conclusions drawn from the results and suggestions for further work is presented in Chapter 5.

2. Theory

2.1. Acoustics of railway vehicles

The noise transmitted from, and into, a train car body can have many sources and transmission paths. It is of importance to identify the sources and transmission paths of railway vehicles, to be able to find measures to reduce them. Generally there are two cases, low-speed and high-speed conditions, where within the two cases different sound sources are dominating.

2.1.1. Auxiliary sources

Under low-speed conditions (below 60 km/h) the traction noise is dominant. At stand-still the noise from cooling systems for the propulsion equipment, air-condition system and the transformer heating and ventilation are dominating. In accelerating conditions, the traction noise can be dominating also for higher velocities.

2.1.2. Rolling noise and curve squeal

At high-speed the sound from the wheel-rail interaction and aerodynamic noise are contributing the most. The vibrations from the wheel-rail contact are caused by irregularities in the contact zone between the wheel and the rail. Vibrations of the wheel and the rail excite the surrounding air and sound is radiated into the surrounding environment. The vibrations are also transmitted into the passenger compartment both through structure-borne and airborne sound [10].

When dealing with noise due to the rail-wheel interaction, curve squeal caused by friction-induced vibrations is also of importance. This phenomenon occurs in tight curves, where a relatively large sliding motion between the rail and the wheel appears. This serves as an energy source for self-excited vibrations involving stick/slip oscillations in the rail-wheel contact and vibrations of the wheel in one of its resonances [11].

2.1.3. Aerodynamic noise

At very high speeds (typically above 300 km/h), the aerodynamic noise contributes significantly to the overall noise radiated by railway vehicles. The main aeroacoustic sources are the pantograph, the recess of the pantograph, the inter-coach spacing, the bogies, the nose of the power car, the coach walls, the rear power car and the louvres. Out of these the most dominating on conventional high-speed trains are the pantograph and the bogie areas, especially the leading bogie.

Aerodynamic noise generated in the bogie area is quite complex, the noise generated by the pantograph on the other side is better understood. It is known that this kind of noise is mainly generated due to vortex shedding around cylinders of the pantograph [14].

2.1.4. Airborne sound

Sound generated in the rail-wheel interaction and aerodynamic noise can be transmitted into a receiving structure through the air, so called airborne sound. This noise can be transmitted into the passenger compartment through openings like ventilation systems, doors and openings for cables. This part of the airborne noise is called primary airborne sound and generally have a marginal influence on the total sound in the coach if the design is reasonably airtight.

More important is the airborne sound that excites structural vibrations in the car body. These vibrations are radiating noise into the passenger compartment. The different propagation paths of airborne sound can be seen in Figure 2.1.

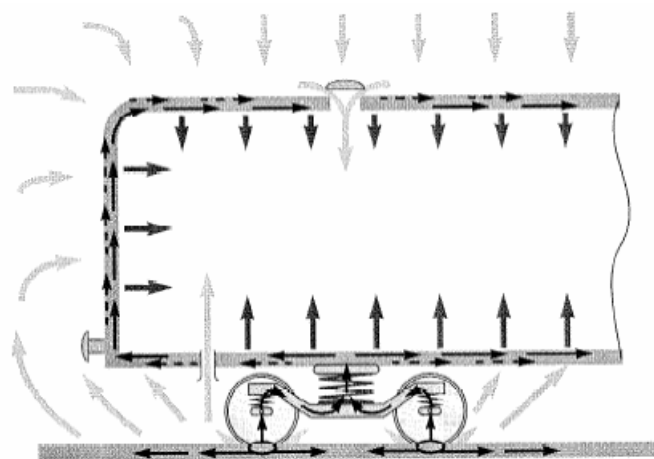


Figure 2.1.: Airborne sound transmitted into the passenger compartment [10].

2.1.5. Structure-borne sound

Vibrations originating from the rail-wheel contact and the drive system, can be transmitted into the passenger compartment through all coupling elements between the bogie and the car body. The amount of sound transmitted into the body of the car depends on the coupling points between the car and the bogie as well as the isolation of the interior. Inside the car body the sound is radiated by elements like floors, walls and ceiling. Also components excited aeroacoustically, like the pantograph, may transmit structure-borne sound.

A distinction between structural vibrations below 20 Hz and those of higher frequencies have to be made. Vibrations under 20 Hz are mainly influencing the ride comfort and higher frequency vibrations are affecting the noise [10].

The amount of structure-borne sound through the bogie is dependent on a variety of factors, like the bogie and carbody design, speed, condition of the track and wheels, position inside the car and the damping. Measurements have shown that the most important radiating structure is typically the coach floor, but for very effective floor designs the lower walls become increasingly important. Over 500 Hz the influence of structure-borne sound normally become less important.

To control the noise it is important to be able to analyze and preferably quantify through which paths the sound is transmitted into the car body. One way of doing this is by a so called Transfer Path Analysis, which will be covered in the following sections.

2.2. The Classical Transfer Path Analysis Method

The classical Transfer Path Analysis (TPA) is a commonly used method, especially in the automotive industry, for analyzing Noise, Vibration and Harshness (NVH) problems. It is a way of estimating and ranking the noise and vibrational contribution of each path in a system, for example the different transmission paths through the bogie of a railway car.

2.2.1. Finding the Frequency Response Function

In the classical TPA the system is divided into two parts: one active part containing the sources, and one passive part including the receiver points where the responses are measured. For this kind of analysis the system is disassembled so that each transfer path is isolated. After isolating each path, a force is applied where the active system is connected to the passive, and at the same time the response is measured at the receiver point. This is done for each transfer path to identify its contribution to the overall response.

When all the Frequency Response Functions (FRF) have been determined, the predicted re-

sponse for each path is calculated by multiplying the force with the FRF. Assuming linearity the predicted response is calculated by:

$$y(j\omega) = H(\omega)x(\omega) \quad (2.1)$$

where $y(\omega)$ is the response, $x(\omega)$ is the input force and $H(\omega)$ is the FRF.

In order to correctly determine the contribution of each path, all transfer paths must be measured separately. To find the total response at the receiver all paths are summed up according to:

$$y_m(\omega) = \sum_{n=1}^N H_{mn}(\omega)x_n(\omega) \quad (2.2)$$

where $y_m(\omega)$ is the response in the receiving point m , $H_{mn}(\omega)$ is the transfer function between point m and path n and $x_n(\omega)$ is the excitation force applied to path n .

The TPA method is in principal able of handling both structure-borne and airborne sound at the same time. If the airborne input is a volume velocity and the structure-borne input is a force the total sound pressure, $p_m(\omega)$, in the receiving position m can be calculated:

$$p_m(\omega) = \sum_{n=1}^k H_n(\omega)F_n(\omega) + \sum_{j=1}^r H_j(\omega)Q_j(\omega) \quad (2.3)$$

where $H_n(\omega)$ and $H_j(\omega)$ are the FRFs, $F_n(\omega)$ is the structure-borne force source at point n and $Q_j(\omega)$ is the airborne volume velocity input in point j [15, 8].

2.2.2. Finding the Operational Forces

There are several ways of finding the operational forces. The input could easily be measured using force transducers, called the *Direct Measurement Method*, however this is not as simple as it might sound. When adding a force transducer the local stiffness can be affected, also since three Degrees of Freedom (DoF) normally are considered the force transducer need to be able to measure in three directions simultaneously.

In practice in vehicle application the mounting of force transducers is often limited due to safety and other operational aspects. Sometimes forces can be indirectly assessed using strain gauges. Instead of directly measuring the force three other commonly used methods are also available.

The most common method is the *Complex Stiffness Method*. This method can be used when the source is mounted to the receiving structure via a resilient connection, in this method the forces are found by comparing the displacements on the active and passive side of the mounting. The excitation forces, $F_n(\omega)$ can be calculated:

$$F_n(\omega) = k_n(\omega) [x_{a,n}(\omega) - x_{p,n}(\omega)] \quad (2.4)$$

where $k_n(\omega)$ is the complex dynamic stiffness of the mounting, $x_{a,n}(\omega)$ are the displacements on the active side and $x_{p,n}(\omega)$ are the displacements on the passive side. The calculation has to be done for all n paths. Commonly the accelerations are measured on the active and passive mounts and thereafter integrated into displacements. Also the complex dynamic stiffness need to be known, this is normally determined on a hydropulse test bench as actual preloads and displacements.

The *Matrix Inversion Method* is used when the mount is rigid, causing the difference in displacement on the active and passive side to be very small and hard to measure correctly. In this method the forces $F_n(\omega)$ are calculated:

$$\begin{bmatrix} F_1(\omega) \\ \vdots \\ F_n(\omega) \end{bmatrix} = \begin{bmatrix} H_{11}(\omega) & \cdots & H_{1N}(\omega) \\ \vdots & \ddots & \vdots \\ H_{M1}(\omega) & \cdots & H_{MN}(\omega) \end{bmatrix}^{-1} \begin{bmatrix} \ddot{x}_1(\omega) \\ \vdots \\ \ddot{x}_m(\omega) \end{bmatrix} \quad (2.5)$$

where $\ddot{x}_m(\omega)$ are the operational accelerations. The number of responses, M , has to be equal to or larger than the number of DoFs, N .

In the last method, which is a simplification of the *Matrix Inversion Method*, the input force in each connecting point is estimated by multiplying the measured transfer function and response at the receiver as follows:

$$F_i = H_{ij}\ddot{x}_j \quad (2.6)$$

where F_i is the force in point i , H_{ij} is the force transfer function from point i to the response at point j and \ddot{x}_j is the measured acceleration at point j . The disadvantage of this method is that it does not take into account cross-talk between the source points, this can lead to high errors. However this method is used quite often, due to its simplicity [7, 8, 15, 17].

2.2.3. Applicability and Limitations of classical Transfer Path Analysis

The classical TPA is well known and widely used for solving NVH problems in the car industry. However, it is a time consuming method since all paths need to be isolated and measured separately. This is typically done by disassembly of the system, which can also create errors in the boundary conditions, since all real world systems are non-linear to some extent. Also with coupling elements dismounted the vehicle can in most cases not be fully operational.

Measuring all paths might also not be as straight forward as it sounds. Sometimes there might simply not be room enough to mount a shaker or fit an impact hammer (inside an engine or train bogie), that is necessary to measure the FRF of the path.

Conversely to the OTPA, in the TPA missed transfer paths will be visible in the result as there will be a discrepancy between the measured response and the synthesized response. This comparison is commonly used as a quality indicator of the TPA [4, 15].

2.3. The Operational Transfer Path Analysis

The classical TPA has been proven to be reliable, but rather complex and time consuming. Therefore it has not yet become a standard tool in the railway industry although some work has been published, for example [10]. This has led to a search for more time efficient methods. One which has gained attention is the Operational Transfer Path Analysis (OTPA). The OTPA does only require operational measurements of the vehicle, hence it is a much faster way of finding the different transfer path contributions [12].

OTPA is a signal processing method using Cross Talk Cancellation (CTC), Singular Value Decomposition (SVD) and Principal Component Analysis (PCA) to find the linearized Transfer Functions (TF) matrix between a chosen set of inputs and outputs of a mechanical system [3].

These sets of input and output quantities can be viewed as Degrees of Freedom (DoF) describing the object's excitation and responses. Like the TPA system the OTPA can be expressed as:

$$\mathbf{Y}(j\omega) = \mathbf{H}(j\omega)\mathbf{X}(j\omega) \quad (2.7)$$

where $\mathbf{Y}(j\omega)$ is the vector of output DoFs, $\mathbf{X}(j\omega)$ is the vector of input DoFs and $\mathbf{H}(j\omega)$ is the linking matrix of transfer functions. Typically, the measured signals are of the type motions (acceleration, velocity or displacement), $\mathbf{u}(j\omega)$, forces, $\mathbf{f}(j\omega)$ and sound pressures, $\mathbf{p}(j\omega)$. The input and output can include all these quantities such that (the dependency of frequency is left out for clarity):

$$\mathbf{X} = \begin{bmatrix} \mathbf{u}_x \\ \mathbf{f}_x \\ \mathbf{p}_x \end{bmatrix} \quad \mathbf{Y} = \begin{bmatrix} \mathbf{u}_y \\ \mathbf{f}_y \\ \mathbf{p}_y \end{bmatrix} \quad (2.8)$$

This means that the entries in the transfer function matrix may have different units. The quantities in Equation 2.8 are vectors:

$$\mathbf{u}_x = \begin{bmatrix} u_x^{(1)} \\ \vdots \\ u_x^{(k)} \end{bmatrix} \quad \mathbf{u}_y = \begin{bmatrix} u_y^{(1)} \\ \vdots \\ u_y^{(l)} \end{bmatrix} \quad \mathbf{f}_x = \begin{bmatrix} f_x^{(1)} \\ \vdots \\ f_x^{(m)} \end{bmatrix} \quad \mathbf{f}_y = \begin{bmatrix} f_y^{(1)} \\ \vdots \\ f_y^{(n)} \end{bmatrix} \quad \mathbf{p}_x = \begin{bmatrix} p_x^{(1)} \\ \vdots \\ p_x^{(o)} \end{bmatrix} \quad \mathbf{p}_y = \begin{bmatrix} p_y^{(1)} \\ \vdots \\ p_y^{(p)} \end{bmatrix} \quad (2.9)$$

where the indices k, l, m, n, o, p are the different measurement points (DoFs). As seen in Equation 2.9 the number of measured points does not have to be the same for all quantities, also not all physical quantities have to be included. The OTPA is not restricted to said quantities, any other physical quantity can be used, as long as they have the same DFT parameter during the measurement.

Since all elements of the transfer function are determined from *one* measurement, several measurement points can be included by taking the transpose of Equation 2.7 so that:

$$\begin{bmatrix} y^{(1)} & \dots & y^{(n)} \end{bmatrix} = \begin{bmatrix} H_{11} & \dots & H_{1n} \\ \vdots & \ddots & \vdots \\ H_{m1} & \dots & H_{mn} \end{bmatrix} \begin{bmatrix} x^{(1)} & \dots & x^{(m)} \end{bmatrix} \quad (2.10)$$

where m and n indicates the number of in- and output DoFs (measurement points) respectively.

In the OTPA the only excitation used is that from the operating forces, this means that it is desirable to measure at several operational states, for example during a run-up of the vehicle. This is done by saving a set of synchronized measurement blocks to disk. Since for this kind of measurement the operating force will vary over time, these blocks will not have the same content. However for each individual measurement block the relation between the input and the output will be linear. Hence, Equation 2.10 can be expanded to:

$$\begin{bmatrix} y_1^{(1)} & \dots & y_1^{(n)} \\ \vdots & \ddots & \vdots \\ y_r^{(1)} & \dots & y_r^{(n)} \end{bmatrix} = \begin{bmatrix} H_{11} & \dots & H_{1n} \\ \vdots & \ddots & \vdots \\ H_{m1} & \dots & H_{mn} \end{bmatrix} \begin{bmatrix} x_1^{(1)} & \dots & x_1^{(n)} \\ \vdots & \ddots & \vdots \\ x_r^{(1)} & \dots & x_r^{(n)} \end{bmatrix} \quad (2.11)$$

where r is the number of measurement blocks¹.

Equation 2.11 can be written in a more compact form:

$$\mathbf{Y} = \mathbf{H}\mathbf{X} \quad (2.12)$$

If the reference matrix is square ($m = r$) it is invertible. This leads to that transfer functions can be calculated by multiplying the inverse of \mathbf{X} on both sides:

$$\mathbf{H} = \mathbf{X}^{-1}\mathbf{Y} \quad (2.13)$$

This is however quite unusual. Commonly the number of measurement blocks is higher than the amount of input measurement points ($r > m$). In this case the problem can be solved as a least-squares optimization problem, which will be discussed in the next section. See also references [3, 15].

2.3.1. Least-Squares Algorithm

If the number of measurement blocks is greater than the number of input measurement points, which it mostly is, this problem can be solved using the least-squares method². This is done by adding an additional residue to Equation 2.12 so that:

$$\mathbf{Y} = \mathbf{H}\mathbf{X} + \boldsymbol{\mu} \quad (2.14)$$

where $\boldsymbol{\mu}$ is the added residue. Solving Equation 2.14 for each frequency line is performed by pre-multiplying the equation by \mathbf{X}^T , requiring that the residual vector is in the null space of the input, i.e. $\mathbf{X}^T\boldsymbol{\mu} = 0$. The transfer function matrix is then found as:

$$\mathbf{H} = \left(\mathbf{X}^T\mathbf{X}\right)^{-1}\mathbf{X}^T\mathbf{Y} = \mathbf{X}^+\mathbf{Y} \quad (2.15)$$

¹Note that this has to be done for each frequency line of the DFT spectrum

²If different physical quantities are used, a weighted least-squares estimate has to be determined.

where the matrix \mathbf{X}^+ is the pseudo-inverse of \mathbf{X} and defined as:

$$\mathbf{X}^+ \triangleq (\mathbf{X}^T \mathbf{X})^{-1} \mathbf{X}^T \quad (2.16)$$

When the transfer function is calculated in Equation 2.15 the residual vector $\boldsymbol{\mu}$, that corresponds to the part of \mathbf{Y} that is not described by the model, can be calculated:

$$\boldsymbol{\mu} = (\mathbf{I} - \mathbf{X}(\mathbf{X}^T \mathbf{X})^{-1} \mathbf{X}^T) \mathbf{Y} \quad (2.17)$$

where \mathbf{I} is an identity matrix. If the OTPA is calculated using the least-squares method, the method is identical to the MIMO technique of finding FRF estimates, if shaker inputs would be used as excitation [3].

Using this method to solve for the transfer functions can cause errors. Especially if the input signals are highly coherent and noisy, since the noise will be amplified in the pseudo-inverse calculation by the term: $(\mathbf{X}^T \mathbf{X})^{-1}$. To overcome this one could instead use the Cross Talk Cancellation (CTC) method consisting of Singular Value Decomposition (SVD) and Principal Component Analysis (PCA), which will be discussed in next section [15].

2.3.2. Cross-Talk Cancellation

Since all measurements are done simultaneously, cross-talk between the channels will occur, which in combination with measurement noise can cause erroneous measurements of the input signals, as discussed in the previous section. This can be avoided by performing a CTC using SVD and PCA. The use of SVD is twofold, first it is a computationally efficient way of finding the principal components, and also it is a good way of finding the pseudo-inverse, \mathbf{X}^+ , of the input matrix \mathbf{X} . [3, 15, 9]

Singular Value Decomposition

SVD is based on the following theorem of linear algebra: Any $M \times N$ matrix \mathbf{X} can be decomposed into:

$$\mathbf{X} = \mathbf{U} \boldsymbol{\Sigma} \mathbf{V}^T \quad (2.18)$$

where \mathbf{U} is an $M \times M$ unitary matrix³, $\boldsymbol{\Sigma}$ is an $M \times N$ matrix with nonnegative elements on the diagonal (the singular values) and zeros elsewhere, \mathbf{V}^T is the transpose of an $N \times N$ unitary matrix \mathbf{V} . The columns of \mathbf{U} are the left singular vectors and the columns of \mathbf{V} are the right singular vectors of \mathbf{X} . [6].

In SVD the correlated components of a dataset is found that such each eigenvector is uncorrelated to all other eigenvectors. Therefor it is important to know that SVD can only separate sources that are either uncorrelated or only partly correlated.

³A unitary matrix has the property that: $\mathbf{U}^T \mathbf{U} = \mathbf{I}$ and $\mathbf{U} \mathbf{U}^T = \mathbf{I}$. This also implies that $\mathbf{U}^T = \mathbf{U}^{-1}$.

The matrix \mathbf{X} is containing the measured inputs to the system. If it includes a combination of sound pressures and vibrations, the matrix must be normalized prior to the SVD calculations.

To find the matrices \mathbf{U} , $\mathbf{\Sigma}$, \mathbf{V} in Equation 2.18 the easiest algorithm is the relationship between the SVD and the eigenvalue decomposition:

$$\mathbf{X}^T \mathbf{X} = \mathbf{V} \mathbf{\Sigma}^T \mathbf{U}^T \mathbf{U} \mathbf{\Sigma} \mathbf{V}^T = \mathbf{V} \left(\mathbf{\Sigma}^T \mathbf{\Sigma} \right) \mathbf{V}^T \quad (2.19)$$

$$\mathbf{X} \mathbf{X}^T = \mathbf{U} \mathbf{\Sigma} \mathbf{V}^T \mathbf{V} \mathbf{\Sigma}^T \mathbf{U}^T = \mathbf{U} \left(\mathbf{\Sigma} \mathbf{\Sigma}^T \right) \mathbf{U}^T \quad (2.20)$$

where the right hand sides describe the eigenvalue decompositions of the left hand sides.

In Equation 2.19 \mathbf{V} is the eigenvector matrix and $\mathbf{\Sigma}^T \mathbf{\Sigma}$ is the eigenvalue matrix with the squared singular values of $\mathbf{X}^T \mathbf{X}$ on the diagonal [15].

Equation 2.20 contains the eigenvector matrix \mathbf{U} , the term $\mathbf{\Sigma}^T \mathbf{\Sigma}$ is the eigenvalue matrix with squared eigenvalues of the term $\mathbf{X} \mathbf{X}^T$ on the diagonal⁴ [15].

This is however not a good algorithm for large matrices, which are often dealt with. Instead there are a number of algorithms that finds the singular values without actually computing $\mathbf{X}^T \mathbf{X}$, for example the *Jacobi Rotation SVD* or the *Golub-Kahan SVD*. These will however not be covered in this thesis, for more information for example [1] can be consulted.

The pseudo-inverse of \mathbf{X} , can be calculated using in the SVD:

$$\mathbf{X}^+ = \mathbf{V} \mathbf{\Sigma}^{-1} \mathbf{U}^T \quad (2.21)$$

where \mathbf{X}^+ is the pseudo-inverse of \mathbf{X} and $\mathbf{\Sigma}^{-1}$ is the inverse of $\mathbf{\Sigma}$.⁵

Substitution of Equation 2.21 in Equation 2.15 yields in an estimation of the transfer function matrix $\tilde{\mathbf{H}}$ using the SVD:

$$\tilde{\mathbf{H}} = \mathbf{V} \mathbf{\Sigma}^{-1} \mathbf{U}^T \mathbf{Y} \quad (2.22)$$

With the SVD the residual vector $\boldsymbol{\mu}$ lays in the null space of \mathbf{U}^T [3, 13, 15].

The singular value matrix ($\mathbf{\Sigma}$) from the SVD can be directly used in a PCA, which will be discussed in the following section.

Principal Component Analysis

The idea of PCA is to reduce the size of a dataset with a large number of interrelated variables, while retaining as much variance as possible. This is done by solving an eigenvalue-eigenvector problem (as done in the SVD). The principal components found are uncorrelated

⁴The singular values on the diagonals of $\mathbf{\Sigma}^T \mathbf{\Sigma}$ and $\mathbf{\Sigma} \mathbf{\Sigma}^T$ are the same [15]

⁵To generate a square matrix ($M \times M$) the additional rows of $\mathbf{\Sigma}$ are deleted prior to the SVD computation.

and ordered so that the first few contain most of the variance present in all of the original variables. This method can be used for noise reduction since the smaller Principal Components (eigenvalues) will be measurement noise and cross-talk [9].

The singular values (Σ) determined by the SVD can be directly used in a PCA. The PCs used in the PCA are found on the diagonal of the matrix Σ , i.e. the singular values. The maximum number of PCs is therefore the number of DoFs (measurement reference positions) included in the analysis.

The contribution of each PC to the overall signal is calculated by dividing the PCs (the diagonal of Σ) with the sum of all PCs. This yields in a percentage contribution of each PC [15].

By looking at the PCs one can roughly estimate the Signal to Noise Ratio (SNR) of the signal. The more PCs with the number zero (or close to zero), the higher the SNR will be. The smaller PCs that have a low contribution to the signal can be removed by setting them to zero. This will yield in a noise and cross-talk reduced matrix [16].

The PCs with low contribution (noise and cross talk) are removed from the matrix Σ , to obtain the noise removed PC matrix Σ_r . The PC matrix in Equation 2.23 can now be replaced with the noise removed PC matrix, generating:

$$\tilde{\mathbf{H}}_r = \mathbf{V}\Sigma_r^{-1}\mathbf{U}^T\mathbf{Y} \quad (2.23)$$

where $\tilde{\mathbf{H}}_r$ is the transfer function matrix with reduced noise and cross-talk. By only using the most contributing PCs the transfer function estimates will be improved (noise will be removed)[3, 15].

2.3.3. Response Synthesis

After calculating the noise removed transfer functions, the response at the measurement position can be synthesized in the frequency domain by multiplying the transfer function matrix, $\tilde{\mathbf{H}}_r(j\omega)$, by the transpose of the reference measurements, $\mathbf{X}^T(j\omega)$:

$$\mathbf{Y}_s(j\omega) = \tilde{\mathbf{H}}_r(j\omega) \cdot \mathbf{X}^T(j\omega) \quad (2.24)$$

where $\mathbf{Y}_s(j\omega)$ is the synthesized response.

This can also be done in time domain by first taking the Inverse Discrete Fourier Transform (IDFT) of $\tilde{\mathbf{H}}_r(j\omega)$ and $\mathbf{X}^T(j\omega)$ and thereafter convolve the two matrices:

$$\mathbf{Y}_s(t) = \tilde{\mathbf{H}}_r(t) * \mathbf{X}^T(t) \quad (2.25)$$

where $\tilde{\mathbf{H}}_r(t)$ and $\mathbf{X}^T(t)$ are the time signals of the noise removed transfer function matrix and reference measurement matrix respectively.

These variables can then be compared to the measured response matrix. If uncorrelated noise sources will be present in the measurements this will be seen as a discrepancy between the

measured and synthesized response. This discrepancy will however only be seen if the noise is uncorrelated to the actual signal as discussed in the next section [15].

2.3.4. Practical implementation of Operational Transfer Path Analysis

Since OTPA is using only operating forces, it is a faster and cheaper way of doing a transfer path analysis than the classical TPA. This is due to that the object under investigation does not have to be disassembled in any way. However it has a few drawbacks and points of attentions, as will be discussed in the following paragraphs.

- The OTPA is conversely to the TPA not based on load-response measurements (since the operational force is unknown), this leads to that the resulting transfer functions will not be FRFs but rather transmissibility functions. OTPA is therefor what we call a response-response method.
- When performing an OTPA it is critical that the engineer is designing the measurement setup correctly. Firstly one has to carefully chose the excitations during the measurement. Since only the excited modes of the structure will have an impact, if the mode is not excited at the time of the measurement, this will be missing in the result. Therefore varying excitations such as run-ups are commonly used to cover all excitation modes.
- Since not a real inversion of the X matrix is done, only a pseudo-inverse solution is done using SVD, errors can occur in the estimated transmissibilities.
- In classical TPA a missed path in the analysis will be noticed as a discrepancy between the measured signal and the synthesized signal. This comparison has become a quality indicator of the TPA. However since this is not seen in OTPA, if the sources are correlated. If one propagation path is forgotten, coherent parts are redistributed over the other signals, it is therefore critical to make sure all significant paths are measured. On the other hand, if the noise is uncorrelated to the operating force this will be seen as an discrepancy as in the TPA.
- If a false path is measured and included in the OTPA this can create an erroneous result. A false path is a path through which no energy is transferred to the receiving point, yet it is still considered and included in the OTPA. Depending on the levels of the vibration or pressure of the false path it can lead to a false interpretation of the real paths in the OTPA [3, 15, 5].

3. Implementation of OTPA on a beam-plate structure

Despite commercial softwares are available an OTPA script is written in MATLAB. The basic purpose of this is to get a better understanding of the technique, the theory behind and to not only rely on a black box solution. A description of the script can be found in the following section.

3.1. MATLAB script

The MATLAB script is performing an OTPA analysis of time data and presenting the results in frequency domain.

The complete OTPA-script with its functions is found in Appendix A, however the script is designed to work with the input files provided from Bombardier Transportation, so it might not work for other file structures without modification. A flow chart of the program can be seen in Figure 3.1.

Firstly, the reference and receiving (input and response) signals loaded are split into measurement blocks. All blocks are then transformed to the frequency domain respectively. Second, the signals are sent into the OTPA-function which first scales the input, then calculates the inverse of the input and the transfer functions, the transfer functions are then descaled and the response is synthesized. Finally, the descaled transfer function and the synthesized response are plotted.

3.1.1. OTPA-function

The OTPA-function performs the OTPA analysis. If the measurement contains both vibration and sound pressure measurements the sound pressure is scaled to the same level as the vibrations prior to the SVD.

Scaling

Prior to the Singular Value Decomposition the reference point measurements are scaled (this has to be done if the analysis contains both sound and vibration measurements). This is simply done by studying the time signals manually and scaling them with a integer so that they are of the same magnitude.

After the Singular Value Decomposition the transfer functions are descaled the same way.

Singular Value Decomposition

The SVD is computed by the built-in MATLAB command:

$$[U, S, V] = \text{svd}(X); \quad (3.1)$$

where U and V are unitary matrices and S contains the singular values on the diagonal, so that the equation $X = USV^T$ is satisfied.

Principal Component Analysis

Principal Component Analysis, PCA, is done by the three MATLAB commands:

$$PC = \text{diag}(S); \quad (3.2)$$

$$COEFF = U*S; \quad (3.3)$$

$$CONT = \text{diag}(S)/\text{sum}(\text{diag}(S))*100; \quad (3.4)$$

where Equation 3.2 takes the singular values on the diagonal of S and puts them in the vector PC . Equation 3.3 finds the principal component coefficients, $COEFF$. This is a matrix where each column contains the coefficient for one principal component. Finally, the percentage of the total variance described by each principal component, $CONT$, is calculated using Equation 3.4.

To reduce the noise, the singular values that contributes less than a specified threshold (e.g 5 %) to the overall variance is disregarded from S and replaced with a zero value.

Inversion of X and calculation of H

The noise reduced version of S is then inverted, forming the variable invSr . Next, the inversion of X is calculated by:

$$X_{\text{inv}} = V*\text{invSr}*U'; \quad (3.5)$$

When X_{inv} has been calculated the transfer functions can be estimated:

$$H = X_{inv}' * Y; \quad (3.6)$$

If the data is normalized prior to the SVD (if it contains both vibrations and sound pressures) the transfer functions are descaled before the synthesized response is calculated.

Synthesize response

After the calculation of the transfer function, H , the partial response from each transfer path can be synthesized by a point-wise multiplication of X and H :

$$Y_s = X .* H; \quad (3.7)$$

3.1.2. Plot-function

Finally the synthesized response and the transfer functions are plotted in a number of ways, specified in the beginning of the OTPA-script.

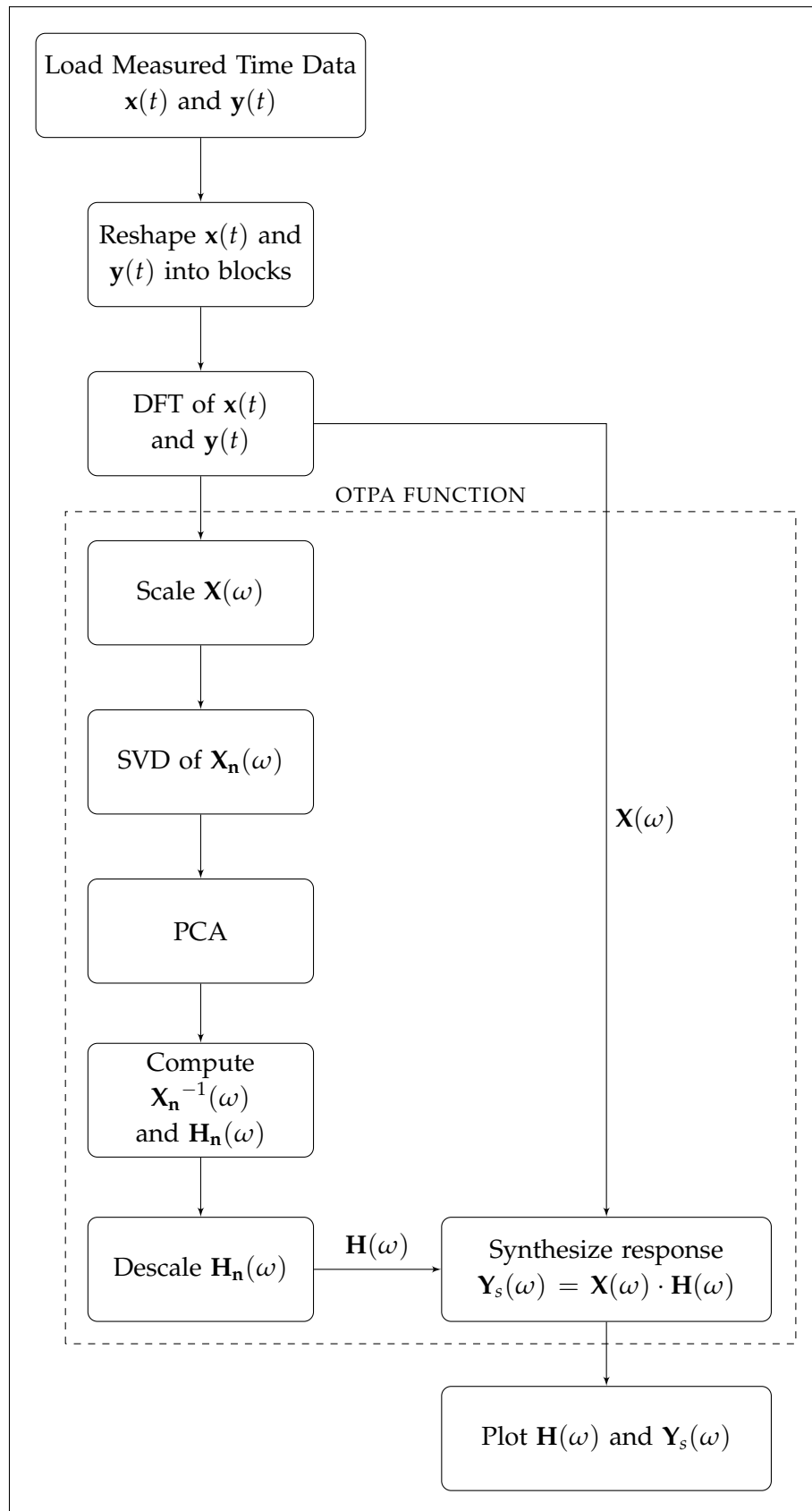


Figure 3.1.: Flow Chart of OTPA script.

3.2. Implementation and validation of OTPA on a test structure

3.2.1. Definition of structure

To test the OTPA script and to carry out parameter studies, the script is firstly applied on simulated displacements, extracted from a Finite Element Method (FEM) model created in COMSOL Multiphysics. The structure, illustrated in Figure 3.2, consists of a rectangular plexiglass beam connected to a plexiglass plate via three cylindrical connectors of steel. Two of the connectors are mounted with a layer of vibration isolating material above and below the steel. This is done to create discrepancy between the transmission of the three connectors. In this way, it is possible to test qualitatively if the OTPA script is generating the expected results. All geometrical measures of the structure can be seen in Table 3.1.

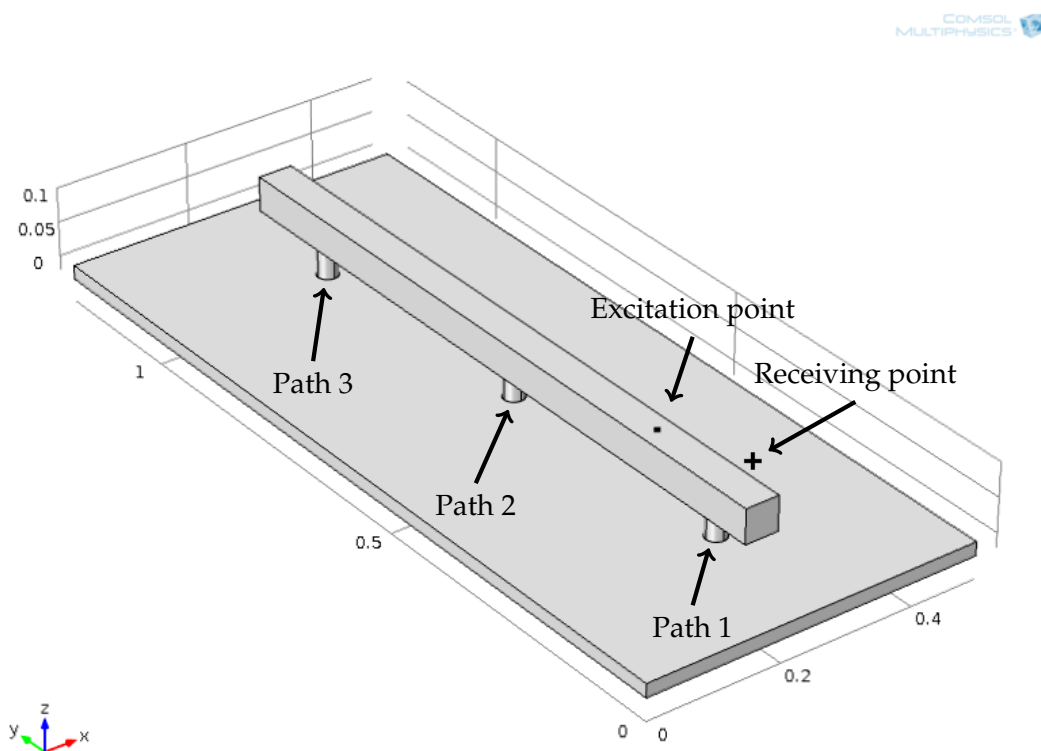


Figure 3.2.: 3D view of COMSOL model used in simulations

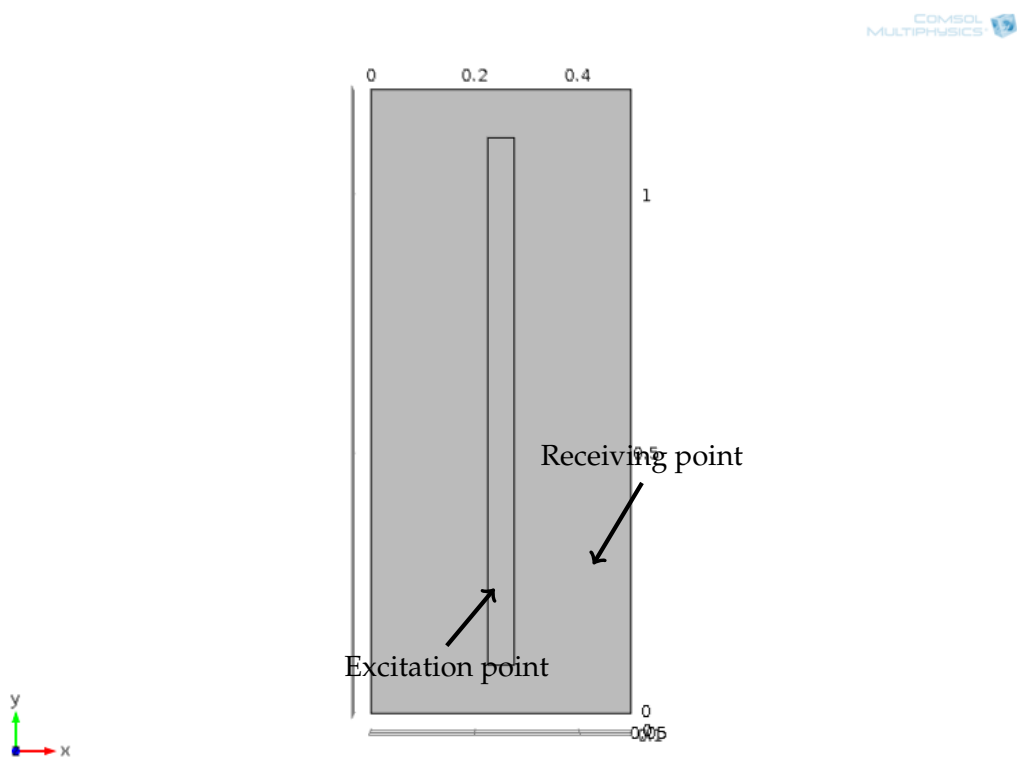


Figure 3.3.: Top view of COMSOL model used in simulations

Plate:	
Thickness	10 mm
Length	1200 mm
Width	500 mm
Young's modulus	$5.6 \cdot 10^9$ Pa
Poisson's ratio	0.3
Density	1150 kg/m^3
Isotropic loss factor	0.13
Connectors:	
Height	50 mm
Diameter	30 mm
Young's modulus	$205 \cdot 10^9$ Pa
Poisson's ratio	0.28
Density	7850 kg/m^3
Isotropic loss factor	0.04
Beam:	
Length	1000 mm
Height	50 mm
Width	50 mm
Young's modulus	$5.6 \cdot 10^9$ Pa
Poisson's ratio	0.3
Density	1150 kg/m^3
Isotropic loss factor	0.13
Vibration isolation:	
Thickness	10 mm ($\times 2$)
Young's modulus	$0.44 \cdot 10^6$ Pa
Poisson's ratio	0.3
Density	220 kg/m^3
Isotropic loss factor	0.2
Excitation point:	
x	250 mm
y	300 mm
z	100 mm
Receiving point:	
x	400 mm
y	300 mm
z	0 mm

Table 3.1.: Material properties of the COMSOL model (the top of the plate is $z=0$ mm)

3.2.2. Calculations

A vertical point force is applied on the top of the beam, and the displacements in the three connectors as well as in the plate are simulated. The excitation and the receiving point used in all OTPA calculations can be seen in Figure 3.2 and Figure 3.3. The displacements in the three points are next imported to the MATLAB script and the OTPA is performed. To simulate several measurement blocks (representing a real measurement) the FRFs are duplicated and random noise is added to each copy when desired.

Thereafter the OTPA model is compared to data extracted from the FE model. The power input (active power), W_{in} , to a structure can be calculated:

$$W_{in} = \frac{1}{2} \Re\{F(\omega)v(\omega)^*\} \quad (3.8)$$

where $F(\omega)$ is the force acting on the structure, $v(\omega)$ is the velocity and $*$ denotes the complex conjugate [2]. The force and the velocity of each connection are extracted from COMSOL and the power input due to each connection is calculated according to Equation 3.8.

3.2.3. Results

Validation of model

The power transmitted through each connecting element is calculated with Equation 3.8 and shown in Figure 3.4. When comparing that to the results from the OTPA seen in Figure 3.5 it is clear that the model actually seems to be working. However it needs to be pointed out that the results can not be directly compared, since Figure 3.4 shows the power input, into the plate, via each connection and Figure 3.5 shows the partial displacement in the receiving point due to each connection. The general behavior is the same, which shows that the OTPA model generates an accurate result.

One can also study Figure 3.5 analytically. Since Path 1 and 2 are treated with a thin layer of vibration isolation material, they should transfer less energy for the high frequencies. Since this is the case (Path 3 is dominant above approximately 200 Hz) also this is indicating that the OTPA model is working properly.

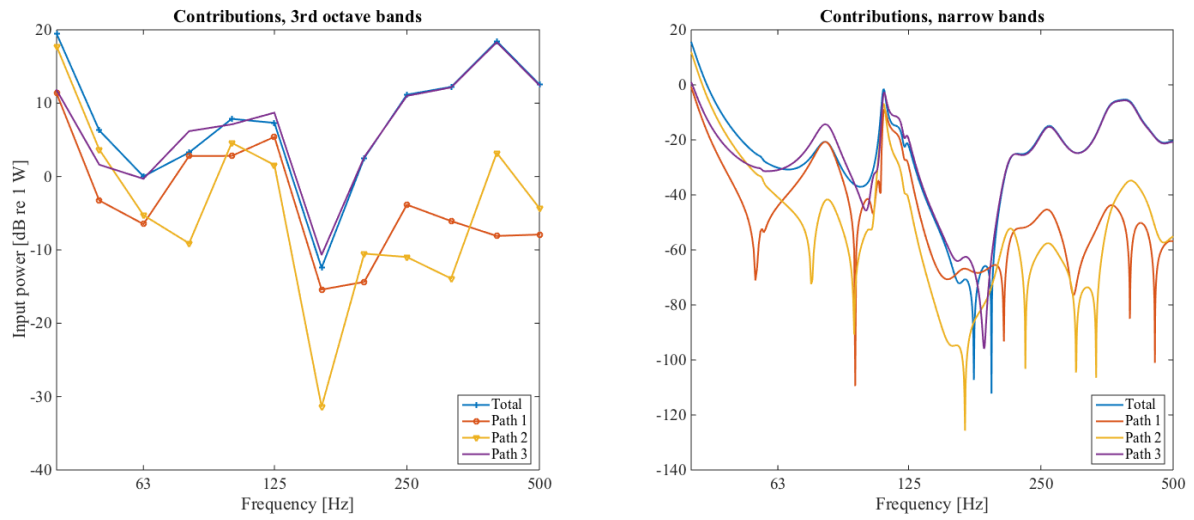


Figure 3.4.: Simulated input power calculated with Equation 3.8, left in third-octave bands and right in narrow bands

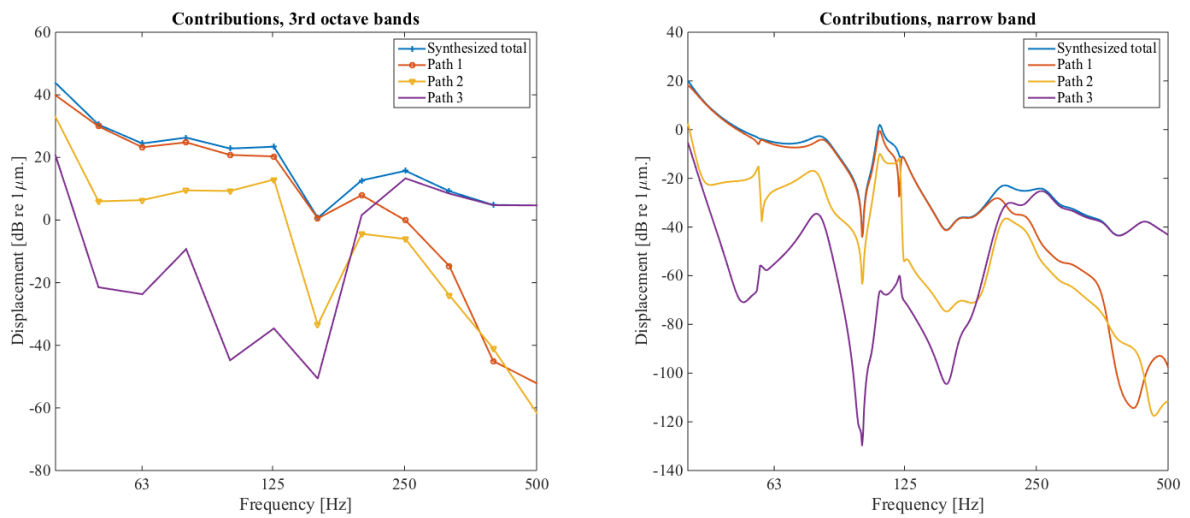


Figure 3.5.: Results from OTPA without noise, narrow and third-octave bands

Noise in receiving point

When a real life measurement is conducted it is always, more or less, affected by noise. To simulate a noisy measurement, uncorrelated noise is added to the calculated velocities prior to the OTPA.

In this section it is investigated how the results from the OTPA are influenced by noise in the receiving point. The effect of noise in the receiving point with a Signal-to-noise ratio (SNR) of 0, 10, 40 and 80 dB is considered.

All figures shown in this section present the synthesized path responses in both narrow and third-octave bands as well as the measured- compared to the synthesized response and the principal component contribution.

SNR=80 dB In Figure 3.6 the synthesized path responses with a SNR of 80 dB (signal 80 dB stronger than the noise) in the receiving point in narrow bands and third-octave bands can be seen. Also the measured vs. synthesized response and the principal component contribution are visible. By studying the graphs, and comparing them to Figure 3.5 (that has no added noise), it can be seen that the responses are noise free.

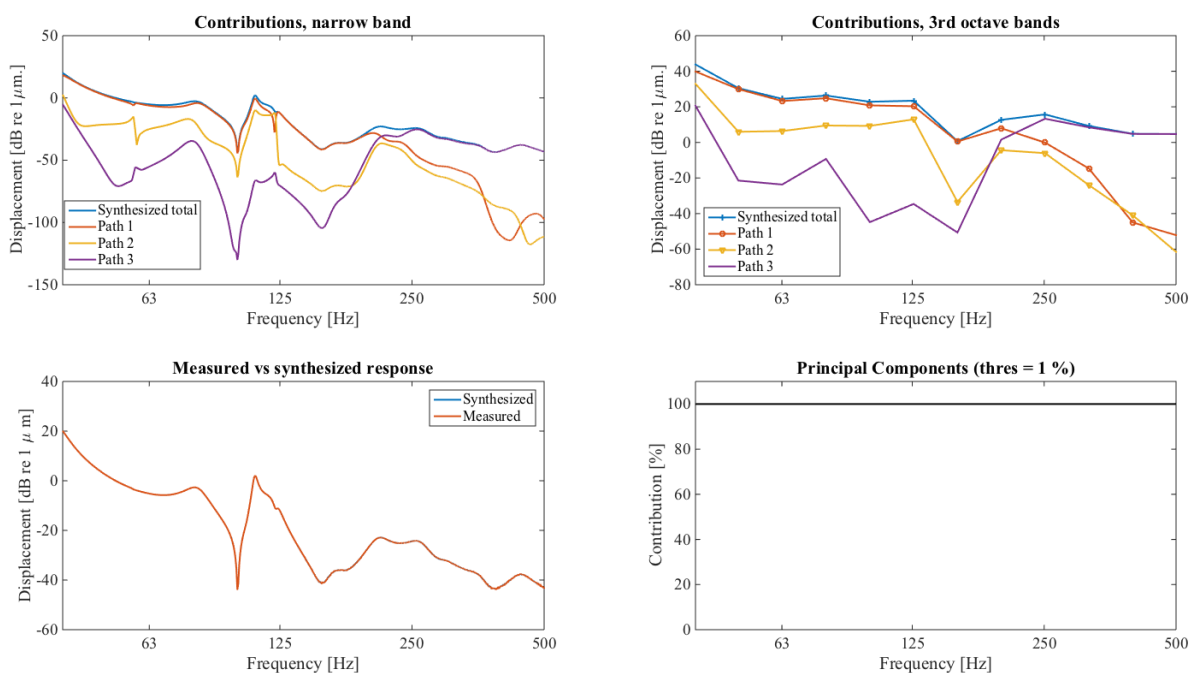


Figure 3.6.: Receiving point SNR=80 dB

SNR=40 dB When comparing the 80 dB figures to Figure 3.7, which have a SNR of 40 dB, it is seen that the shape of the responses are equal, even though the latter figures are containing

more noise.

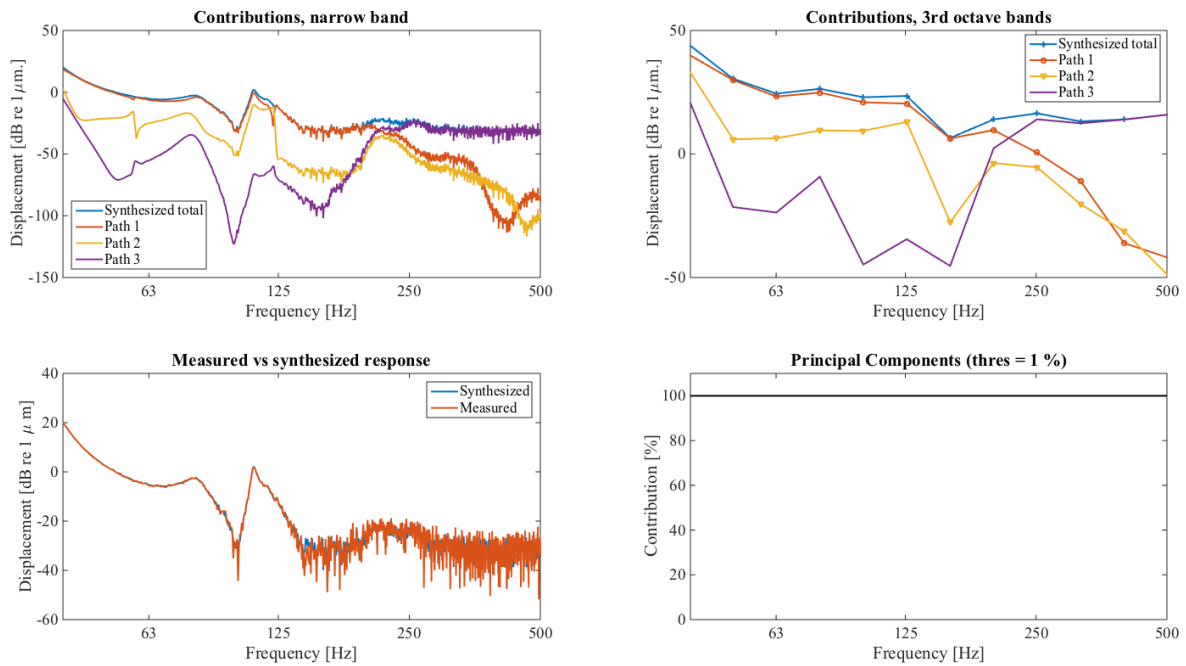


Figure 3.7.: Receiving point SNR=40 dB in narrow bands

SNR=10 dB Figure 3.8 is showing the responses with a SNR of 10 dB in the receiving point. Due to the added noise, the total response is overestimated in the mid and high frequencies. Still, it can be seen that the relation between the different paths is correct.

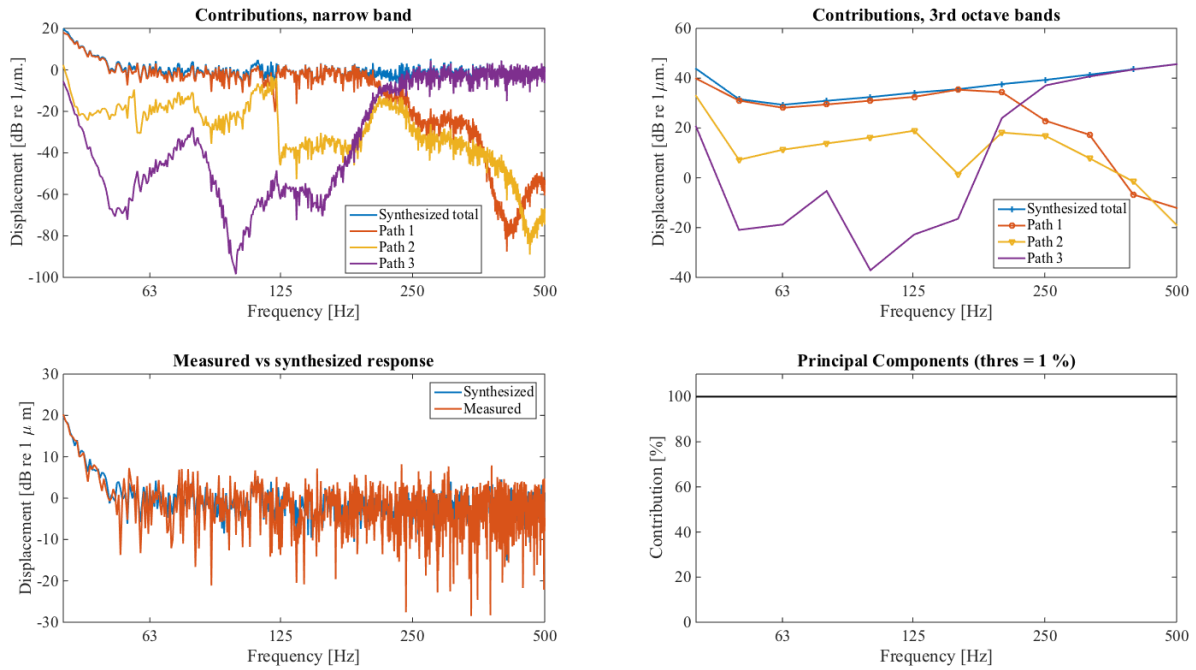


Figure 3.8.: Receiving point SNR=10 dB

SNR=0 dB In Figure 3.9 the signal and the noise are of equal strength, hence a SNR of 0 dB. Even though this is a very noisy signal, the contribution due to each path still can be estimated with a good accuracy. Like in the SNR=10 dB case the total response is flattened out and overestimated from the high noise level.

When comparing the synthesized- to the measured response, and looking at the principal component contribution, also seen in Figure 3.9 it is clearly visible that the response is noisy (which it should be, since the noise is equally strong as the signal). However, the synthesized response is less noisy compared to the measured, this is partly due to the PCA which is noise reducing¹.

Also it can be seen that the Principal Components are not affected by the noise, this is due to that they are calculated from just the input (reference) signal (see Equation 3.1 and Equation 3.4).

This investigation indicates that the estimated relation between the paths is not much affected by having noise in the receiving point. However, with increasing noise the total response smears out over the frequencies, and it is becoming harder to see in which frequency range the response is strong and in which range the response is weak. This is of course a setback, but still it is able to relate the different paths to each other.

Having uncorrelated noise in the receiving point is not uncommon. For example in the train case one can have fans inside the train cabin (or people talking), which are generating uncor-

¹Also in this case since the measurement blocks (vibration responses from COMSOL) are copies of the same response, some of the noise is averaged out.)

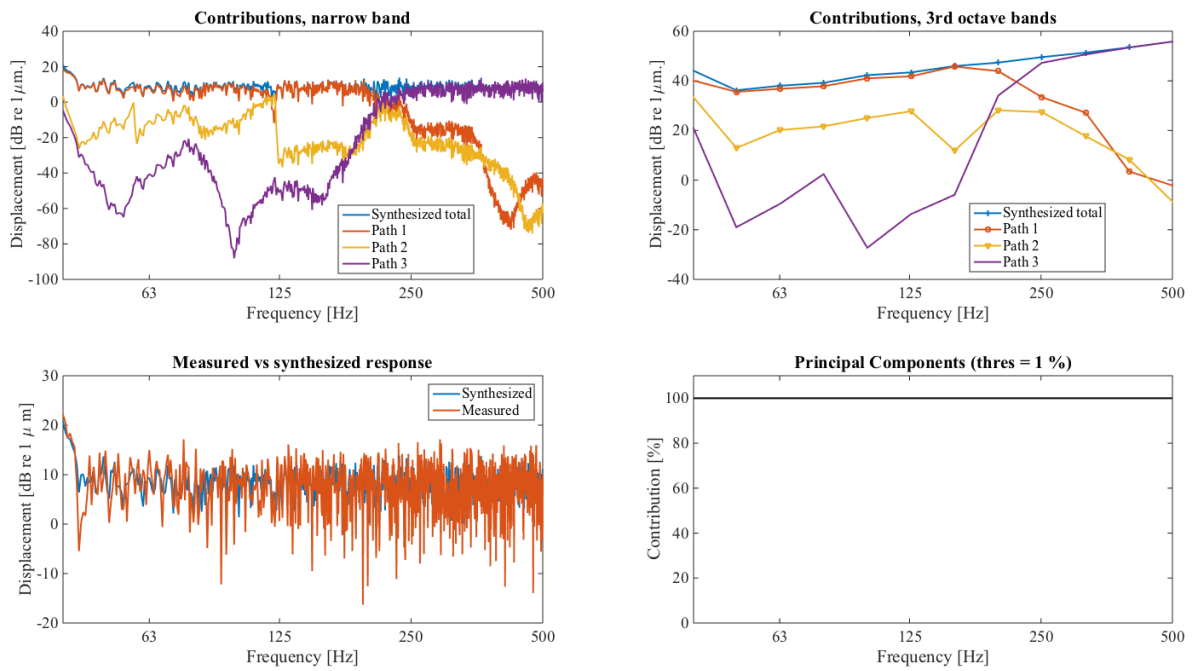


Figure 3.9.: Receiving point SNR=0 dB

related noise in the receiving microphone measurements. This is as seen not strongly affecting the possibility to rank the different paths.

It is also shown that the frequency response of the receiving signal can be used as an estimator for the noise in the receiving point.

Noise in reference points

Like in the previous section, also the measurements of the reference points (connectors) are always containing noise to some extent. In this section it therefor is investigated how noise at the reference measurements are affecting the results. Noise is added to the extracted velocities prior to the OTPA, and the receiving points are kept noiseless.

All figures shown in this section will present the synthesized path responses in both narrow and third-octave bands as well as the measured- compared to the synthesized response and the principal component contribution.

SNR=120 dB Figure 3.10 is showing the case with an SNR in the reference points of 120 dB.

When this is compared to Figure 3.5, which is a case without any added noise, it is visible that having an SNR of 120 dB in the reference points is like adding no noise at all. In Figure 3.10 it can be seen that one principal component contributes to all the energy in the signal.

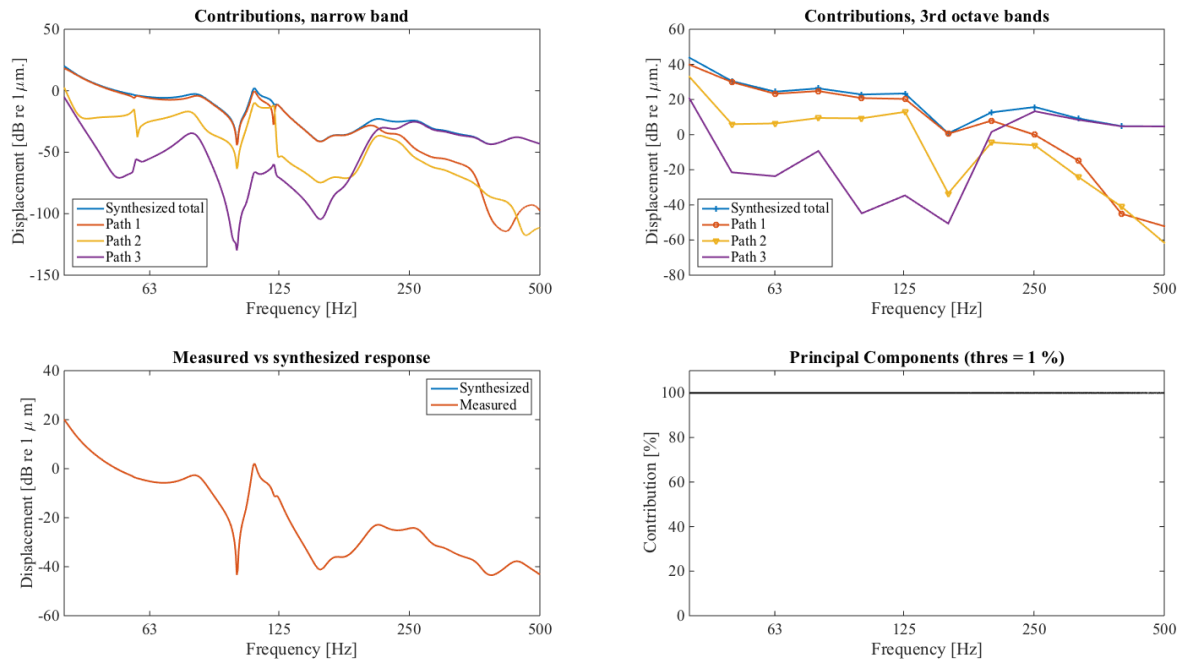


Figure 3.10.: Reference point SNR=120 dB in third-octave bands

SNR=80 dB In Figure 3.11 the SNR in the reference points is 80 dB.

Just like the plot with SNR=120 dB a SNR of 80 dB are giving good results. When studying the principal component contribution it can be seen that for 80 dB not all of the information is in the strongest principal component. Also the weaker parts of the signal (path 2 and 3 above 250 Hz) are a bit distorted in the narrow band plot.

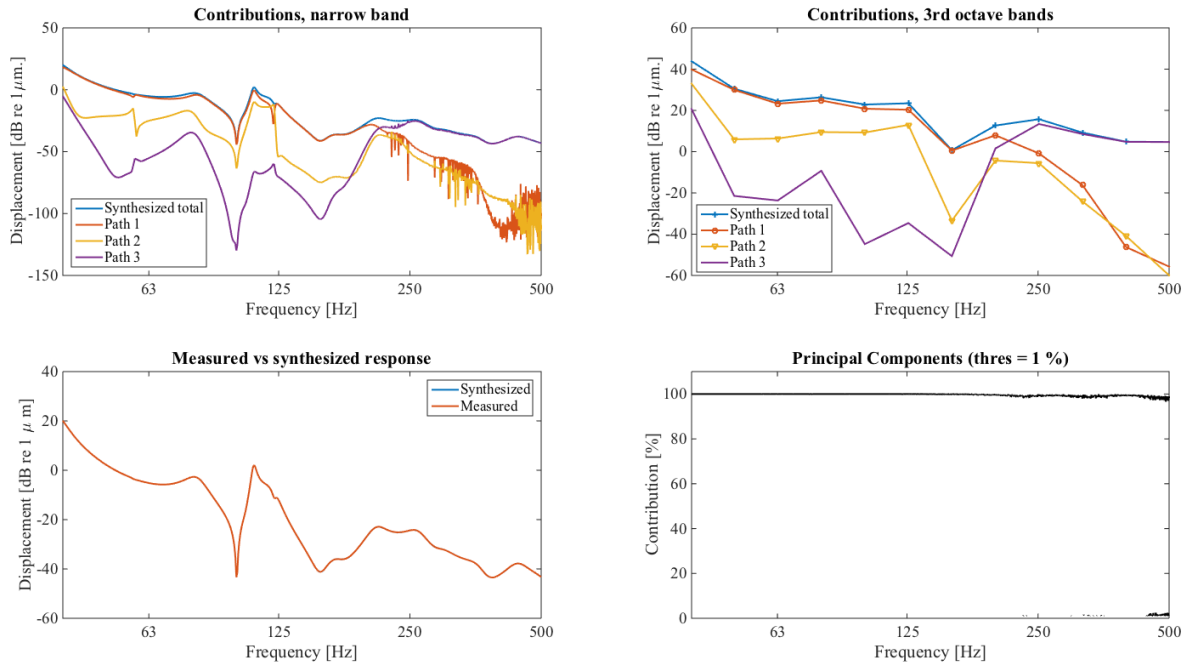


Figure 3.11.: Reference point SNR=80 dB

SNR=40 dB For a SNR of 40 dB Figure 3.12 is shown.

The third-octave plot is still showing the contribution of the paths in a decent way to being able to do a good ranking. However the narrow band plot is noisy (over 63 Hz) and hard to interpret.

When having a look at the principal component contribution it can be seen that with a noisy reference signal, even the lower order principal components are contributing to the signal.

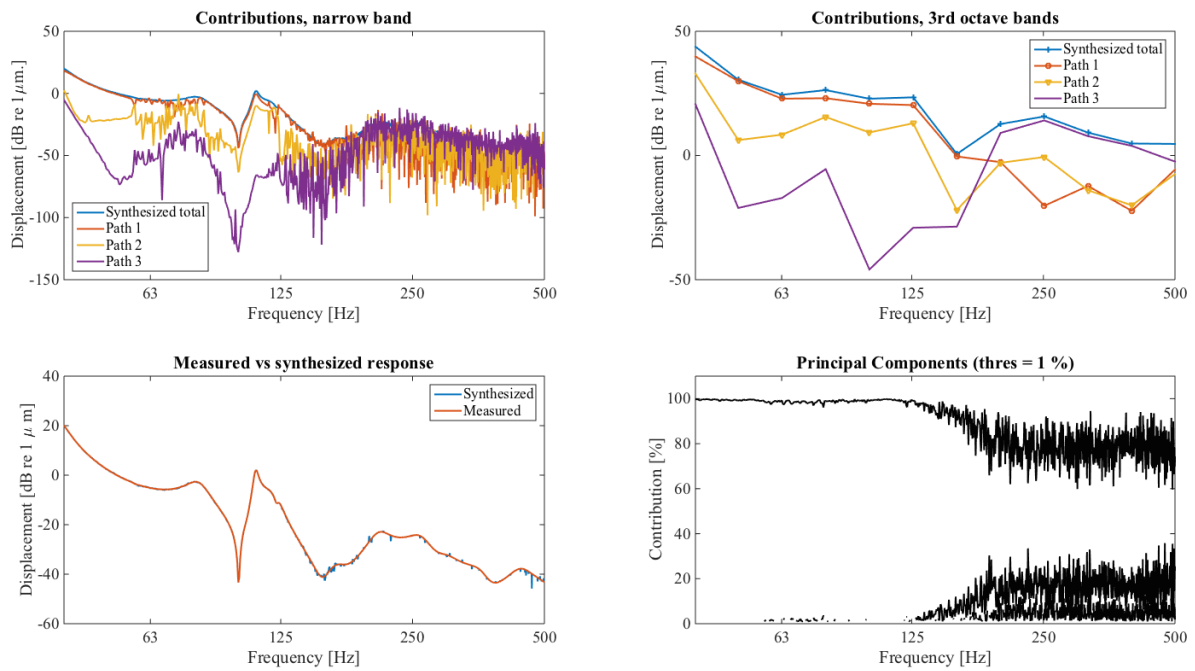


Figure 3.12.: Reference point SNR=40 dB

SNR=10 dB In Figure 3.13 the SNR has been adjusted to 10 dB in the reference points. it can be seen in the figure that the signal is too distorted to generate a good estimation of the paths both in third-octave bands and narrow bands.

When studying the principal component contribution in Figure 3.13 it can be seen that even more information is in the lower ranked principal components.

From the experiment with noise in the reference points it can be concluded that the principal component contribution is a good estimator of the noise in the reference points. With increasing noise, more energy is spread to the lower order principal components.

It can also be concluded that the reference points are more sensitive to noise than the receiving points, and a good SNR is needed to get good results from the OTPA.

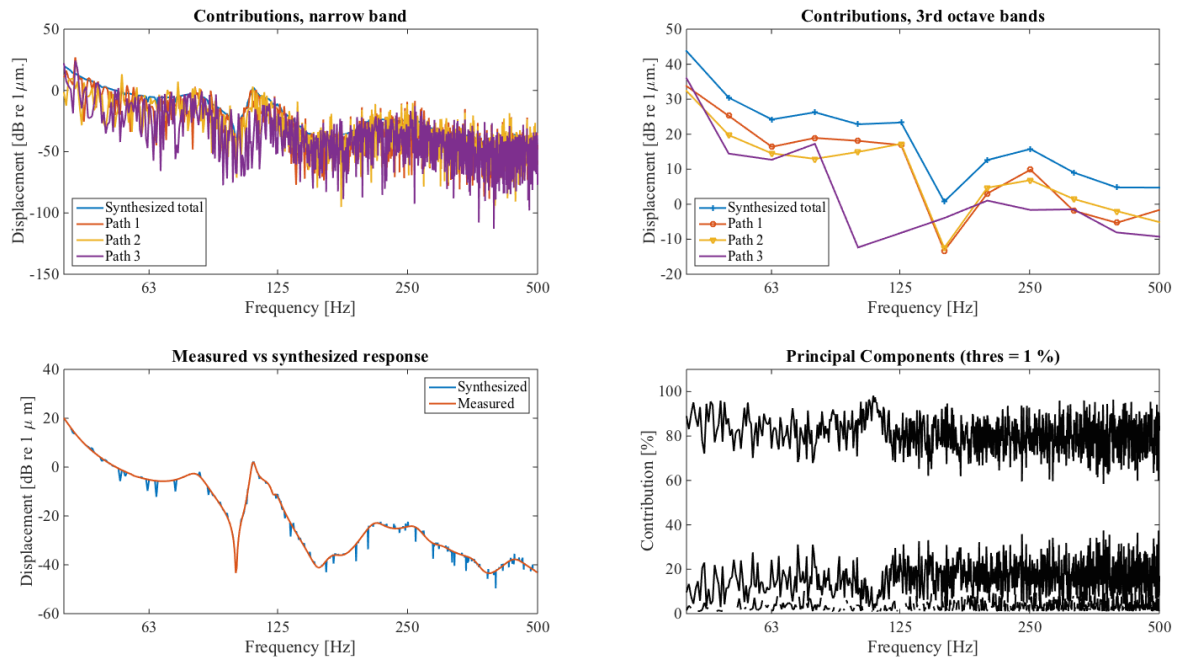


Figure 3.13.: Reference point SNR=10 dB

Missing path

In this section the effects of a missing path is investigated. If a path is excluded from the OTPA analysis, according to the theory, the energy from the missing path will be distributed on to the other paths in the analysis.

Only path 1 and 2 included In Figure 3.14 path 3 is excluded from the OTPA analysis and the contribution due to path 1 and 2 is calculated. Of course, path 3 is still contributing to the vibrations in the plate (the total response), however the transmission path is not included in the analysis.

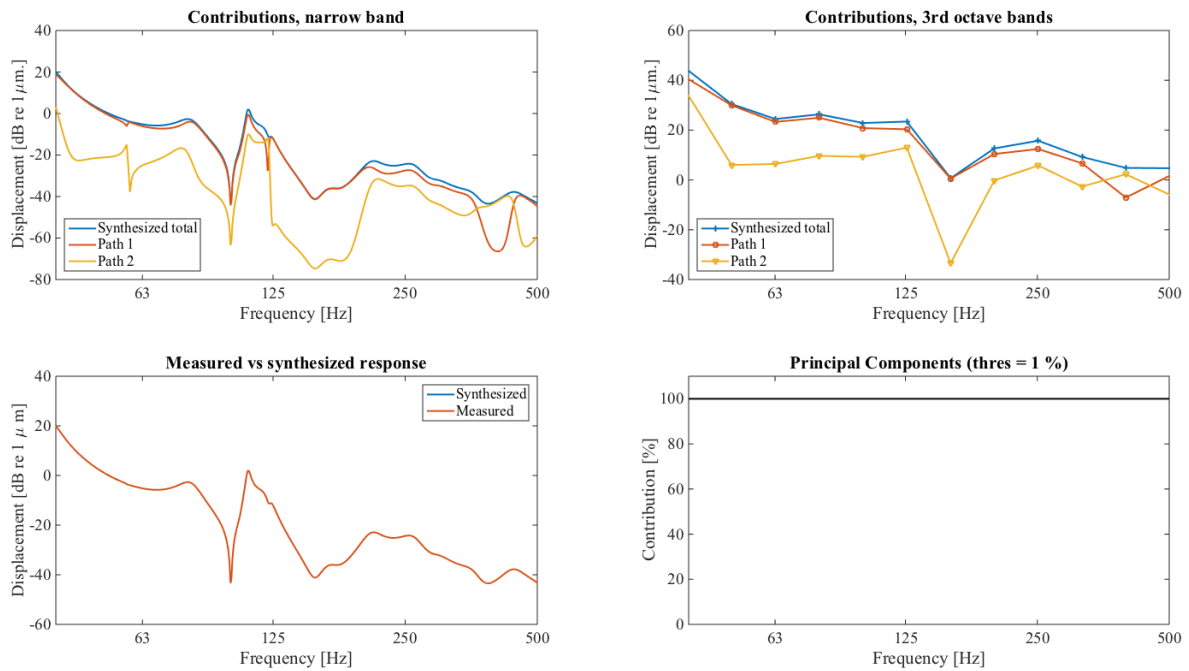


Figure 3.14.: Contribution due to path 1 and 2, with path 3 excluded

Only path 1 and 3 included Figure 3.15 is showing the contribution from path 1 and 3 when path 2 is excluded in third-octave bands and narrow bands respectively.

In this experiment the relation of the paths is preserved even if one path is not included in the analysis. However, if a strong path is excluded, the other paths will be overestimated. This is causing that path 1 and 2 are looking stronger than they really are in Figure 3.14 for high frequencies (over 200 Hz). This is due to that the energy from path 3 (which is excluded) are spreading to path 1 and 2. If this analysis was used as a base for how to lower the vibrations in the plate, resulting in that path 1 and 2 are treated, this would not give a good result, since path 3 would still be the major transmission path (especially over 200 Hz).

As seen in Figure 3.14 and Figure 3.15 the synthesized and measured responses are equal even though a path is excluded. This is according to the theory since the energy from the missing path is spread to the other paths included in the analysis. Hence, the comparison between the measured and synthesized response can not be used as an indicator that all paths are measured (as it often is in classical TPA).

The conclusion can be drawn, that it is critical to have a good knowledge about the system prior to the analysis. If not, and a transmission path is not measured, the other paths will look stronger than they really are. This is not seen in the comparison between the synthesized and measured response or principal components. This might result in that a path that seem strong is treated, with an unsatisfying result. Paths can be neglected from the analysis, but only if it is known that they do not contribute much to the response.

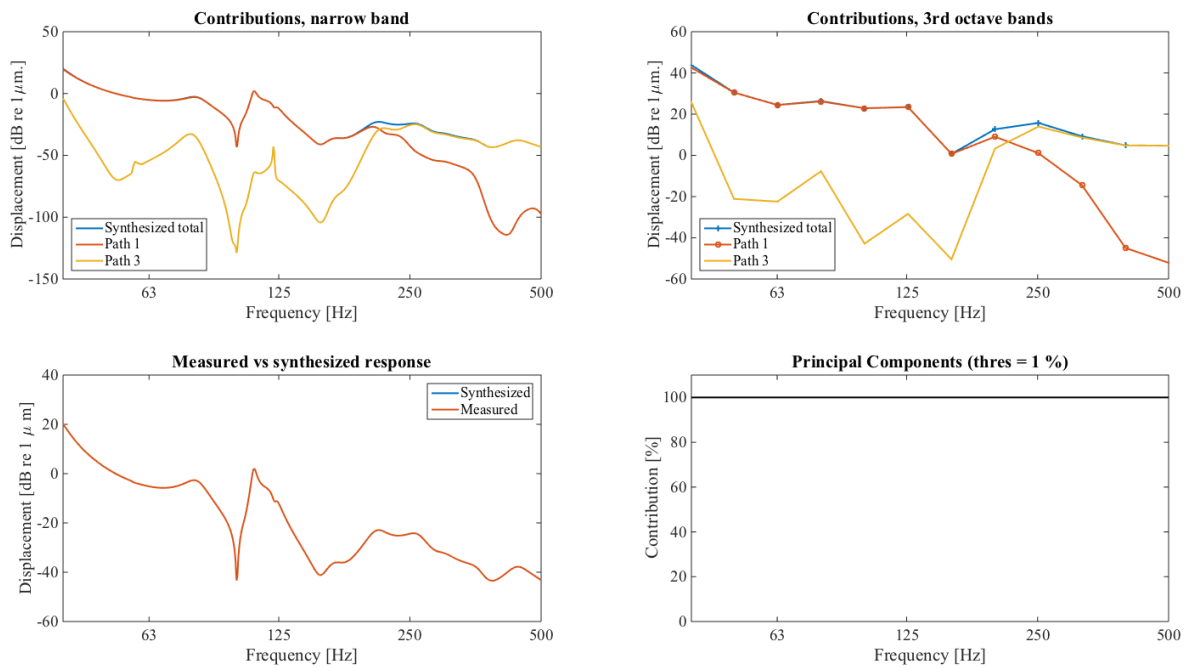


Figure 3.15.: Contribution due to path 1 and 3, with path 2 excluded

4. Implementation of OTPA on a high-speed train

4.1. The high-speed train

The primary suspension of a train bogie, normally a steel spring, is the link between the wheelsets and the bogie frame. The bogie frame is connected to the carbody via the secondary suspension consisting of airsprings and vertical and lateral dampers.

The bolster is used to connect the carbody to the bogie, and is fixed under the carbody.

The airsprings allow articulation of the bogie under the carbody around the x-, y-, and z axis and are introducing some vertical damping. Yaw damping (ride stabilization) is provided by hydraulic yaw dampers located between the bogie frame and the bolster. They damp rotational movements of the bogie relative to the carbody about the z-axis. The lateral suspension provides damping in the y-direction. To resist the carbody's rolling movements an anti-roll bar is used. The system comprises a torsion bar mounted to the bolster by rubber-metal bearings, with one lever at each end to take the anti-rolling moments transmitted by linkage rods from the bogie frame.

A drawing of a secondary suspension can be seen in Figure 4.1.

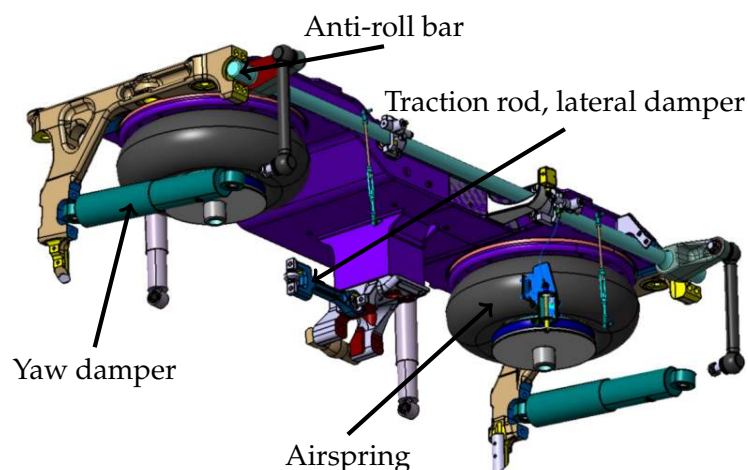


Figure 4.1.: Secondary suspension of a high-speed train

4.2. Measurements

Measurements of a Bombardier high-speed train are conducted in 2013 at a railway test circuit.

At the time of the measurements, the train was not yet in final serial design status which meant that the saloons were not finalized. There were only some interior insulation installed, no chairs or interior panels. Also, the cab door could not be closed. Since several other test teams apart from the acoustic were aboard the train this resulted in some speech disturbances in the microphone signal in the driver's cab. The noise in the receiving microphones should not be a problem, as discussed in section 3.2.3.

The OTPA script is implemented on the measured accelerations and sound pressures. The reference measurement points can be seen in Figure 4.1.

Description	Name	Direction	Position
Yaw Damper	YDLx	X	L
Yaw Damper	YDLy	Y	L
Yaw Damper	YDLz	Z	L
Yaw Damper	YDRx	X	R
Anti-roll bar	ARBLz	Z	L
Anti-roll bar	ARBRz	Z	R
Traction rod/Lateral damper	CPx	X	C
Traction rod/Lateral damper	CPy	Y	C
Traction rod/Lateral damper	CPz	Z	C
Airspring (bolster)	BBLz	Z	L
Airspring (bolster)	BBRz	Z	R
Bogie space microphone	MBOG	S	C

Table 4.1.: Measured reference points.

Description	Name	Direction
Acc. below driver's seat	A1Z	Z
Acc. floor right side	A2Z	Z
Acc. lower sidewall right side	A3Y	Y
Acc. higher sidewall right side	A4Y	Y
Acc. floor left side	A5Z	Z
Mic. H=1.6 m, right side	M5	S
Mic. H=1.5 m (driver's ear), right side	M6	S
Mic. H=0.5 m, right side	M7	S

Table 4.2.: Measured receiving points

4.3. Results

Results from the OTPA of the measurements from the high-speed train will be presented in this section. All analysis is done with a block size of 1 second and a PCA Threshold of 5 %.

Since all measurements were made during a run-up, all results are for run-up conditions.

4.3.1. Campbell diagrams

First on the Campbell diagrams of the measured and OTPA results are shown and compared.

Figure 4.2 shows the sound pressure level in the microphone position at the driver's ear inside the cabin (M5) as a function of speed and frequency. When comparing the response from the OTPA to the measured one it is visible that there is a good match between the two. One can also see that the OTPA diagram is noise reduced.

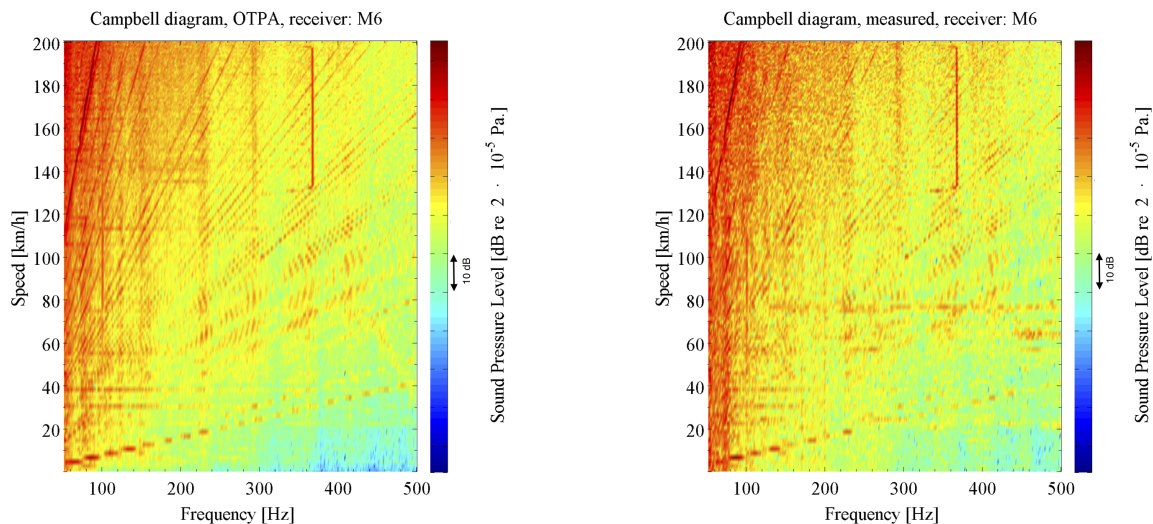


Figure 4.2.: Campbell diagram of receiver microphone at the driver's ear, $h=1.5$ m (M6). Right: Measured, Left OTPA. Both graphs have the same scale.

Figure 4.3 shows the Campbell diagram of the measured sound pressure in the bogie room. When analyzing the figure it is clear that the traction motor cooling fan is starting to operate in full speed at ca 130 km/h, which leads to a clear peak around 370 Hz. This noise is also transmitted into the driver's cabin, which can be seen in Figure 4.2.

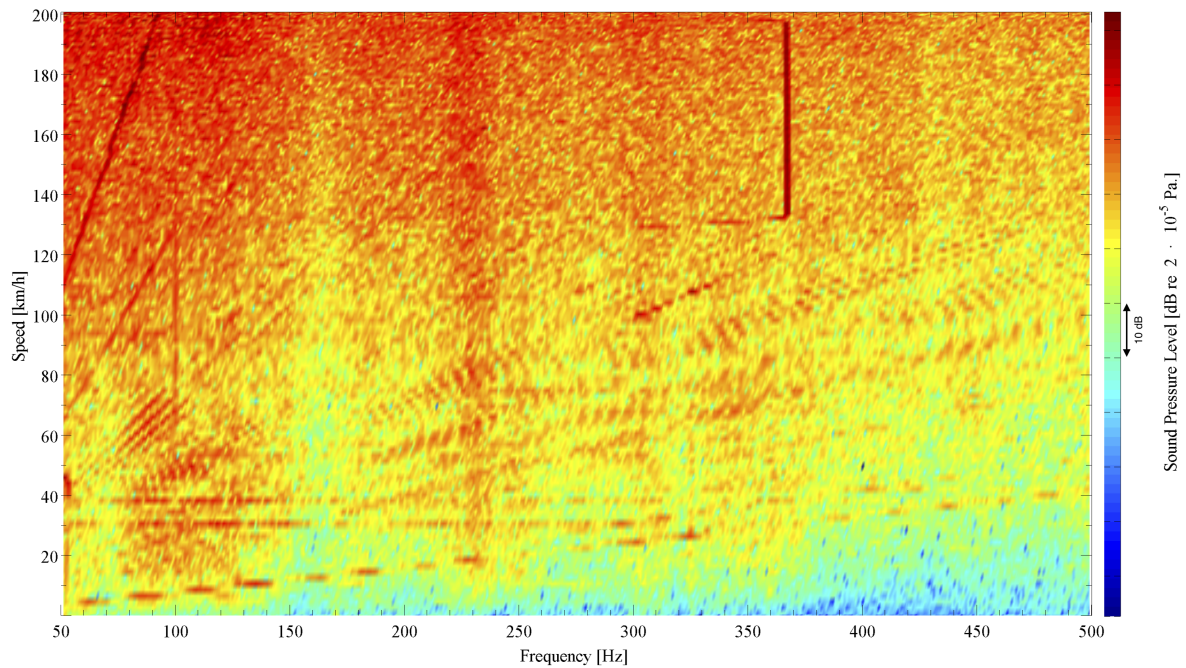


Figure 4.3.: Campbell diagram of reference microphone in the bogie spacing (MBOG1)

4.3.2. Transfer Functions

Structure-borne vs airborne sound

Figure 4.4 is showing the transfer functions of the airborne and structure-borne sound from the bogie to the microphone position at the driver's ear as determined from the OTPA.

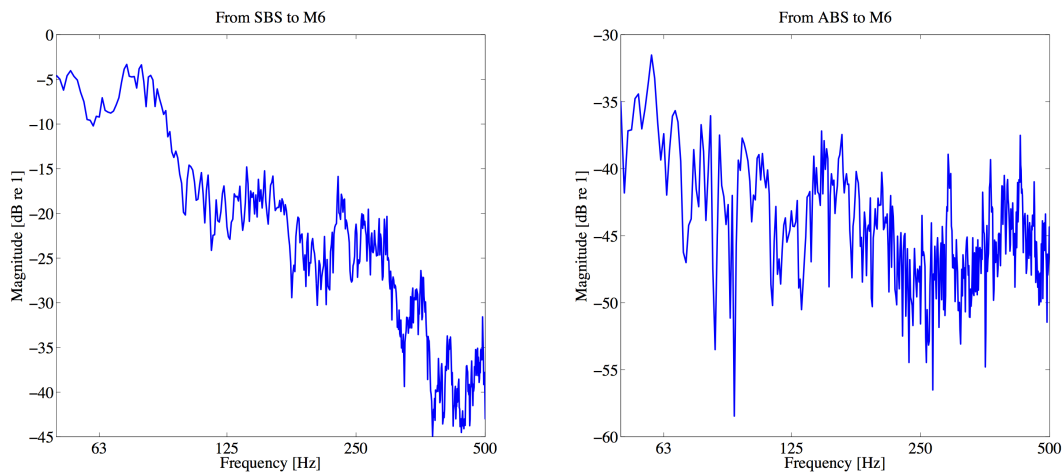


Figure 4.4.: Transfer functions of the airborne (ABS) and structure-borne sound (SBS) from the bogie to the microphone at the driver's ear (M6)

Comparison with loudspeaker measurements

One of the other test cases performed during the measurements was to test the airborne transmission through the bogie. This is done by, at standstill, feeding a loudspeaker placed in the bogie spacing with a white noise signal. Simultaneously the sound pressure is measured in the bogie as well as inside the train. From those measurements the transfer function from the bogie spacing (MBOG) to the receiving microphone at the driver's ear inside the cabin is calculated. This is compared to the transfer function between the same transducers from the OTPA calculations and the result is shown in Figure 4.5.

When comparing the transfer function from the OTPA to the one from the loudspeaker measurement it is seen that they are not equal. This might be due to that in the loudspeaker case more of a plane wave is created, compared to the operational case with more sound sources (4 wheels and two rails). This may affect the transfer function to be less modal as seen in the narrow band case in Figure 4.5.

However it can be seen that the transfer functions are at approximately the same level almost throughout the frequency range and for some frequency bands they match perfectly.

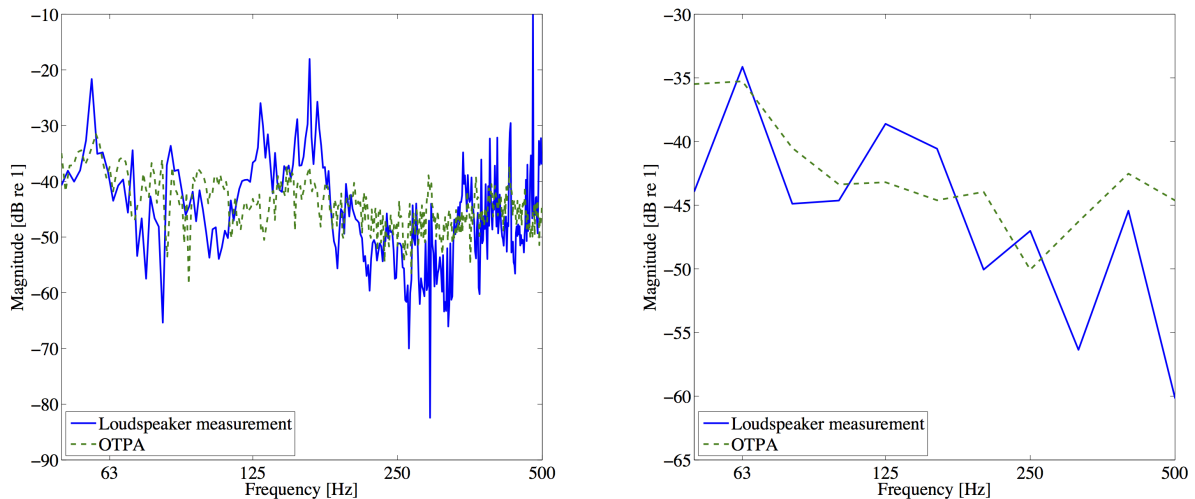


Figure 4.5.: Transfer functions from the airborne bogie spacing microphone (MBOG) to the microphone at the driver's ear (M6) calculated with OTPA and from loudspeaker measurements

Transfer functions to microphones

When the transfer functions from a certain reference to the three interior microphones are compared, it is seen that they are similar (i.e the transfer function from MBOG to M5 are very similar to the one from MBOG to both M6 and M7). Due to this, only receiving microphone M6 (at the driver's ear) will be used in the upcoming analysis.

Plots of the transfer functions can be seen in Appendix B.

Transfer functions to structure-borne receivers (accelerometers)

The transfer functions to all structure-borne receivers can be seen in Appendix B. Since not all data can be presented the accelerometer below driver's seat (A1z) is chosen for further analysis.

All following results will be presented for the accelerometer below the driver's seat and the microphone at the driver's head.

4.3.3. Structure-borne vs. airborne sound

In the first stage, all structure-borne paths are added up, and the amount of structure-borne versus airborne sound transferred into the carbody is investigated. This is done for the speeds 40, 80, 120, 160 and 200 km/h.

Receiver: Microphone at driver's ear

For the airborne receiver at the driver's ear is the separation of structure-borne and airborne sound presented in Figure 4.6, Figure 4.7, Figure 4.8, Figure 4.9 and Figure 4.10 for speeds 40, 80, 120, 160 and 200 km/h respectively.

For the frequency range analysed it is clearly seen that the structure-borne sound is most significant all over the speed range, even though for high speeds in the high frequencies the airborne contributes the most to the sound pressure at the driver's ear. Please note that no data above 0.5 kHz is analysed. If such data were included airborne sound would be relatively more important.

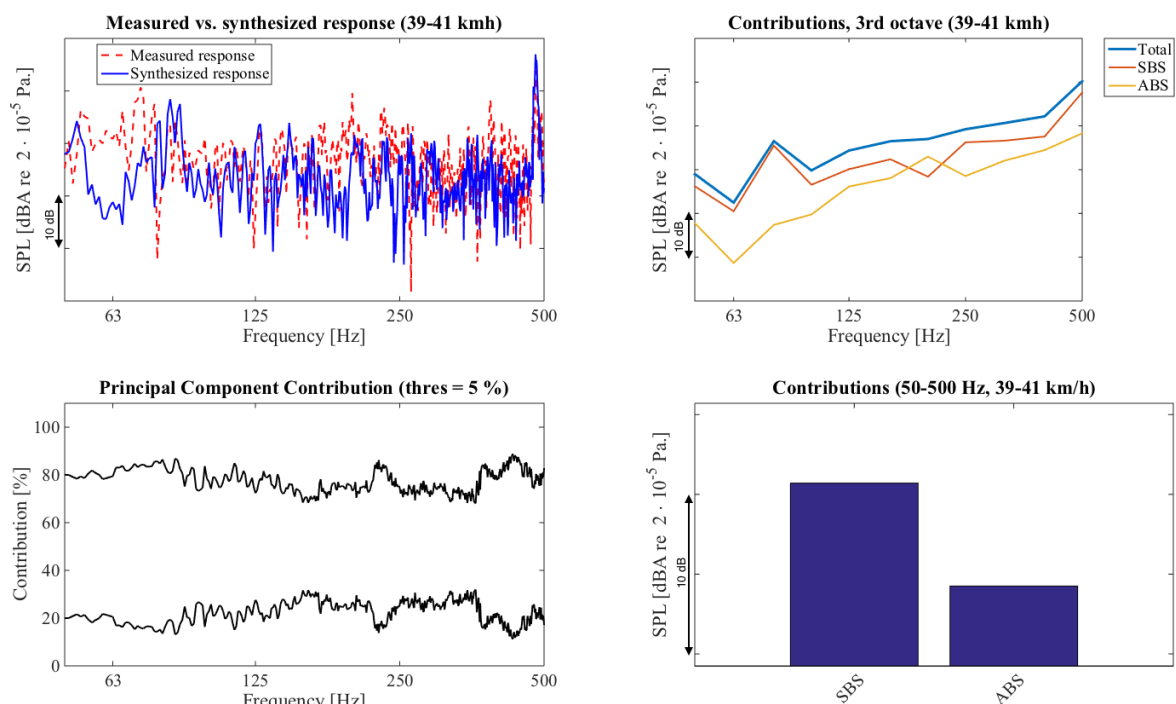


Figure 4.6.: Airborne and structure-borne sound in microphone at driver's ear at 40 km/h

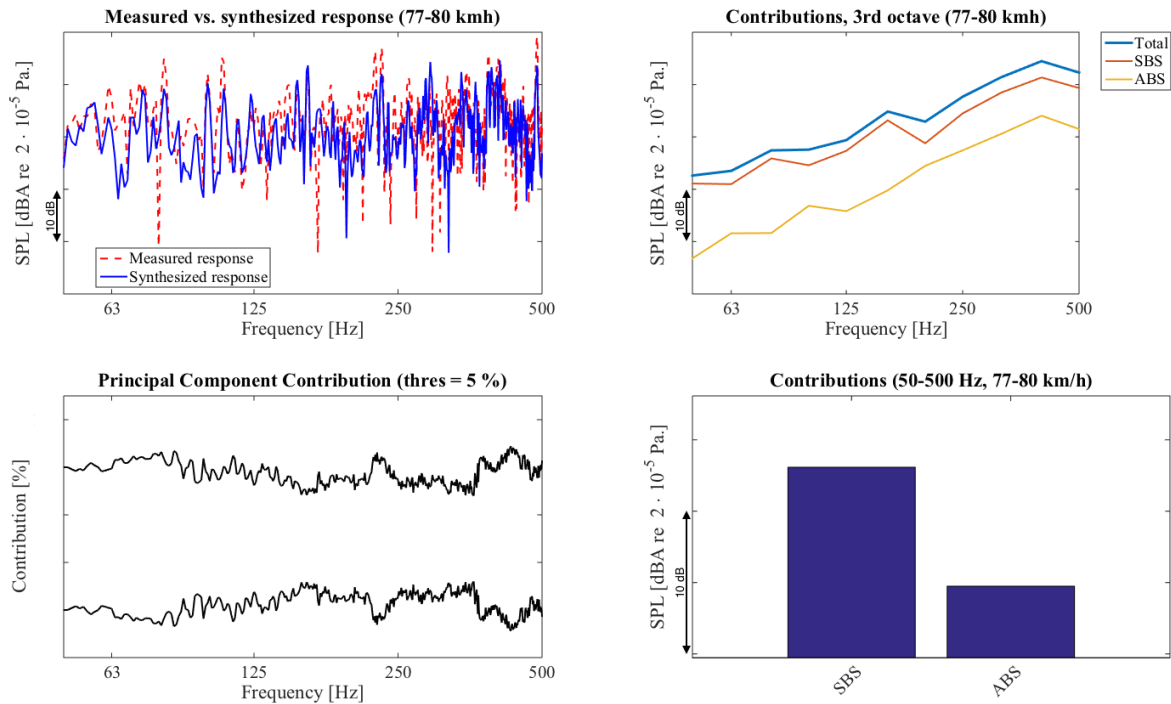


Figure 4.7.: Airborne and structure-borne sound in microphone at driver's ear at 80 km/h

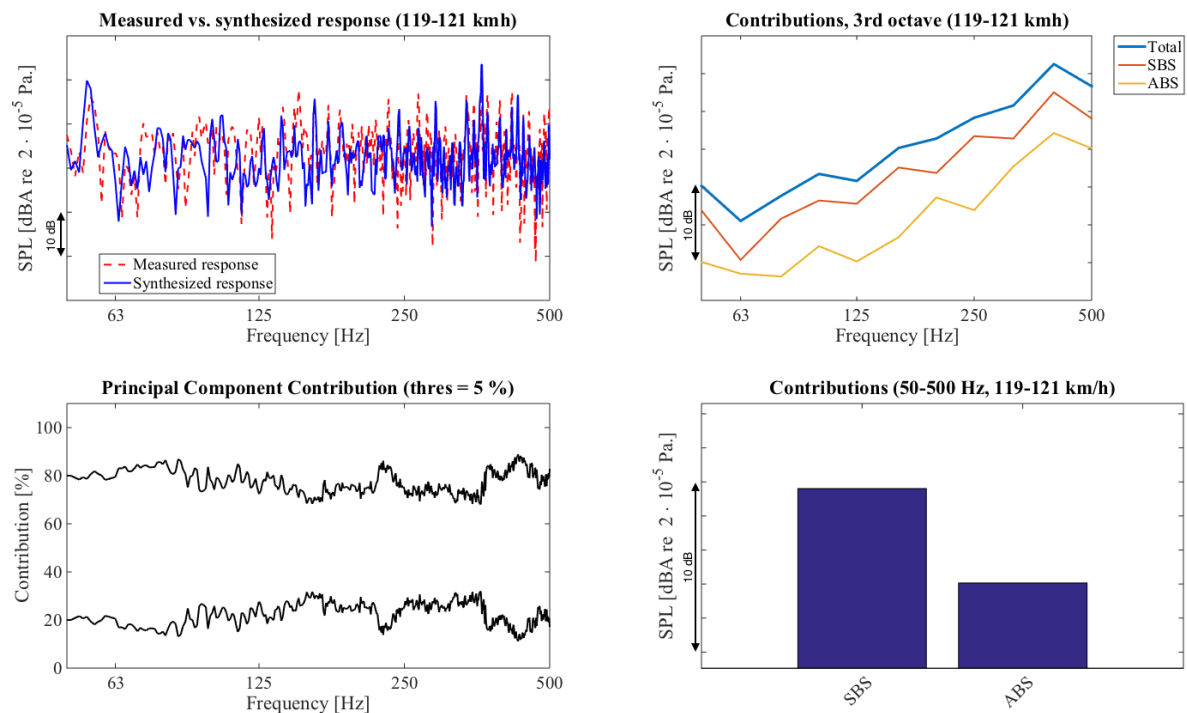


Figure 4.8.: Airborne and structure-borne sound in microphone at driver's ear at 120 km/h

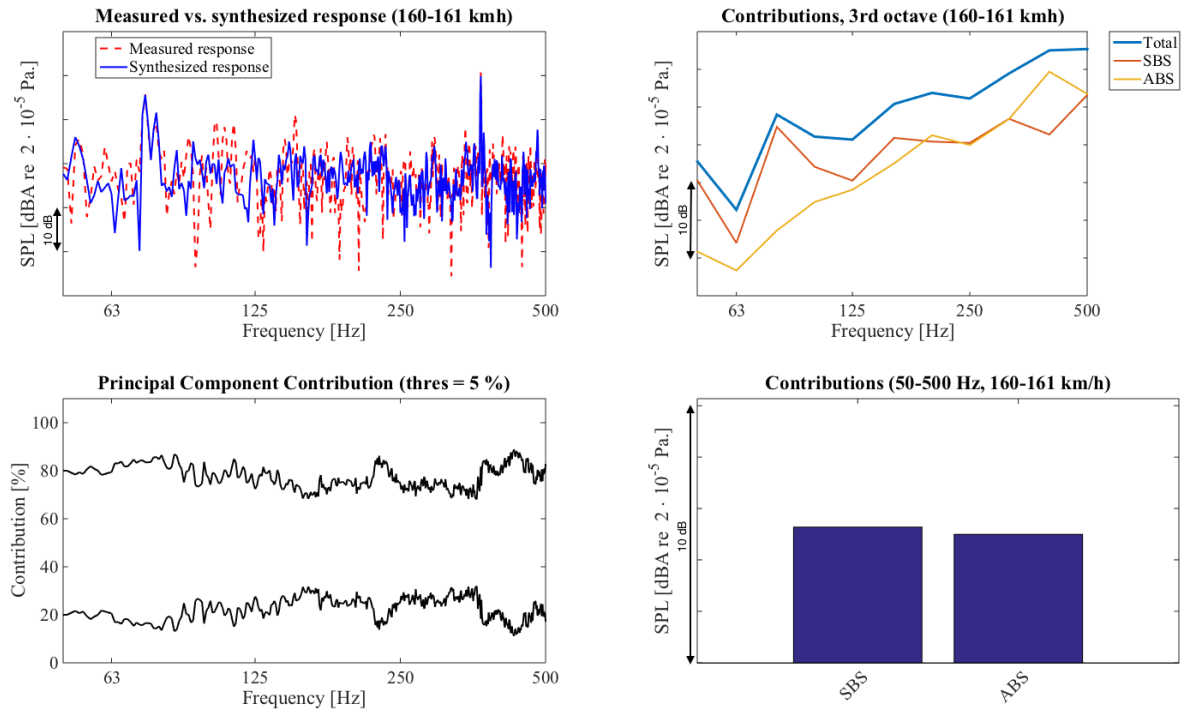


Figure 4.9.: Airborne and structure-borne sound in microphone at driver's ear at 160 km/h

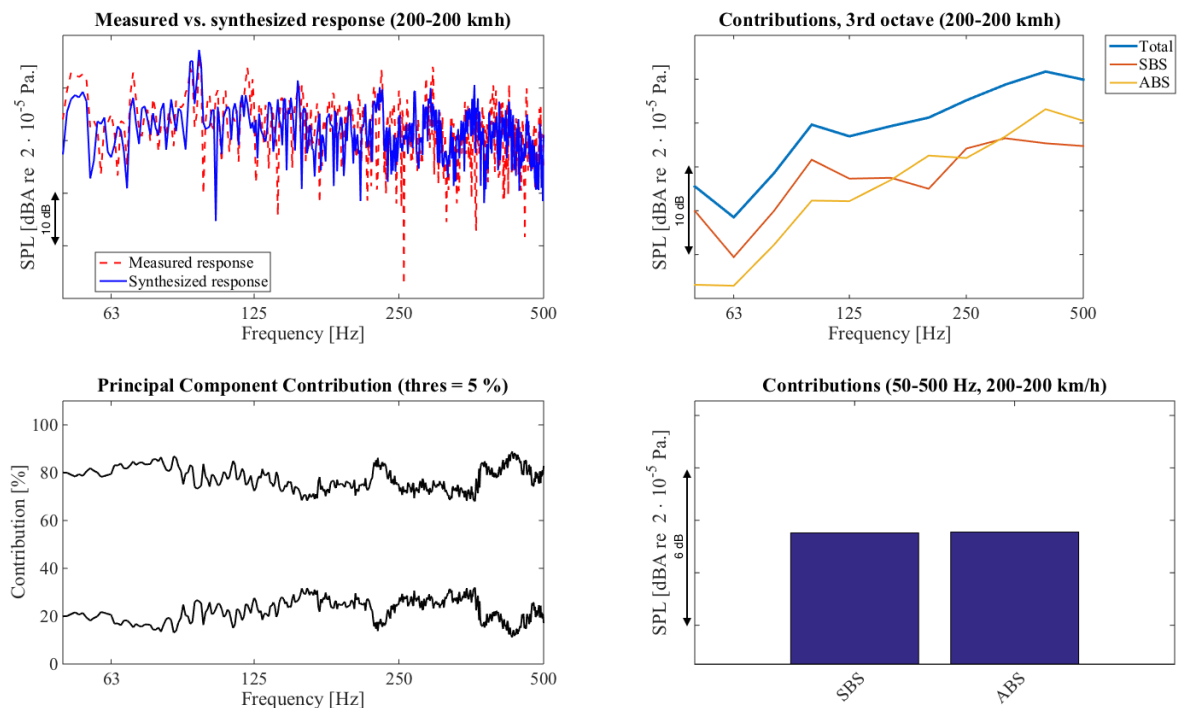


Figure 4.10.: Airborne and structure-borne sound in microphone at driver's ear at 200 km/h

Receiver: Accelerometer on floor below driver's seat

The contributions to the floor accelerations due to the structure-borne and airborne sound transmission can be seen in Figure 4.11, Figure 4.12, Figure 4.13, Figure 4.14 and Figure 4.15. The speeds plotted for are 40, 80, 120, 160 and 200 km/h.

From the graphs it can be seen that the structure-borne transmission contributes most to the floor accelerations in the low speeds, while for the high speeds the airborne sound is dominant. This might be due to that the floor is well isolated, so that it does not let through much sound from the bogie. This leads to that the biggest contribution to the vibrations in the driver's cabin floor

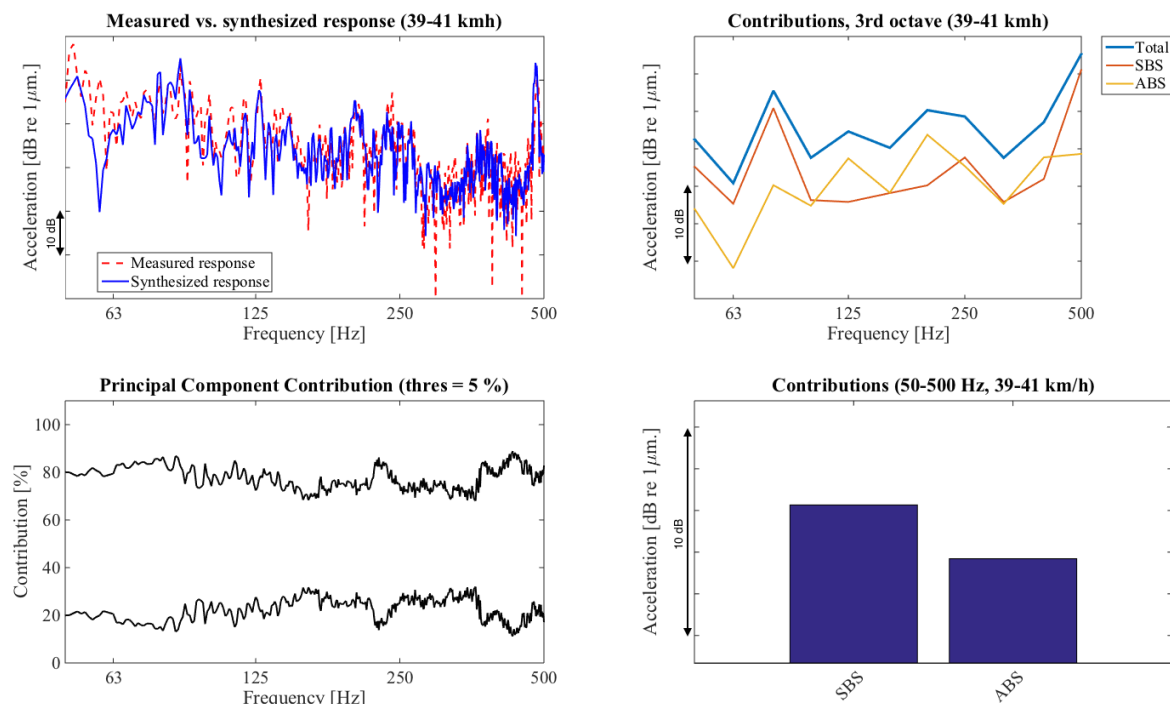


Figure 4.11.: Airborne and structure-borne sound in accelerometer at driver's seat at 40 km/h

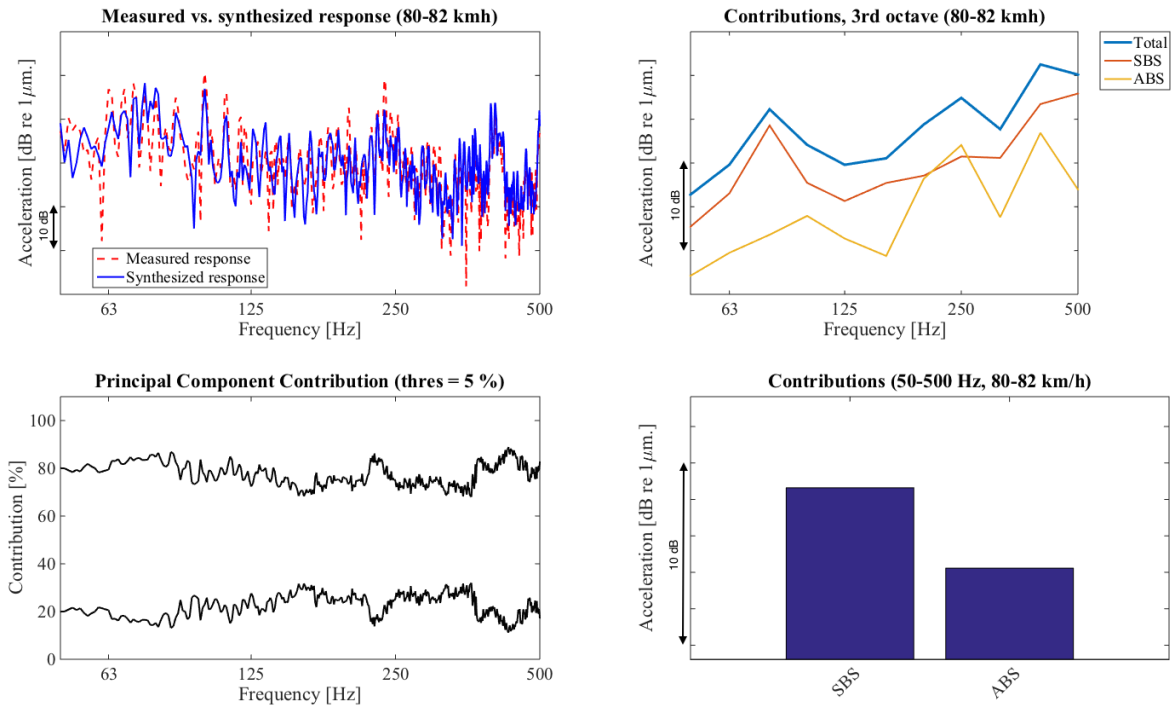


Figure 4.12.: Airborne and structure-borne sound in accelerometer at driver's seat at 80 km/h

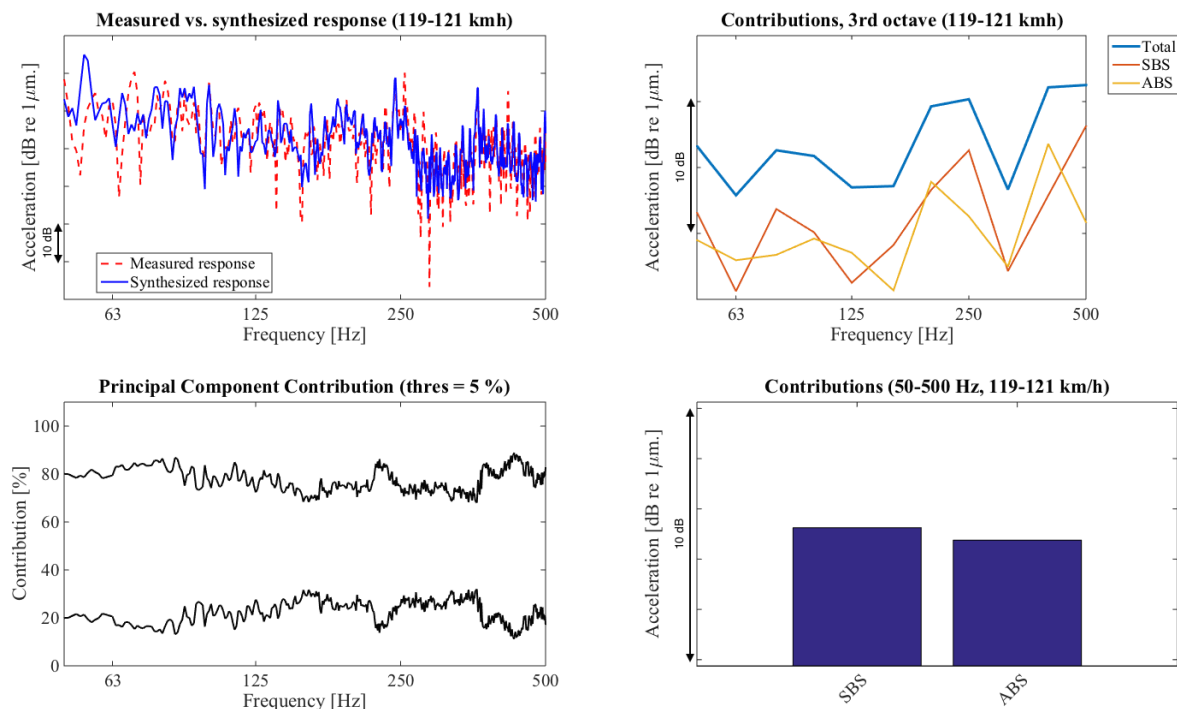


Figure 4.13.: Airborne and structure-borne sound in accelerometer at driver's seat at 120 km/h

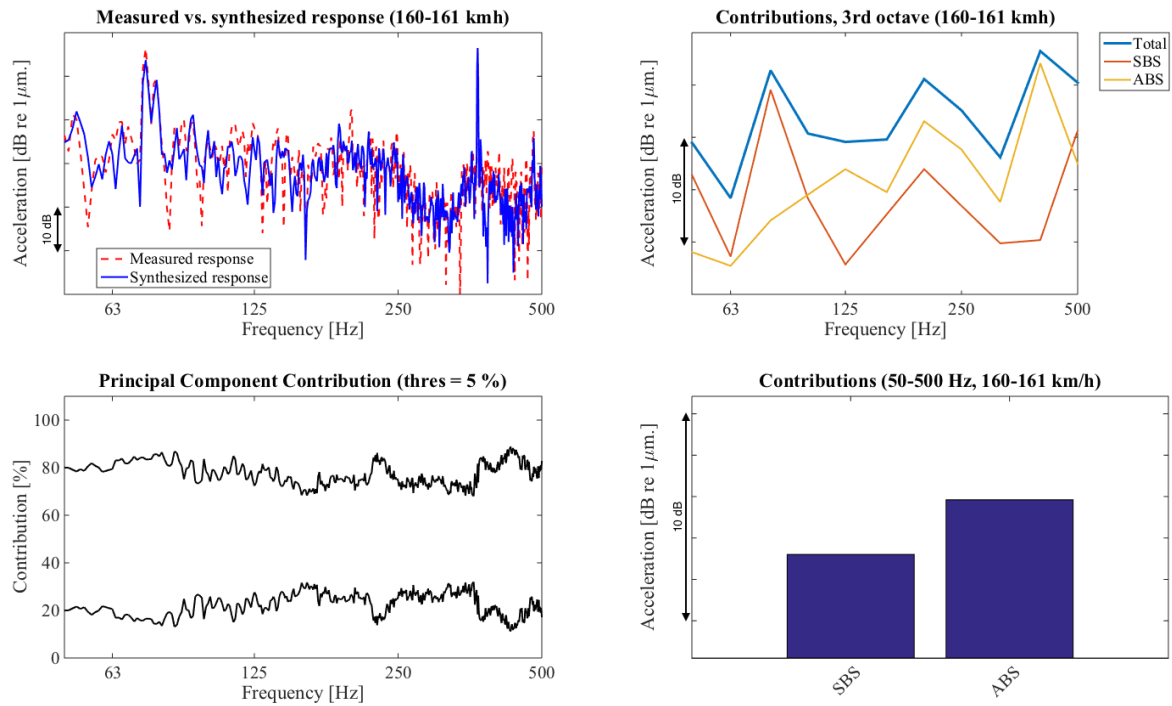


Figure 4.14.: Airborne and structure-borne sound in accelerometer at driver's seat at 160 km/h

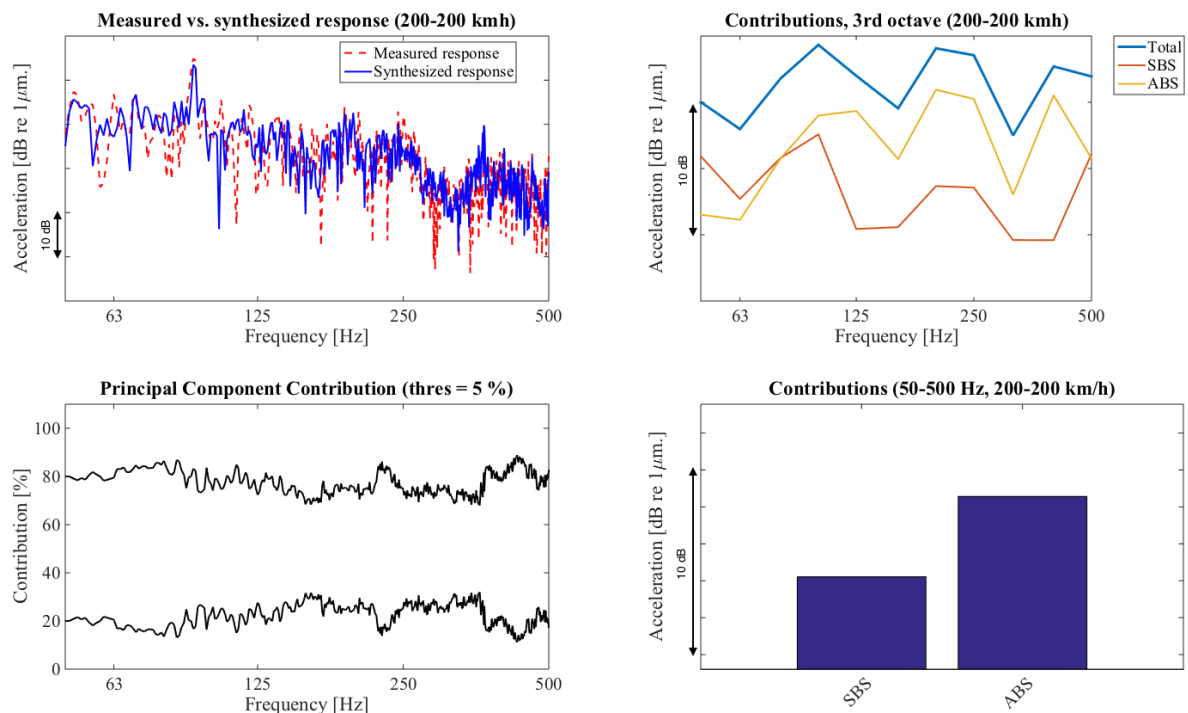


Figure 4.15.: Airborne and structure-borne sound in accelerometer at driver's seat at 200 km/h

4.3.4. Transfer Paths

In this section, the contribution due to all transfer paths in the bogie is investigated.

Receiver: Microphone at driver's ear

The contributions in the microphone at the driver's ear are shown in Figure 4.16, Figure 4.17, Figure 4.18, Figure 4.19 and Figure 4.20 for the speeds 40, 80, 120, 160 and 200 km/h respectively.

From the graphs it can be seen that the airspring is not contributing much to the overall sound pressure throughout the speed range. For low speeds the yaw damper and traction rod seem to be most significant. As the speed increases, the airborne path becomes more and more important and for high speeds are the traction rod and airborne transmission most significant.

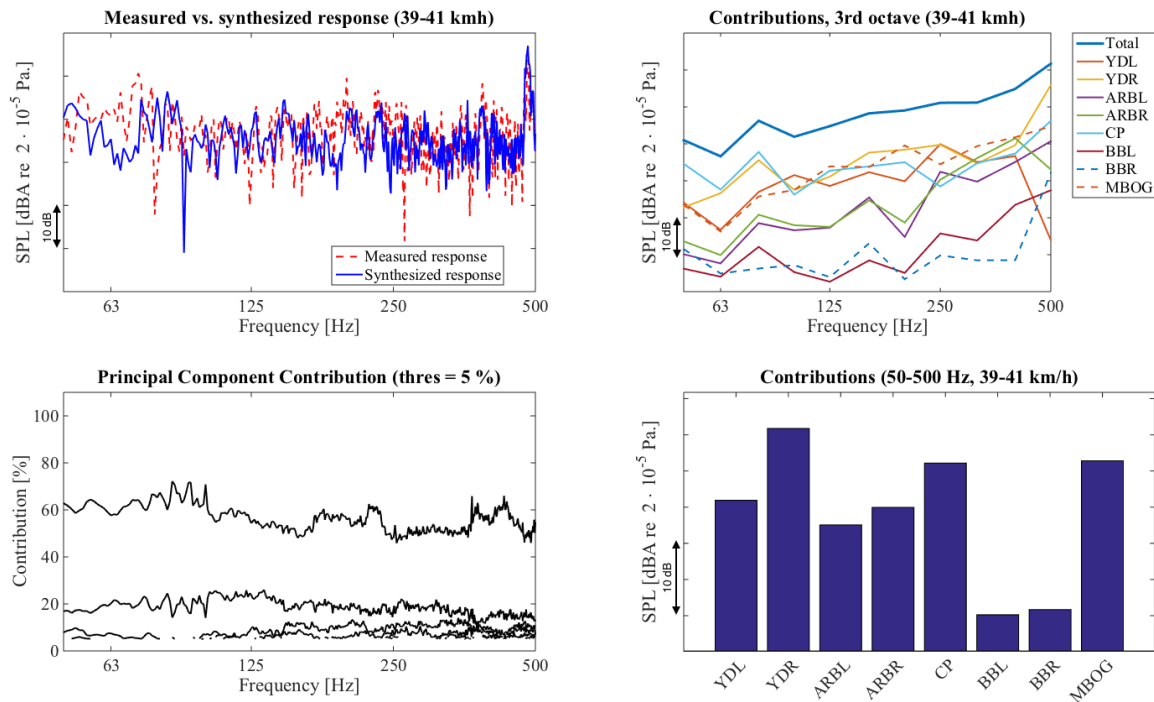


Figure 4.16.: Contribution due to different transfer paths in microphone at driver's ear at 40 km/h

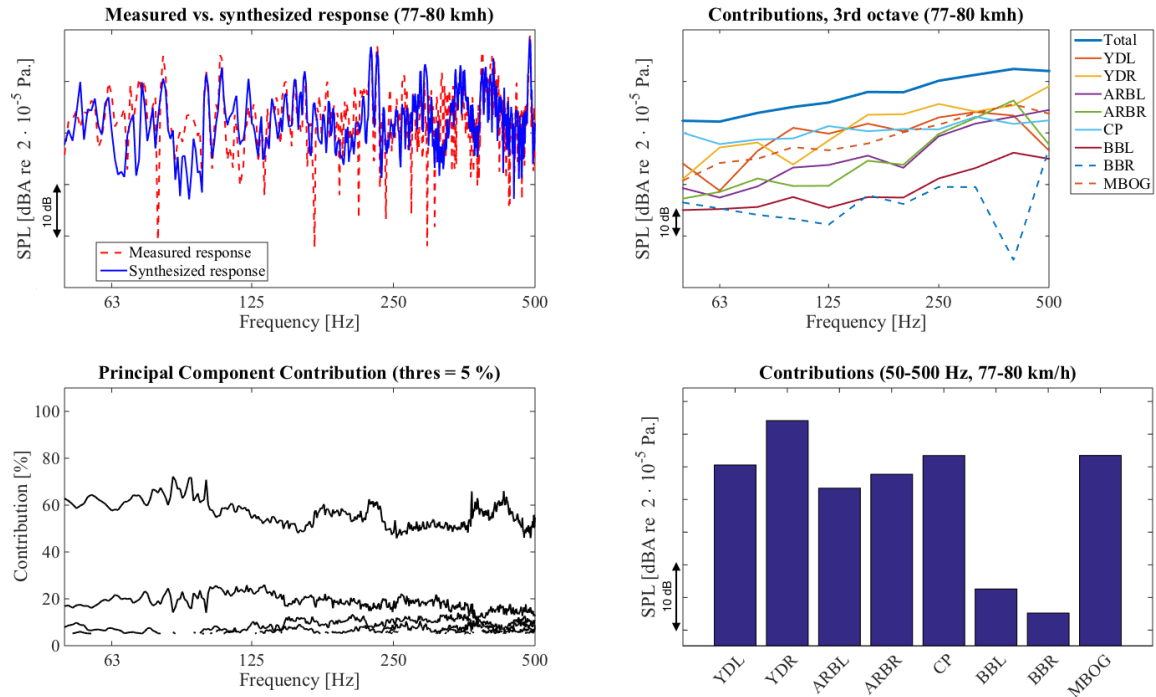


Figure 4.17.: Contribution due to different transfer paths in microphone at driver's ear at 80 km/h

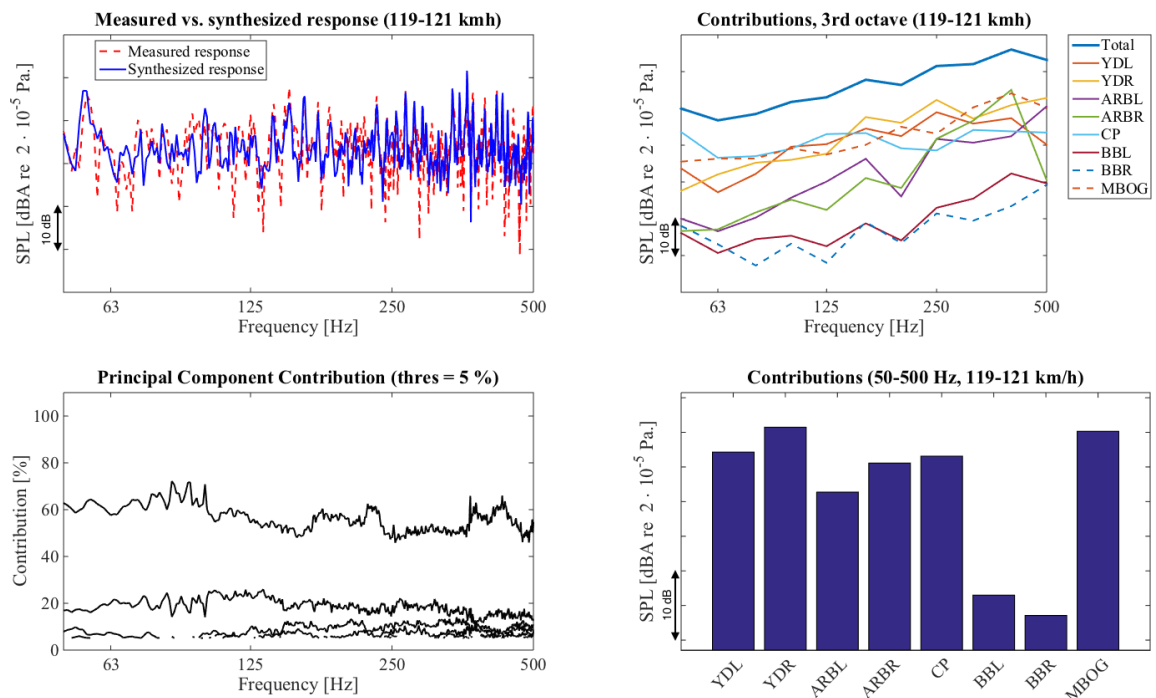


Figure 4.18.: Contribution due to different transfer paths in microphone at driver's ear at 120 km/h

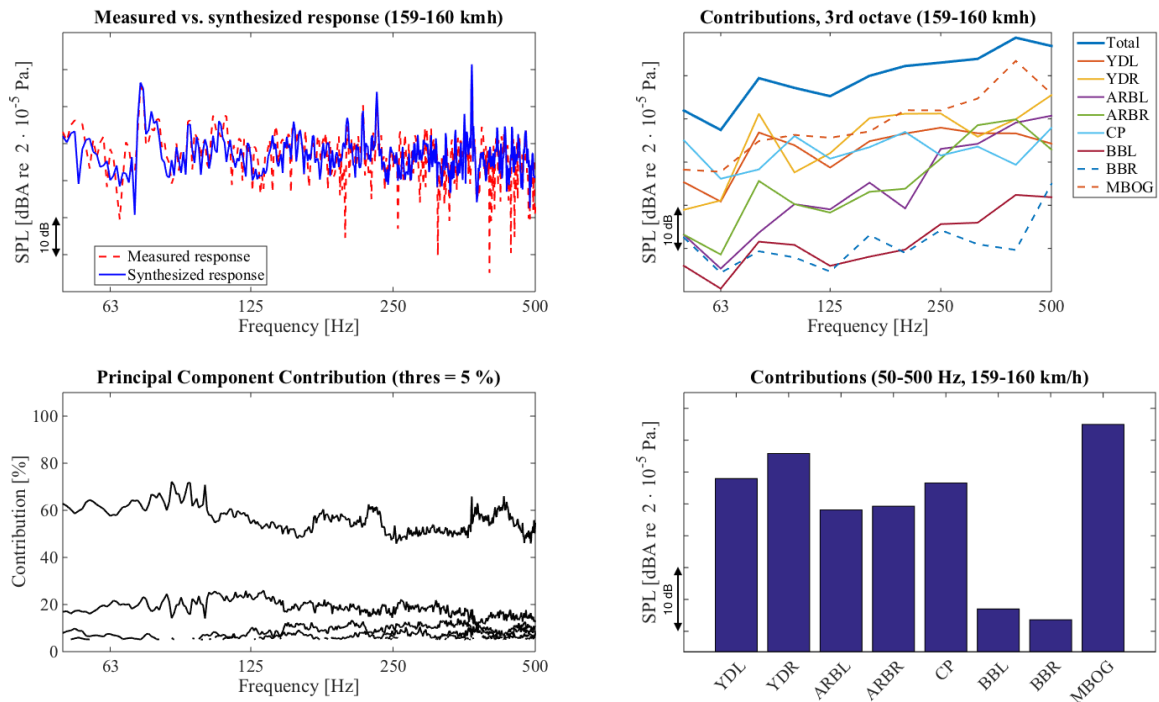


Figure 4.19.: Contribution due to different transfer paths in microphone at driver's ear at 160 km/h

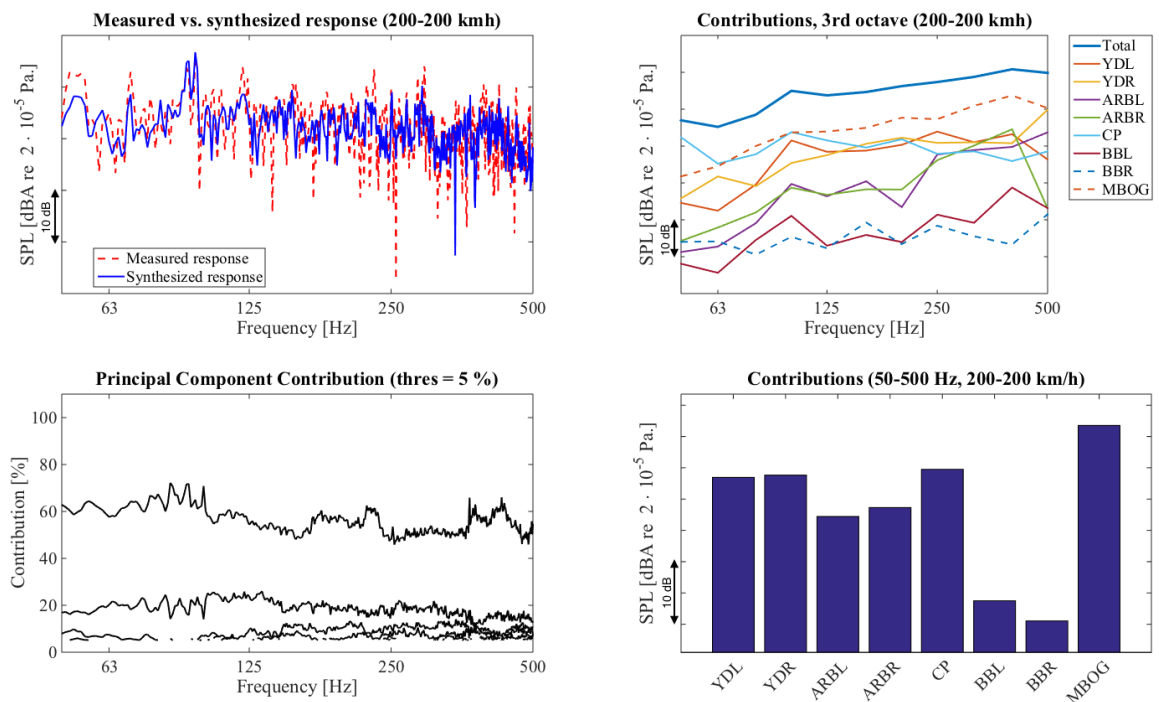


Figure 4.20.: Contribution due to different transfer paths in microphone at driver's ear at 200 km/h

Receiver: Accelerometer on floor below driver's seat

The contributions in the accelerometer on the floor below driver's seat can be seen in Figure 4.21, Figure 4.22, Figure 4.23, Figure 4.24 and Figure 4.25 for the speeds 40, 80, 120, 160 and 200 km/h respectively.

As in the sound pressure, the airspring does not transmit much energy to the floor vibrations. For high speeds it is clear that the airborne transmission is most significant, it is about 10 dB higher than the strongest structure-borne path. Also in low speeds the airborne sound is most important, however not as clear as in high speeds. For the lowest speeds the yaw dampers and the traction rod is almost equally strong as the airborne contribution.

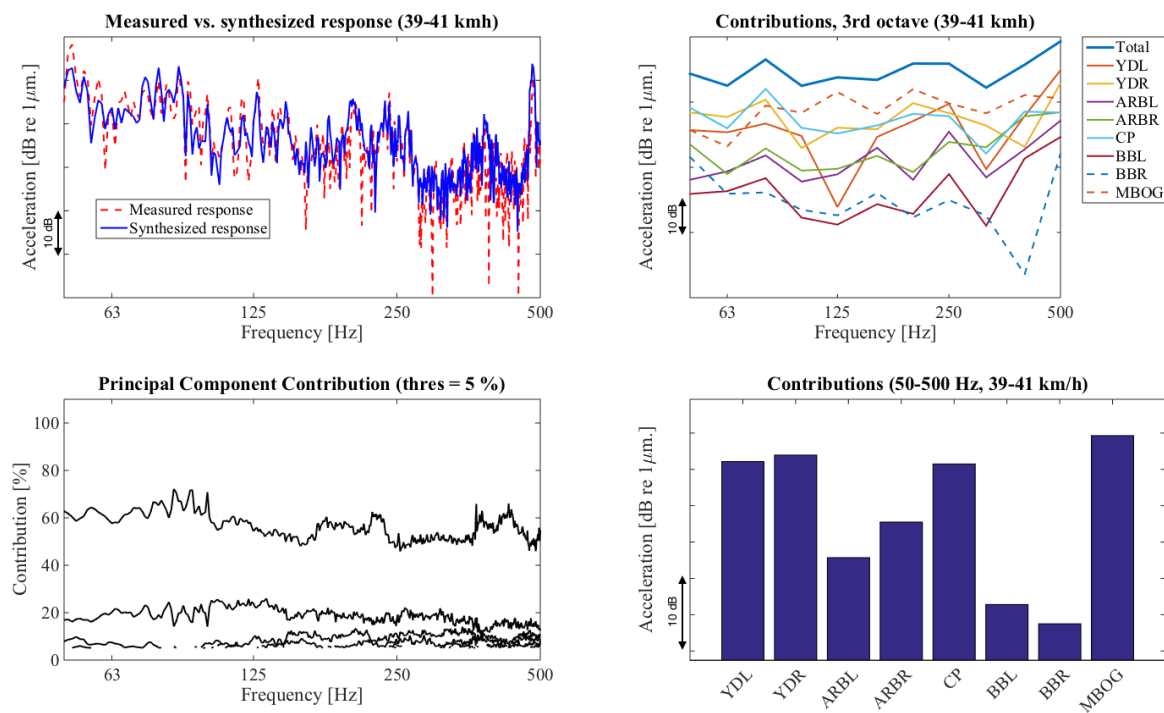


Figure 4.21.: Contribution due to different transfer paths in accelerometer on the floor at the driver's seat at 40 km/h

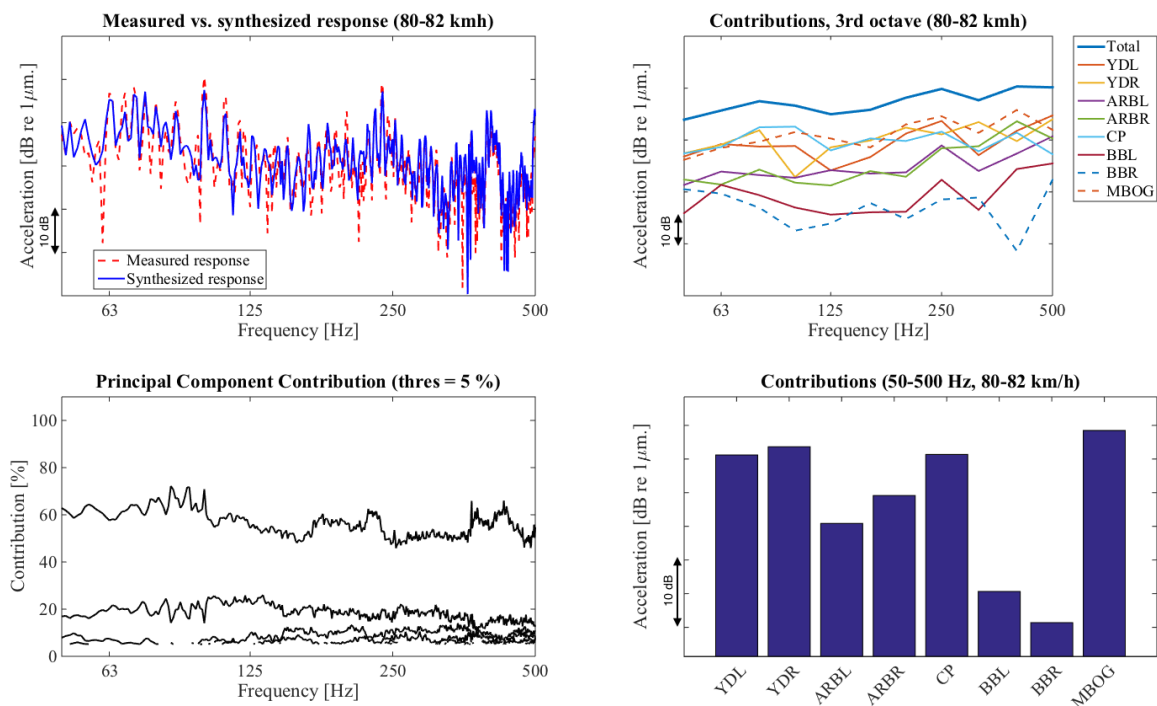


Figure 4.22.: Contribution due to different transfer paths in accelerometer on the floor at the driver's seat at 80 km/h

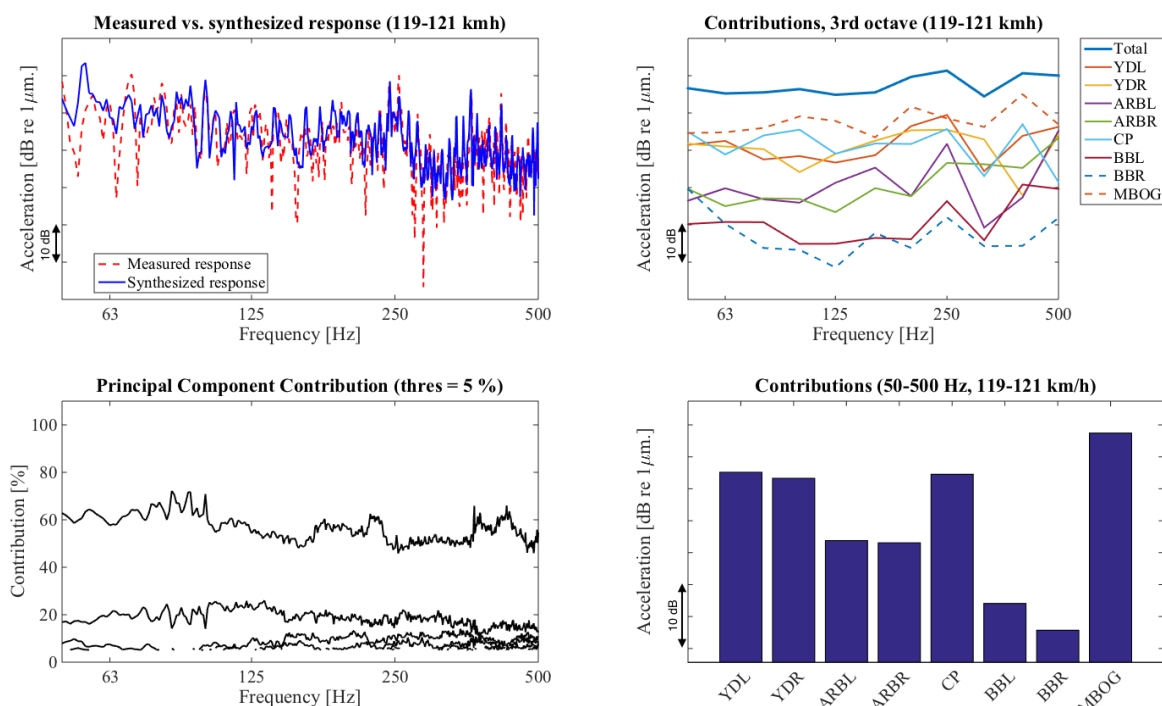


Figure 4.23.: Contribution due to different transfer paths in accelerometer on the floor at the driver's seat at 120 km/h

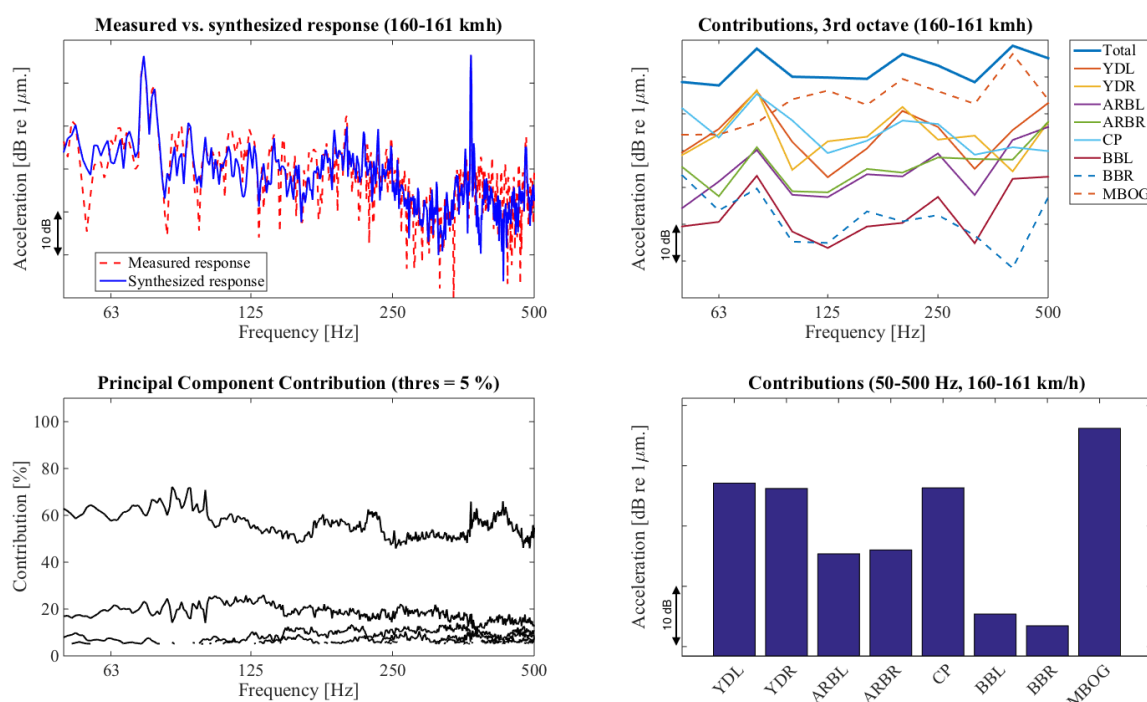


Figure 4.24.: Contribution due to different transfer paths in accelerometer on the floor at the driver's seat at 160 km/h

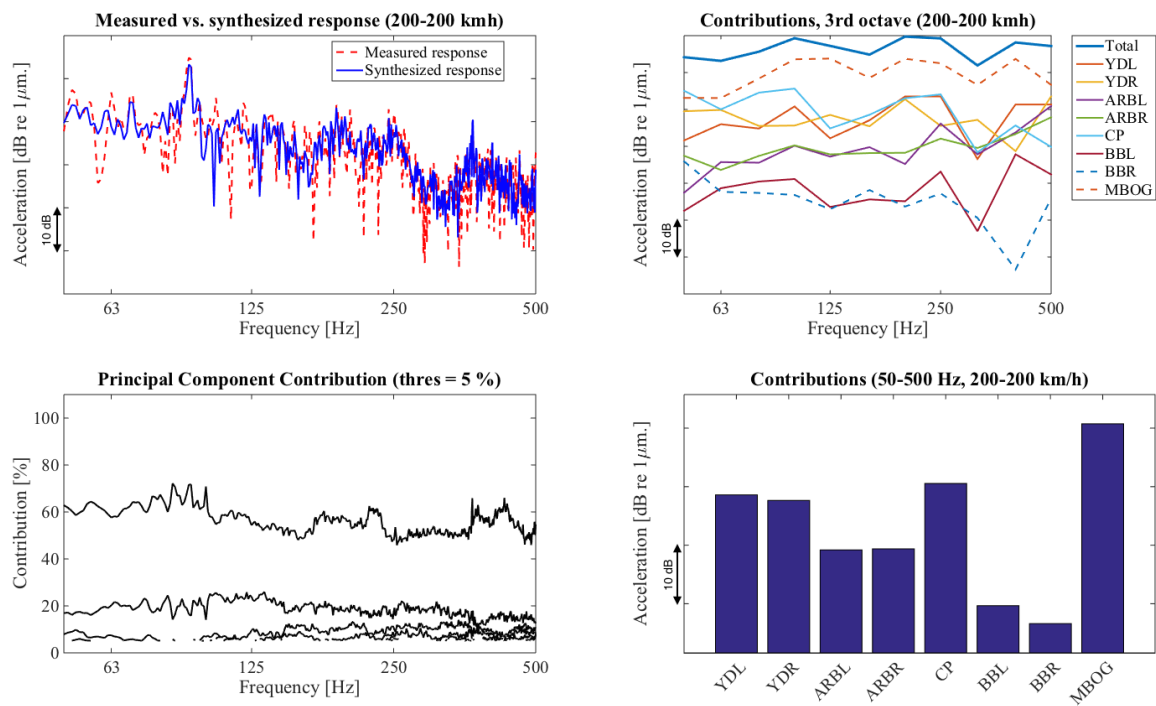


Figure 4.25.: Contribution due to different transfer paths in accelerometer on the floor at the driver's seat at 200 km/h

4.3.5. Traction motor fan

In this section the impact of the traction motor fan is investigated. The OTPA is performed on two speeds, just before the traction motor fan goes in to full speed (130 km/h) and just after (135 km/h).

Both in the receiving sound pressure and floor vibrations most of the energy in the strong peak at 0.3 kHz caused by the traction motor fan is airborne transmitted.

Receiver: Microphone at driver's ear

Figure 4.26 is showing the contribution at 130 km/h, when the traction motor fan is still on low speed and Figure 4.27 is showing the contribution when the fan is on full speed (at 135 km/h).

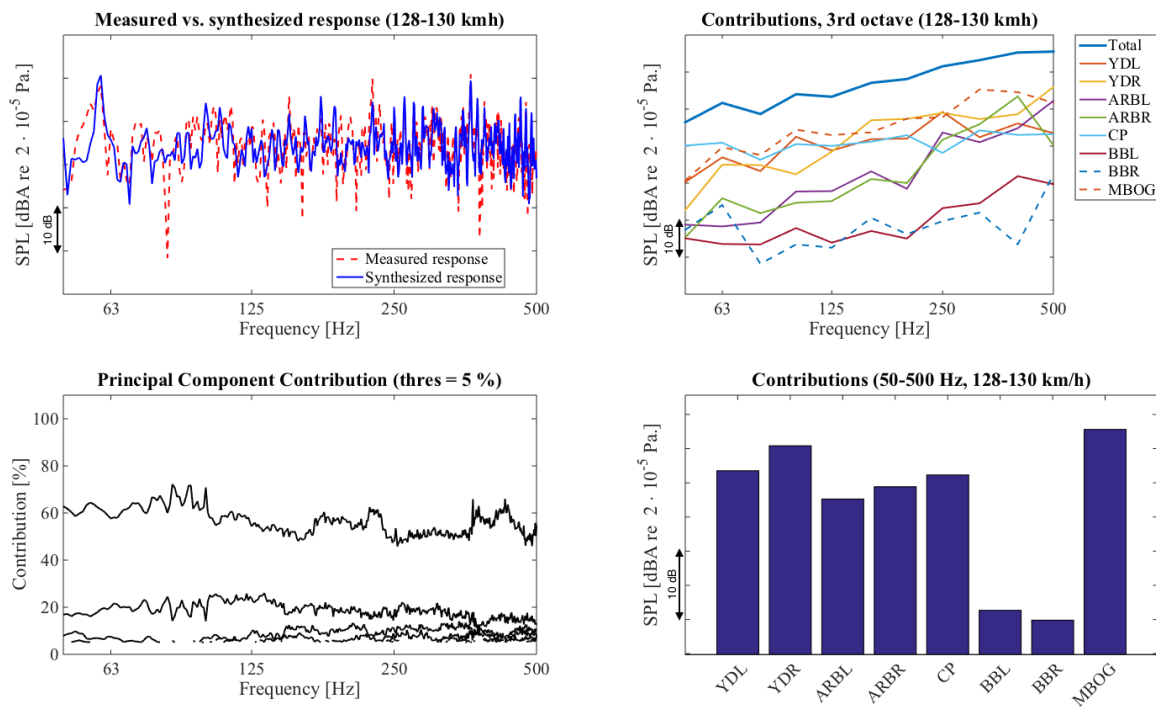


Figure 4.26.: Contribution due to different transfer paths in microphone at the driver's head at 130 km/h, traction motor fan on low speed

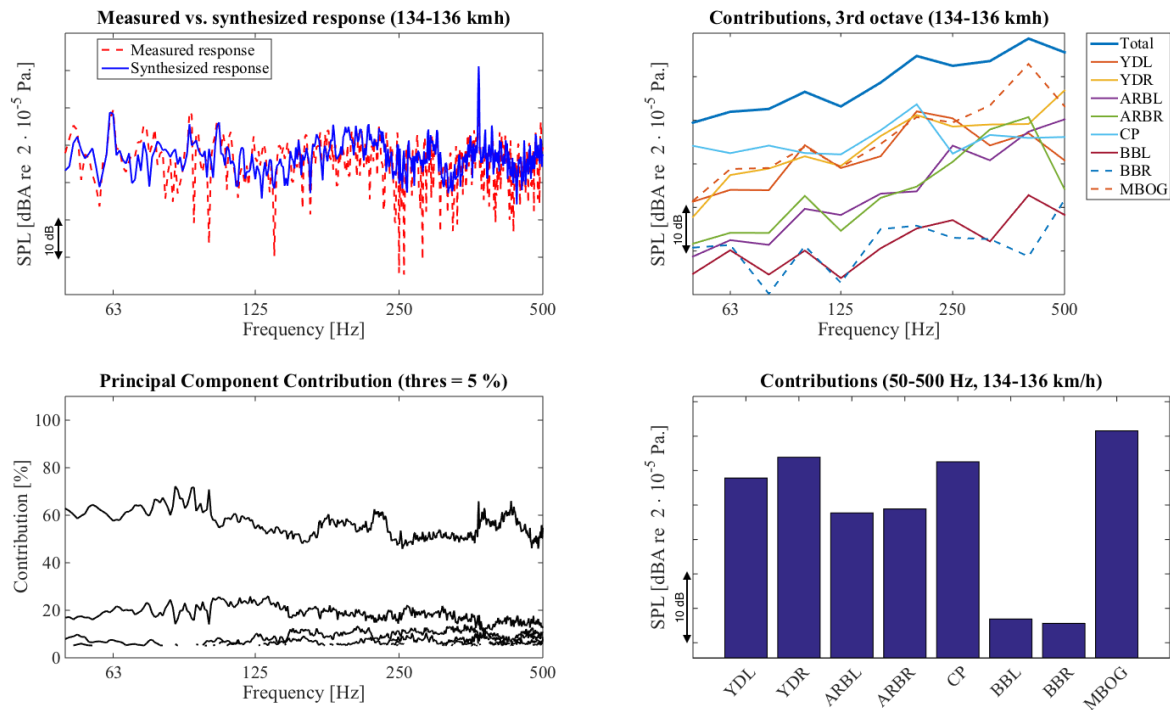


Figure 4.27.: Contribution due to different transfer paths in microphone at the driver's head at 135 km/h, traction motor fan on full speed

Receiver: Accelerometer on floor below driver's seat

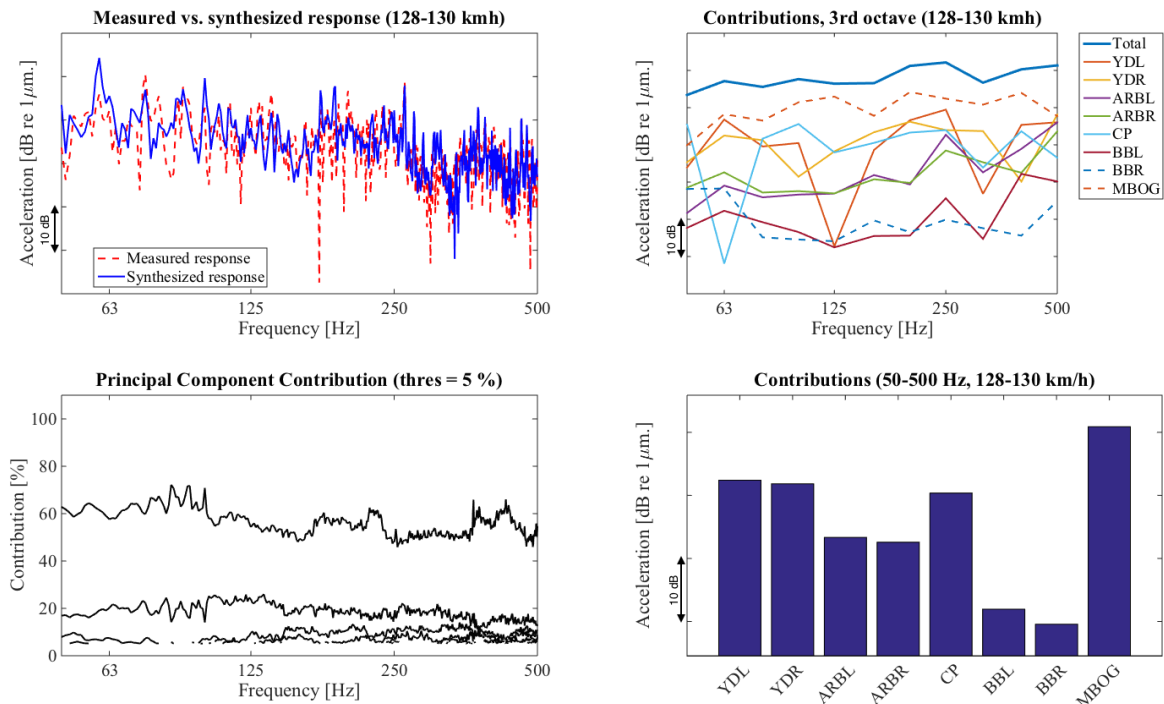


Figure 4.28.: Contribution due to different transfer paths in accelerometer on the floor at the driver's seat at 130 km/h, traction motor fan on low speed

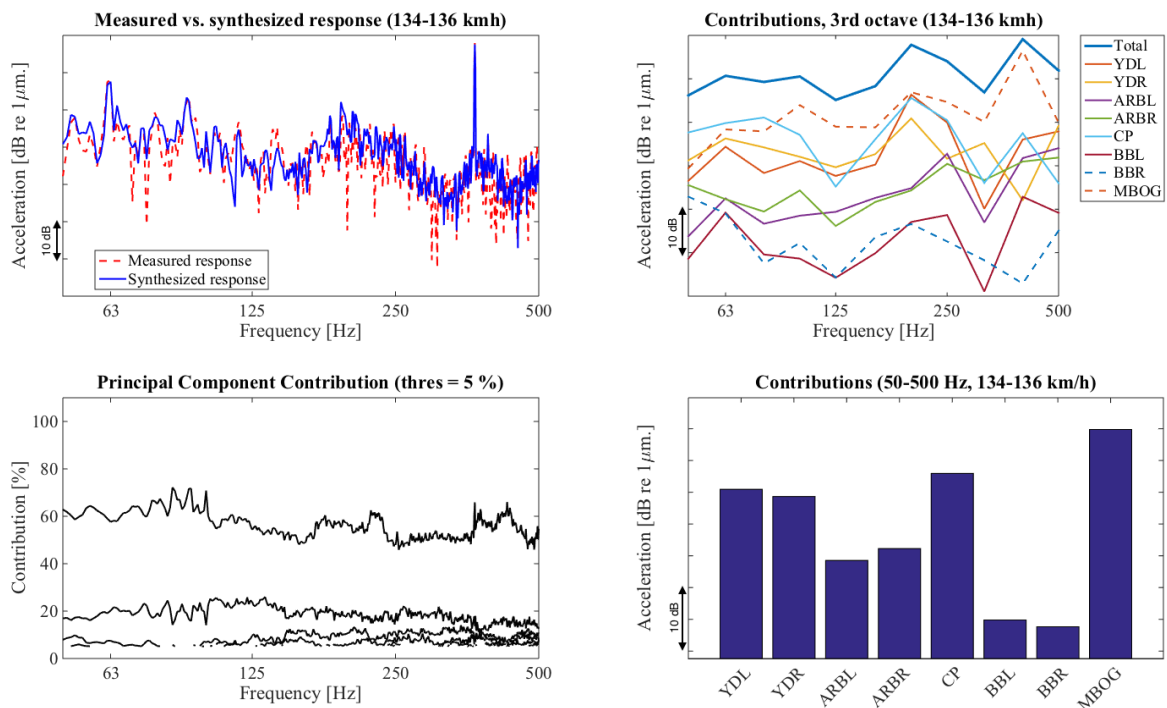


Figure 4.29.: Contribution due to different transfer paths in accelerometer on the floor at the driver's seat at 135 km/h, traction motor fan on full speed

4.3.6. Validity of results

Since OTPA is a method where a lot of errors can occur, the accuracy of the results will in this section discussed.

In the measurements a lot of noise is present in the receiving points (especially the microphone). This should however not affect the results (as showed in section 3.2.3).

On the other hand a couple of other things can have caused errors in the results. Firstly, the right yaw damper was only measured in x-direction, this can affect the results, since the energy in the unmeasured degrees of freedom is spread to the measured transfer paths. This can cause an error, especially in low speeds where the yaw dampers seem to transfer a lot of energy.

One other insecurity is the sound in the bogie. Since only one bogie microphone is used in the measurements errors in the results might be present. This is due to that the sound field might not be consistent throughout the bogie spacing.

5. Conclusions and suggestions for further work

5.1. Summary

Operational Transfer Path Analysis (OTPA) is a good method of diagnosing which paths contribute to most of the sound pressure and/or vibration inside a vehicle. The method is relatively simple and fast, especially compared to the traditional Transfer Path Analysis which often requires more time and money.

Although OTPA is a fast and often cheap way a lot of planning has to be done prior to the measurements. It is for example critical to measure all transmission paths under several operating conditions, otherwise can easily errors occur that might give a wrong interpretation of the system.

The created program seems to work fine, which is validated with a couple of comparisons, for example with the transfer function through the bogie for airborne sound, measured with loudspeakers.

When comparing the structure-borne and airborne sound it is seen that the structure-borne sound is dominating the sound pressure in the driver's cabin in the frequency range analysed. That is also true for the floor vibrations in low speeds, however at 120 km/h the two contributes to equally much of the vibrations and above the airborne sound is dominating. Please note that for higher frequencies the airborne path is likely to dominate.

In the next step, when the transmission paths in the secondary suspension are split into its connections, it is seen that for all speeds the airspring is not contributing to much of neither the sound pressure nor floor vibrations.

When it comes to the sound pressure in the driver's cabin it is visible that the yaw damper and traction rod are most significant, closely followed by the airborne sound. With increasing speed the airborne path becomes more important, and for the highest speeds the traction rod and airborne transmission are contributing most.

For the floor vibrations in the driver's cabin it is seen that the airborne transferred sound is contributing most. In lower speeds airborne transmission, the yaw dampers and the traction rod are almost equally strong.

It is also seen that the strong peak from the traction motor fan in full speed is being airborne

transmitted into the driver's cabin.

5.2. Suggestions for further work

How to correctly scale the in-data prior to the SVD, and a creation of a standard procedure upon how to do it would be interesting to study further.

It would also be interesting to have a deeper look into how the threshold in the PCA should be set to obtain an as good result as possible.

Further, it would be interesting to increase the frequency range of the study and have a look into how this method applies to higher frequencies.

Since OTPA is a method where results can be inaccurate without it being easily seen, it would be of importance to validate the results with actual measurements, for example with dampers disconnected.

Also, for the validation of the OTPA method using FE calculated results in Section 3.2.3, the partial contribution of the space averaged kinetic plate energy could be compared to the power transmitted through the different connector elements. This approach would result in a more representative comparison of physical properties than the present approach.

Finally, if this method is to be further used by Bombardier Transportation, it would be beneficial to turn the script in to a more graphical and user friendly version. Also more features could be added, as for example automatic scaling of the reference measurements prior to the SVD.

Bibliography

- [1] A. K. Cline and I. S. Dhillon. *Handbook of Linear Algebra*, chapter 58. CRC Press, 2nd edition, 2013.
- [2] L. Cremer, M. Heckl, and B.A.T. Petersson. *Structure-Borne-Sound*. Springer-Verlag, Berlin Heidelberg, 2005.
- [3] D. de Klerk and A. Ossipov. Operational transfer path analysis: Theory, guidelines and tire noise application. *Journal of Mechanical Systems and Signal Processing*, 24(7):1950–1962, 2010.
- [4] G. de Sitter, C. Devriendt, P. Guillaume, and E. Pruyt. Operational transfer path analysis. *Journal of Mechanical Systems and Signal Processing*, 27(7):416–431, 2010.
- [5] P. Gajdatsy. *Advanced Transfer Path Analysis Methods*. PhD thesis, Katholieke Universiteit Leuven, 2011.
- [6] L. Han and M. Neumann. *Handbook of Linear Algebra*, chapter 5. CRC Press, 2nd edition, 2013.
- [7] GK. Jalics, R. Arndt, and G. Schleinzer. Application of the TPA Method for Railway Bogies. *Proceedings from IWRN9 Feldafing*, 2007.
- [8] K. Janssens, P. Gajdatsy, and H. Van der Auweraer. Operational Path Analysis: a critical review. *Proceedings from ISMA 2008, Belgium*, 2008.
- [9] I.T. Jolliffe. *Principal Component Analysis*. Springer-Verlag, New York, 2nd edition, 2002.
- [10] S. Kraft. Structure-borne sound in railway vehicles: Transfer path analysis of the secondary suspension. Master’s thesis, Bombardier Transportation, Västerås, 2011.
- [11] A. Pieringer. *Time-domain modelling of high-frequency wheel/rail interaction*. PhD thesis, Department of Applied Acoustics, Chalmers University of Technology, Göteborg, 2011.
- [12] A. Sievi, A. Martner, and S. Lutzenberger. Noise Reduction of Trains Using the Operational Transfer Path Analysis. In *Noise and Vibration Mitigation for Rail Transportation Systems*, pages 453–461. Springer Japan, 2012.
- [13] J. Stoer and R. Arndt. *Introduction to Numerical Analysis*. Springer-Verlag, New York, 3rd

edition, 2002.

- [14] C. Talotte, P.-E. Gautier, D.J. Thompson, and C. Hanson. Identification, modelling and reduction potential of railway noise sources: A critical survey. *Journal of Sound and Vibration*, 267(3):447–468, 2003.
- [15] M. Toome. Operational transfer path analysis: A study of source contribution predictions at low frequency. Master’s thesis, Department of Applied Acoustics, Chalmers University of Technology, 2012.
- [16] W.-X. Yang and P.W. Tse. Development of an advanced noise reduction method for vibration analysis based on singular value decomposition. *NDT&E International*, 36(6):419–432, September 2003.
- [17] N. Zafeiropoulos, A.T. Moorhouse, A. Mackay, and U. Senapati. A comparison of two in-situ transfer path analysis methods. *Proceedings from RASD 2013 Pisa*, 2013.

A. MATLAB Script

A.1. Main script (*analysis.m*)

```
clear all; close all; clc
tic;

set(0,'defaultlinelength',2)
set(0,'defaultAxesFontSize',21)
set(0, 'DefaultAxesFontName', 'Times New Roman')

load X_and_Y_SB+AB.mat

time=toc;
fprintf('Loading time: %f seconds \n', time);
clear time

%%%%%%%%% Input settings %%%%%%%%%%%

block = 1; % Which block to plot for in spectrum, surface

x_limits = [50 500]; % limits of frequency axis in plots

% Turn figures on/off
audio_play='off'; % play signal 'chno' as audio
% stop sound by writing stop(sound) in Command Window

plot_results = 'on'; % Turn plotting 'on/off'
plot_coherence = 'off'; % Plot coherence blockwise
plot_subplots = 'on'; % Main plot w. four subplots 'on/off'
plot_campbell = 'off'; % Plot Campbell diagram 'on/off'
plot_scaling = 'off'; % Plot scaled and unscaled levels prior to OTPA
plot_transfer_functions = 'off'; % Plot transfer functions
sum_directions = 'on'; % Sum all degrees of freedom (x,y,z) for each path
sum_structure_borne = 'off'; % Sum all structure-borne sound
```

```

rec_type = 'airborne'; % Choose 'airborne/structure-borne' receiver
% will plot SPL/displacement in dB

rec=7; % Which receiving point to evaluate (7 and 1)
chno=9; % Which X channel to evaluate coherence of

% PCA Threshold
thres = 5; %Threshold: Minimum PCs % contribution towards PCs score
% (e.g. %5, thres=5)

Y_all = Y;
Y = Y(:,rec);

Y_header_used = Y_header(rec);

% Change names of X_header.RespId and X_header.Title
X_header(1).RespId = 'Yaw damper, left, X';
X_header(2).RespId = 'Yaw damper, left, Y';
X_header(3).RespId = 'Yaw damper, left, Z';
X_header(4).RespId = 'Yaw damper, right, X';
X_header(5).RespId = 'Anti-roll bar, left';
X_header(6).RespId = 'Anti-roll bar, right';
X_header(7).RespId = 'Traction rod, X';
X_header(8).RespId = 'Traction rod, Y';
X_header(9).RespId = 'Traction rod, Z';
X_header(10).RespId = 'Airspring, left';
X_header(11).RespId = 'Airspring, right';
X_header(12).RespId = 'Bogie microphone';

X_header(1).Title = 'YDLx';
X_header(2).Title = 'YDLy';
X_header(3).Title = 'YDLz';
X_header(4).Title = 'YDRx';
X_header(5).Title = 'ARBLz';
X_header(6).Title = 'ARBRz';
X_header(7).Title = 'CPx';
X_header(8).Title = 'CPy';
X_header(9).Title = 'CPz';
X_header(10).Title = 'BBLz';
X_header(11).Title = 'BBRz';
X_header(12).Title = 'MBOG';

%%%%%%%% Sum all DoFs %%%%%%%%%%

```

```

% If sum_directions is 'on' sum YD and CP (over all DoFs) respectively
if strcmp(sum_directions,'on')
    X_YD = sum(X(:,1:3),2);
    X_CP = sum(X(:,7:9),2);

    X_summed = [X_YD X(:,4) X(:,5) X(:,6) X_CP X(:,10) X(:,11) X(:,12)];

    % Cut X_header due to summation
    X_summed_header = [X_header(1) X_header(4:7) X_header(10:12)];
    % Change names of X_header
    X_summed_header(1).RespId = 'Yaw damper, left';
    X_summed_header(2).RespId = 'Yaw damper, right';
    X_summed_header(3).RespId = 'Anti-roll bar, left';
    X_summed_header(4).RespId = 'Anti-roll bar, right';
    X_summed_header(5).RespId = 'Traction rod';
    X_summed_header(6).RespId = 'Airspring, left';
    X_summed_header(7).RespId = 'Airspring, right';
    X_summed_header(8).RespId = 'Bogie microphone';

    X = X_summed;
    X_header = X_summed_header;

    X_header(1).Title = 'YDL';
    X_header(2).Title = 'YDR';
    X_header(3).Title = 'ARBL';
    X_header(4).Title = 'ARBR';
    X_header(5).Title = 'CP';
    X_header(6).Title = 'BBL';
    X_header(7).Title = 'BBR';
    X_header(8).Title = 'MBOG';
end

if strcmp(sum_structure_borne,'on')

    % sum structure-borne sound
    X_SB = sum(X(:,1:end-1),2);
    % Put SB sound and AB sound in a matrix
    X_summed = [X_SB X(:,end)];

    X = X_summed;

    X_summed_header = [X_header(1) X_header(end)];

```



```

X_summed_header(1).RespId = 'Structure-borne sound';
X_summed_header(2).RespId = 'Airborne sound';
X_header = X_summed_header;

X_header(1).Title = 'SBS';
X_header(2).Title = 'ABS';

end

%%%%%%%%%% Create blocks %%%%%%%%%%%%%%

block_length=1; % length of each block [s]
nref=size(X,2); % number of references
dt=X_header.xIncrement; % time step
fs=1/dt; % sampling frequency

samples=block_length*fs; % number of samples in each block

nb = floor(size(X,1)/samples); % number of blocks

sig_length = nb*samples; % number of samples in entire signal

X_cut=X(1:sig_length,:); % cut X to have even number of blocks
Y_cut=Y(1:sig_length,:); % cut Y to have even number of blocks

% cut speed vector
speed_cut=speed(1:sig_length);

% create time vector
t_cut=((0:length(speed_cut)-1)*dt)'; % time vector

tic;
% Cut signal to blocks with reshape function
for ii=1:size(X_cut,2)
    % reshape X
    X_blocks(ii,:,:)= reshape(X_cut(:,ii),samples,nb)';
    % X_SVD_blocks(ii,:,:)= reshape(X_SVD_cut(:,ii),samples,nb)';
end
% reshape Y
Y_blocks=reshape(Y_cut,samples,nb)';
% reshape speed

```

```

speed_blocks=reshape(speed_cut,samples,nb)';
% reshape time
t_blocks=reshape(t_cut,samples,nb)';

time=toc;
fprintf('Reshape time: %f seconds \n', time);
clear time

tic;
% apply hanning window on X_blocks and Y_blocks
hw=hann(samples)';
% hw scaling due to the lost energy in the windowing
hw_scale=sqrt(sum(hw.^2)/length(hw));

% Apply Hanning window
for ii=1:nb
    Y_hw(ii,:) = Y_blocks(ii,:).*hw/hw_scale;
    for jj=1:nref
        % Original X
        X_temp(:,1)=X_blocks(jj,ii,:);
        X_hw(jj,ii,:) = X_temp.*hw'/hw_scale;
        clear X_temp
    end
end
time=toc;
fprintf('Windowing time: %f seconds \n', time);
clear time

% Dimensions after reshape
% Y = (blocks,frequencies)
% X = (points,blocks,frequencies)

%%%%%%%% Create variables %%%%%%%%%

Nf=size(X_blocks,3); % number of frequency components

df=fs/Nf; % frequency step
f=(0:Nf-1)*df; % frequency vector

%%%%%%%% FFT %%%%%%%%%

tic;
X_freq=fft(X_hw,Nf,3)/Nf; % fft

```

```

Y_freq=fft(Y_hw,Nf,2)/Nf;
time=toc;
fprintf('FFT time: %f seconds \n', time);
clear time

%%%%%%%%% Scaling %%%%%%%%%%%%%%

X_freq_unscaled = X_freq;

% Create scale vector to scale (divide) X with
scale_vector = [1 1 1 1 1 1 1 1 1 1 1 10];

% If sum_directions is 'on' create other (shorter) manual scale vector
if strcmp(sum_directions,'on')
    scale_vector = [1 1 1 1 1 1 1 10];
end

if strcmp(sum_structure_borne,'on')
    scale_vector = [1 7];
end

% Create scale matrix
scale_ref = diag(scale_vector);

% Loop over all blocks and scale each block individually
for ii = 1:size(X_freq,2)
    % Scale Reference measurement (X)
    temp(:, :) = X_freq(:, ii, :);
    temp_scaled(:, :) = inv(scale_ref)*temp;
    X_freq_scaled(:, ii, :)=temp_scaled;
    clear temp temp_scaled
end

if strcmp(plot_scaling,'on')
    % Plot scaled and unscaled signals
    X_plot_scaled(:, :) = X_freq_scaled(:, block, :);
    X_plot_unscaled(:, :) = X_freq(:, block, :);

    X_plot_scaled=X_plot_scaled';
    X_plot_unscaled=X_plot_unscaled';
end

```

```

figure
semilogx(20*log10(abs(X_plot_scaled(:,1:end-1)))), 'b')
hold on
semilogx(20*log10(abs(X_plot_scaled(:,end)))), 'r')
title('Scaled. Blue is SB, red is AB.')
xlim(x_limits)
set(gca,'XTick',[16 31.5 63 125 250 500 1000])

figure
semilogx(20*log10(abs(X_plot_unscaled(:,1:end-1)))), 'b')
hold on
semilogx(20*log10(abs(X_plot_unscaled(:,end)))), 'r')
title('Unscaled. Blue is SB, red is AB.')
xlim(x_limits)
set(gca,'XTick',[16 31.5 63 125 250 500 1000])
clear X_plot_scaled X_plot_unscaled
end

X_freq_scaled = abs(X_freq_scaled);
Y_freq = abs(Y_freq);
X_freq_unscaled = abs(X_freq_unscaled);

% Call OTPA function, performs SVD and PCA, also calculates the
% synthesized response at the receiver
[Ys,Ys_tot,COEFF,PC,CONT,Cont,H]=otpa_function_w_scaling(f,...
    X_freq_scaled,Y_freq,thres,nb,scale_ref,X_freq_unscaled);

% Calculate 3rd octave band levels
for ii=1:nref
    for jj=1:nb
        [f_3rd,Ys_3rd(ii,jj,:)] = thirdlevels(f,Ys(ii,jj,:));
    end
end

%%%%%% Plotting %%%%%%%%%%

if strcmp(plot_results,'on')
    DlgH = figure('name','Break');
    set(DlgH,'OuterPosition',[1000 500 50 100])
    handle_campbell = uicontrol('Style','PushButton', ...
        'String','Break', ...
        'Callback','delete(gcf)');
    while (ishandle(handle_campbell))

```

```

% Create Campbell plot to choose speed in
[clicked_block]=campbell_plot(Ys_tot,f,x_limits,speed_blocks,...
    Y_header_used,rec_type);

tic;
% otpa_plot.m function
otpa_plot(Ys,Ys_3rd,Y_freq,Ys_tot,f,f_3rd,clicked_block,nref,Cont,...
    thres,x_limits,speed_blocks,X_header,plot_campbell,...
    plot_subplots,Y_header_used,rec_type,plot_transfer_functions,H,X_freq);

time=toc;
fprintf('Plotting time: %f seconds \n', time);
clear time
pause
end
end

fprintf('End\n');

```

A.2. OTPA-function (*otpa_function.m*)

```

function [ Ys,Ys_tot,COEFF, PC, CONT, Cont, H_s] = otpa_function_w_scaling(...
    f,X,Y,thres,Nb,scale_ref,X_unscaled)
% OTPA_FUNCTION - Operational Transfer Path Analysis
% Performs SVD, PCA, descaes H and calculates the synthesized response at the
% receiver.

N = length(f); % Find number of frequency components
tic;
for ii=1:N % Loop through all N frequency components

    % Singular Value Decomposition (SVD) ('S' is matrix of PCs)
    % Use "econ" to ensure S is a square Matrix
    [U,S,V] = svd(X(:, :, ii), 'econ');

    % Principal Component Analysis (PCA)
    % COEFF - The coefficients corresponding to the PCs
    % PC - The Principal Components (i.e. the Singular Values)
    % CONT - The contribution to the overall signal (%)

```

```

PC = diag(S);
COEFF = U*S;
CONT = diag(S)/sum(diag(S))*100;

% Find PCs that correspond to PCA method input
numPC = find(CONT>thres,1,'last');

% Calculate "invSr" - The noise reduced inverse of S.
invSr = zeros(size(S)); % Allocate zeros for size of the invSr matrix
S1 = diag(diag(inv(S(1:numPC,1:numPC))));
invSr(1:numPC, 1:numPC) = S1(1:numPC, 1:numPC);

% Save PC values for plot
Cont(:,ii) = NaN*CONT;
Cont(1:numPC,ii) = CONT(1:numPC);

% Calculate noise reduced inverse of X
X_inv(:, :, ii) = V*invSr*U'; % Noise reduced inverse of X

% Transfer function estimate
H(:,ii) = X_inv(:, :, ii)'*Y(:,ii);

end

time=toc;
fprintf('SVD and PCA time: %f seconds \n', time);
clear time

% Descale H
H_s = H'*inv(scale_ref);

% Transpose H_s
H_s = H_s';

% Calculate Synthesized Response at the receiver
tic;

for ii=1:Nb % Loop over all blocks
    for jj=1:N % Loop over all frequencies

        % Calculate the synthesized 'Ys' by Y=HX for all reference points
        % in a loop over all frequencies and blocks

```

```

        Ys(:,ii,jj) = X_unscaled(:,ii,jj).*H_s(:,jj);

        % Sum the total synthesized response
        Ys_tot(ii,jj) = sum(Ys(:,ii,jj));

    end
end

time=toc;
fprintf('Synthesized response time: %f seconds \n', time);
clear time

end

```

A.3. Plot-function (*otpa_plot.m*)

```

function [ ] = otpa_plot(Ys,Ys_3rd,Y,Ys_tot,f,f_3rd,block,Nref,Cont,...
    thres,x_limits,speed_blocks,X_header,plot_campbell,plot_subplots,...
    Y_header_used,rec_type,plot_transfer_functions,H,X)

% OTPA_PLOT Plotting of OTPA results
% Plot OTPA results:
% - Main figure with four subplots containing:
%     1. Measured vs. synthesized response
%     2. Contribution of each path in 3rd octave bands
%     3. Principal Component contribution in %
%     4. Bar plot of contribution in the chosen frequency range
% - Campbell diagram of:
%     1. Synthesized response of chosen receiver
%     2. Measured response of chosen receiver
%     3. Measured response of chosen reference
% - Transfer function from chosen reference to receivers

% Put synthesized responses for chosen block in a matrix for plotting
Ys_plot_3rd(:, :) = Ys_3rd(:, block, :);

% Structure-borne reference and label if structure-borne receiver
if strcmp(rec_type, 'structure-borne')
    ref=10^(-6); % acceleration reference value

```

```

        y_label = ('Acceleration [dB re 1\mum.]');
end

% Airborne reference and label if airborne receiver
if strcmp(rec_type,'airborne')
    ref=2e-5; % pressure reference value
    y_label = ('Sound Pressure Level [dB re 2 \cdot 10^{-5} Pa.]');
end

% Calculate speed range of chosen block
speed_plotted=[min(speed_blocks(block,:)) max(speed_blocks(block,:))];

% Create label with all path names
x_tick_bar = {X_header.Title};
% Add 'Synthesized total' to created label
xtick_plus_total=cat(2,'Total ',x_tick_bar);
% Find index of first and last frequency to set range of plotting
f_limit_indices=[find(x_limits(1)<f, 1 ) find(f<x_limits(2), 1, 'last' )];

%% Plot figure with four subplots %%

if strcmp(plot_subplots,'on')

%% Create main figure for subplots %%

    str_title = sprintf('Rec: %s, %.f-%.f km/h',Y_header_used.RespId,...
        speed_plotted(1),speed_plotted(2));

    FigHandle=figure('name',str_title);

    % Maximize figure
    %     pause(0.001);
    %     frame_h = get(handle(gcf),'JavaFrame');
    %     set(frame_h,'Maximized',1);

    set(FigHandle, 'Position', [-10, -10, 1680, 1050]);
%% Plot synthesized vs measured response, subplot 1 %%

    % Create string for title and name of saved figure
    str_title=sprintf('Measured vs. synthesized response (%.f-%.f kmh)'...
        ,speed_plotted(1),speed_plotted(2));

```



```

% Plot measured vs synthesized response
subplot(2,2,1)
semilogx(f,20*log10(abs(Y(block,:)/ref)), 'r') % Measured response
hold on;
semilogx(f,20*log10(abs(Ys_tot(block,:)/ref))) % Synthesized response
legend('Measured response','Synthesized response','Location','Best')
xlim(x_limits)
set(gca,'XTick',[16 31.5 63 125 250 500 1000])
title(str_title)
ylabel(y_label)
xlabel('Frequency [Hz]')

clear str_title
%% Plot contributions due to each path, subplot 2 %%
% Sum synthesized 3rd octave responses over all paths

Ys_3rd_total=sum(Ys_plot_3rd);

% Plot all different contributions compared to total response
plot_3rd = zeros(Nref,size(f_3rd,2));
for ii=1:Nref
    % Create matrix of all 3rd octave bands to plot
    plot_3rd(ii,:)=20*log10(abs(Ys_plot_3rd(ii,:)/ref));
end

% Create string for title and name of saved figure
str_title=sprintf('Contributions, 3rd octave (%.f-%.f kmh)'\dots
    ,speed_plotted(1),speed_plotted(2));

% Plot synthesized total and all paths in 3rd octave bands
subplot(2,2,2)
h2=semilogx(f_3rd,20*log10(abs(Ys_3rd_total/ref)),f_3rd,plot_3rd);
ylabel(y_label)
xlabel('Frequency [Hz]')
title(str_title)
legend(xtick_plus_total,'Location','NorthEastOutside')
xlim(x_limits)
set(gca,'XTick',[16 31.5 63 125 250 500 1000])
set(h2(1),'LineWidth',2) % Double linewidth for synthesized total

% If more paths than 7 change linestyle for paths > 7
if length(h2) > 7
    set(h2(8:end),'LineStyle','--')

```

```

end

clear str_title
hold off

%% Plot contribution of each principal component, subplot 3

subplot(2,2,3)
% Loop over all PCs and plot contribution
for ii=1:size(Cont,1)
    semilogx(f,Cont(ii,:), 'k')
    hold on;
end
title(['Principal Component Contribution (thres = ',num2str(thres),' %)']);
ylabel('Contribution [%]');
xlabel('Frequency [Hz]')
xlim(x_limits)
ylim([0 110])

set(gca,'XTick',[16 31.5 63 125 250 500 1000])
%% Plot bar graph, total response within the frequency limits, subplot 4 %%

% Sum synthesized responses over frequencies between limits
Ys_limits(:, :) = Ys(:, block, f_limit_indices(1):f_limit_indices(2));
Ys_sum = sum(Ys_limits, 2);

% Create string for title and name of saved figure
str_title=sprintf('Contributions (%d-%d Hz, %.f-%.f km/h)',...
    x_limits(1),x_limits(2),speed_plotted(1),speed_plotted(2));
%     str_figure

subplot(2,2,4)
% Plot bar graph
bar(20*log10(abs(Ys_sum/ref)))
ylabel(y_label)
ylim([ min(20*log10(abs(Ys_sum/ref)))-5 ...
    max(20*log10(abs(Ys_sum/ref)))+5 ])
title(str_title)
set(gca,'XTickMode','manual')
set(gca,'XTick',1:size(X,1))
set(gca,'XTickLabel',x_tick_bar)
%     set(gca,'XTickLabelRotation',45)
rotateXLabels( gca, 45 ) % Rotate XTickLabels 45° for prior matlab

```

```

%     versions
set(gca,'XLim',[0 length(x_tick_bar)+1])

hold off

clear str str_title;

spd=round(mean(speed_plotted));
set(gcf,'PaperPosition',[0 0 40 25])
name=sprintf('%dkmh_%s',spd,Y_header_used.Label);
%     name=cat(2,spd,'kmh_',Y_header_used.Label);
eval(['print -depsc2 Plots/',name])
%     saveSameSize(gcf, 'format', '-depsc2', 'file', 'test.eps')

end

%% %% Plot Campbell diagrams %% %%

if strcmp(plot_campbell,'on')
    % Cut f to plotted range
    f_plot_range=f(f_limit_indices(1):f_limit_indices(2));
    % Cut total synthesized response to plotted freq. range
    Ys_tot_plot_range=Ys_tot(:,f_limit_indices(1):f_limit_indices(2));
    % Calculate average speed for each block
    speed_average=mean(speed_blocks,2);

    %% Campbell diagram bogie mic
    X_freq_plot_range(:,:)=X(8,:,f_limit_indices(1):f_limit_indices(2));
    % Create string for title and name of saved figure
    str=sprintf('Campbell diagram, measured, reference: %s', X_header(8).RespId);
    figure('name',str);
    % Maximize figure
    pause(0.001);
    frame_h = get(handle(gcf),'JavaFrame');
    set(frame_h,'Maximized',1);
    % Create surface plot of measured response
    surface(f_plot_range,speed_average,20*log10(abs(X_freq_plot_range/ref)))
    shading('interp');
    colormap jet
    xlabel('Frequency [Hz]')
    ylabel('Speed [km/h]')
    axis tight;

```

```

set(gca,'YDir','normal');
set(gca,'XMinorTick','on');
set(gca,'YMinorTick','on');
set(gca,'Layer','top');
set(gca,'Box','on');
ylim([min(speed_average) max(speed_average)])
xlim(x_limits)
caxis([min(20*log10(abs(X_freq_plot_range(:)/ref)))...
      max(20*log10(abs(X_freq_plot_range(:)/ref)))])
cbar=colorbar('EastOutside');
ylabel(cbar,y_label)
clear str

figure('name','Campbell')

% Maximize figure
pause(0.001);
frame_h = get(handle(gcf),'JavaFrame');
set(frame_h,'Maximized',1);

% % OTPA campbell diagram
% Create string for title and name of saved figure
str=sprintf('Campbell diagram, OTPA, receiver: %s',Y_header_used.RespId);

subplot(1,2,1)
% Create surface plot of synthesized response
surface(f_plot_range,speed_average,20*log10(abs(Ys_tot_plot_range/ref)))
shading('interp');
colormap jet
xlabel('Frequency [Hz]')
ylabel('Speed [km/h]')
axis tight;
set(gca,'YDir','normal');
set(gca,'XMinorTick','on');
set(gca,'YMinorTick','on');
set(gca,'Layer','top');
set(gca,'Box','on');
ylim([min(speed_average) max(speed_average)])
xlim(x_limits)
caxis([min(20*log10(abs(Ys_tot_plot_range(:)/ref)))...
      max(20*log10(abs(Ys_tot_plot_range(:)/ref)))])
title(str)
cbar=colorbar('EastOutside');

```

```

ylabel(cbar,y_label)

clear str

% % Measured campbell diagram
Y_freq_plot_range=Y(:,f_limit_indices(1):f_limit_indices(2));
% Create string for title and name of saved figure
str=sprintf('Campbell diagram, measured, receiver: %s',Y_header_used.RespId);
subplot(1,2,2)
% Create surface plot of measured response
surface(f_plot_range,speed_average,20*log10(abs(Y_freq_plot_range/ref)))
shading('interp');
colormap jet
xlabel('Frequency [Hz]')
ylabel('Speed [km/h]')
axis tight;
set(gca,'YDir','normal');
set(gca,'XMinorTick','on');
set(gca,'YMinorTick','on');
set(gca,'Layer','top');
set(gca,'Box','on');
ylim([min(speed_average) max(speed_average)])
xlim(x_limits)
caxis([min(20*log10(abs(Ys_tot_plot_range(:)/ref)))...
      max(20*log10(abs(Ys_tot_plot_range(:)/ref)))])
title(str)
cbar=colorbar('EastOutside');
ylabel(cbar,y_label)

clear str

end

%% %% Plot transfer functions %% %%

if strcmp(plot_transfer_functions,'on')

    str = cat(2,'Transfer functions to ',Y_header_used.RespId);

    if Nref == 2
        figure('name',str)

```

```

% Maximize figure
pause(0.001);
frame_h = get(handle(gcf),'JavaFrame');
set(frame_h,'Maximized',1);
for ii=1:Nref
    subplot(1,2,ii)
    semilogx(f,20*log10(abs(H(ii,:))));
    title_str = sprintf('From %s to %s',X_header(ii).Title,...
        Y_header_used.RespId);
    title(title_str)
    xlim(x_limits)
    xlabel('Frequency [Hz]')
    ylabel('Magnitude [dB re 1]')
    set(gca,'XTick',[16 31.5 63 125 250 500 1000])
    clear title_str
    hold on;
end
hold off
end

if Nref == 8
    % Transfer functions 1-4
    figure('name',str)
    % Maximize figure
    pause(0.001);
    frame_h = get(handle(gcf),'JavaFrame');
    set(frame_h,'Maximized',1);
    for ii=1:4
        subplot(2,2,ii)
        semilogx(f,20*log10(abs(H(ii,:))));
        title_str = sprintf('From %s to %s',X_header(ii).Title,...
            Y_header_used.RespId);
        title(title_str)
        xlim(x_limits)
        xlabel('Frequency [Hz]')
        ylabel('Magnitude [dB re 1]')
        set(gca,'XTick',[16 31.5 63 125 250 500 1000])
        clear title_str
        hold on;
    end
    hold off
    % Transfer functions 5-8
    figure('name',str)

```

```

% Maximize figure
pause(0.001);
frame_h = get(handle(gcf),'JavaFrame');
set(frame_h,'Maximized',1);
for ii=5:8
    subplot(2,2,ii-4)
    semilogx(f,20*log10(abs(H(ii,:))));
    title_str = sprintf('From %s to %s',X_header(ii).Title,...
        Y_header_used.RespId);
    title(title_str)
    xlim(x_limits)
    xlabel('Frequency [Hz]')
    ylabel('Magnitude [dB re 1]')
    set(gca,'XTick',[16 31.5 63 125 250 500 1000])
    clear title_str
    hold on;
end
hold off
end

if Nref == 12
    % Transfer functions 1-4
    figure('name',str)
    % Maximize figure
    pause(0.001);
    frame_h = get(handle(gcf),'JavaFrame');
    set(frame_h,'Maximized',1);
    for ii=1:4
        subplot(2,2,ii)
        semilogx(f,20*log10(abs(H(ii,:))));
        title_str = sprintf('From %s to %s',X_header(ii).Title,...
            Y_header_used.RespId);
        title(title_str)
        xlim(x_limits)
        xlabel('Frequency [Hz]')
        ylabel('Magnitude [dB re 1]')
        set(gca,'XTick',[16 31.5 63 125 250 500 1000])
        clear title_str
        hold on;
    end
    hold off
    % Transfer functions 5-8
    figure('name',str)

```

```

% Maximize figure
pause(0.001);
frame_h = get(handle(gcf),'JavaFrame');
set(frame_h,'Maximized',1);
for ii=5:8
    subplot(2,2,ii-4)
    semilogx(f,20*log10(abs(H(ii,:))));
    title_str = sprintf('From %s to %s',X_header(ii).Title,...
        Y_header_used.RespId);
    title(title_str)
    xlim(x_limits)
    xlabel('Frequency [Hz]')
    ylabel('Magnitude [dB re 1]')
    set(gca,'XTick',[16 31.5 63 125 250 500 1000])
    clear title_str
    hold on;
end
hold off
% Transfer functions 9-12
figure('name',str)
% Maximize figure
pause(0.001);
frame_h = get(handle(gcf),'JavaFrame');
set(frame_h,'Maximized',1);
for ii=9:12
    subplot(2,2,ii-8)
    semilogx(f,20*log10(abs(H(ii,:))));
    title_str = sprintf('From %s to %s',X_header(ii).Title,...
        Y_header_used.RespId);
    title(title_str)
    xlim(x_limits)
    xlabel('Frequency [Hz]')
    ylabel('Magnitude [dB re 1]')
    set(gca,'XTick',[16 31.5 63 125 250 500 1000])
    clear title_str
    hold on;
end
hold off
end

end
end

```


B. Transfer functions

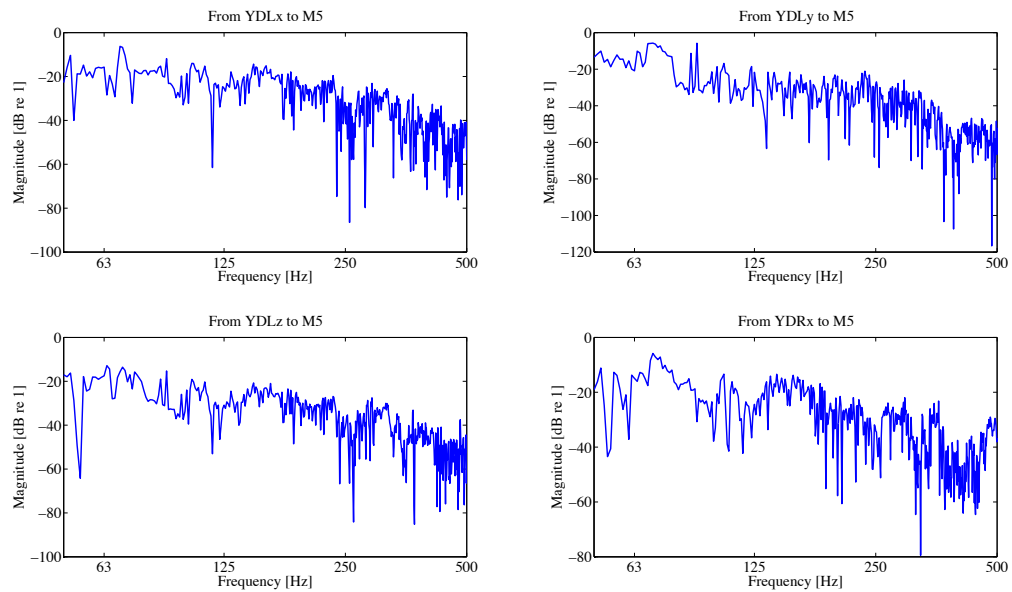


Figure B.1.: Transfer functions to microphone at right side, 1.6 m above floor (M5)

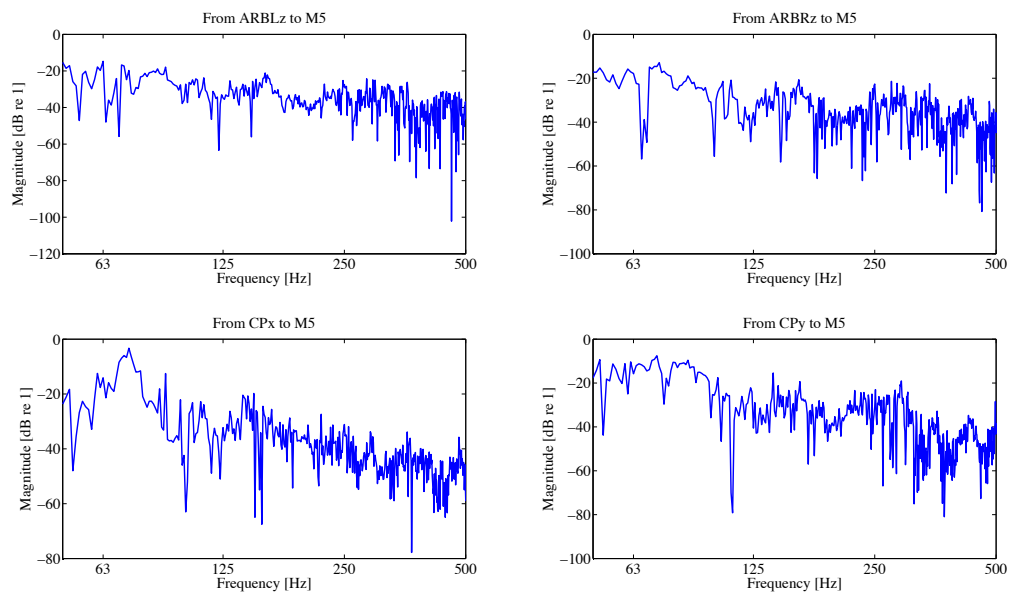


Figure B.2.: Transfer functions to microphone at right side, 0.5 m above floor (M5)

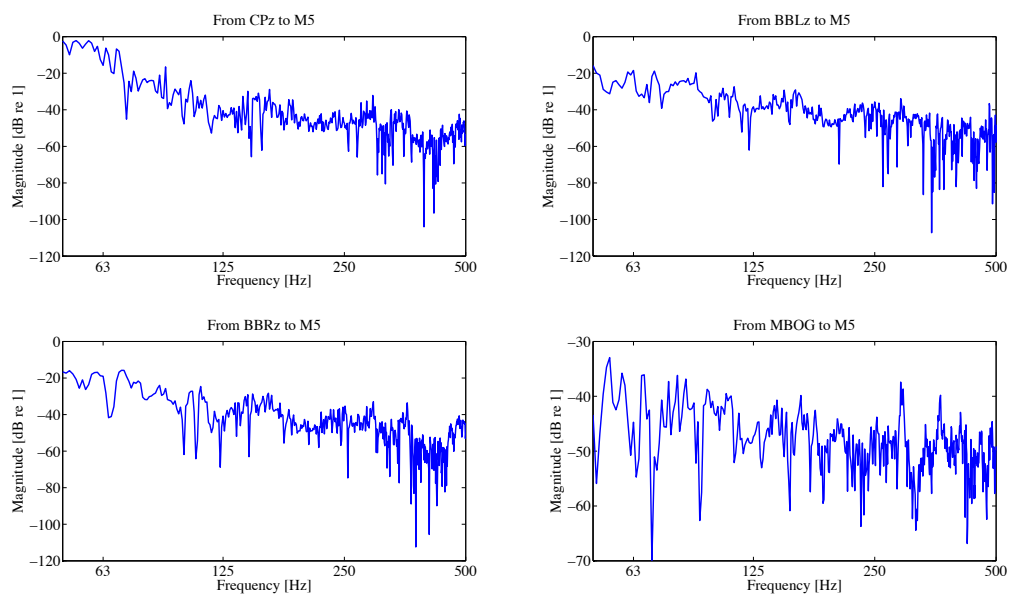


Figure B.3.: Transfer functions to microphone at right side, 0.5 m above floor (M5)

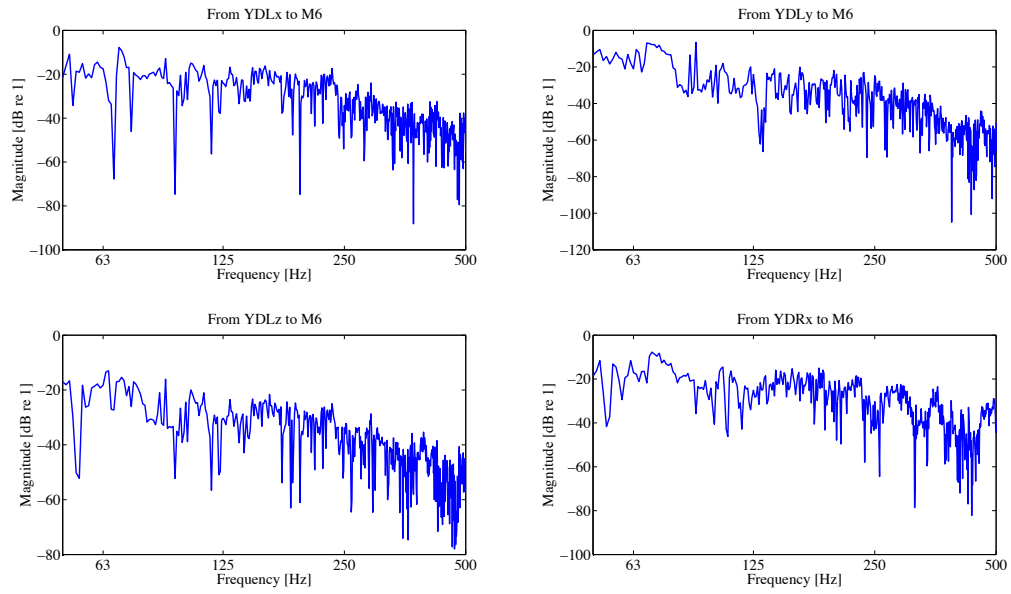


Figure B.4.: Transfer functions to microphone at driver's ear, 1.5 m above floor (M6)

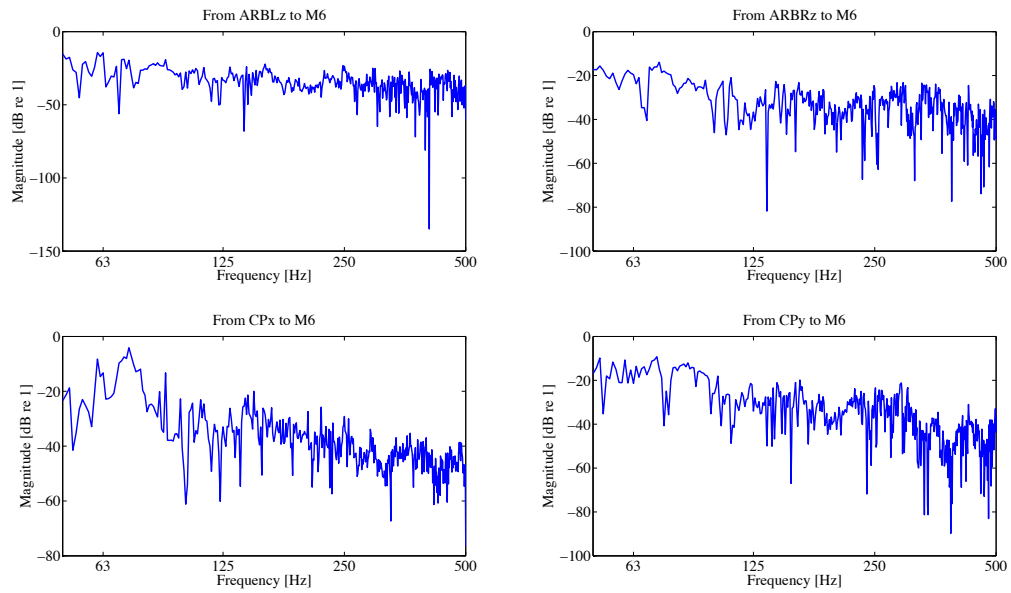


Figure B.5.: Transfer functions to microphone at driver's ear, 1.5 m above floor (M6)

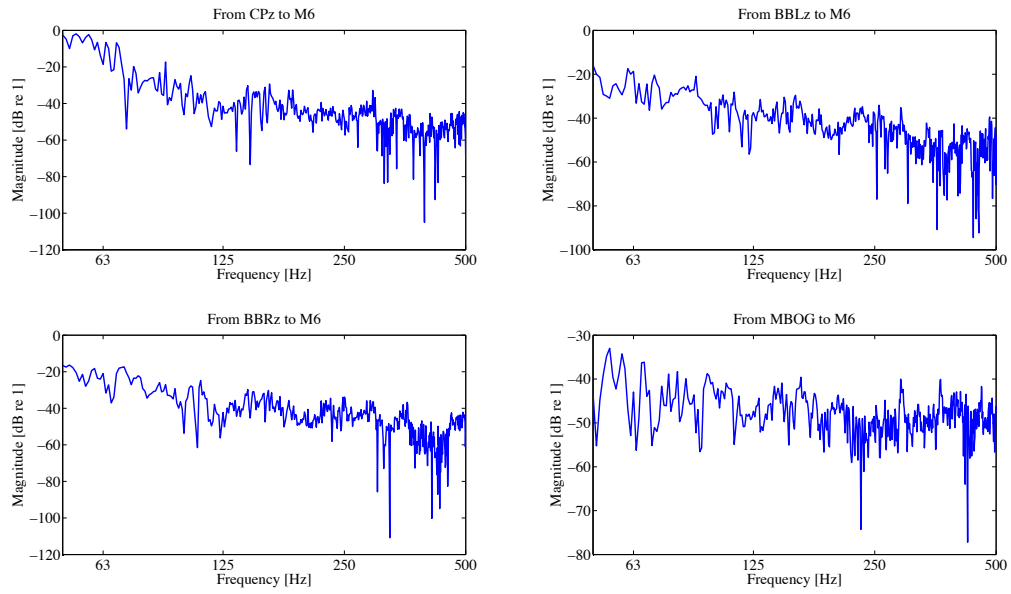


Figure B.6.: Transfer functions to microphone at driver's ear, 1.5 m above floor (M6)

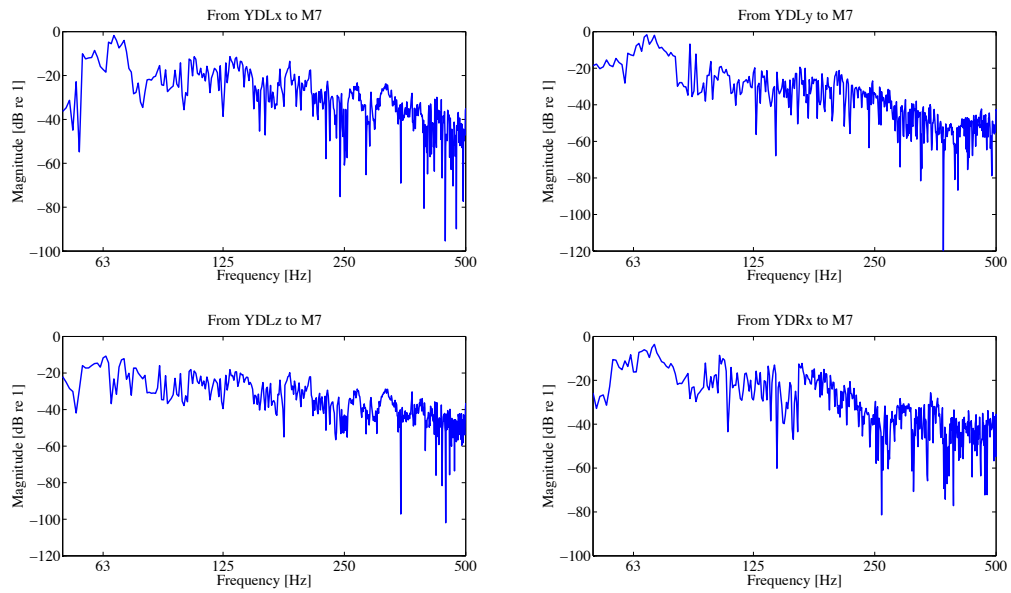


Figure B.7.: Transfer functions to microphone at right side, 0.5 m above floor(M7)

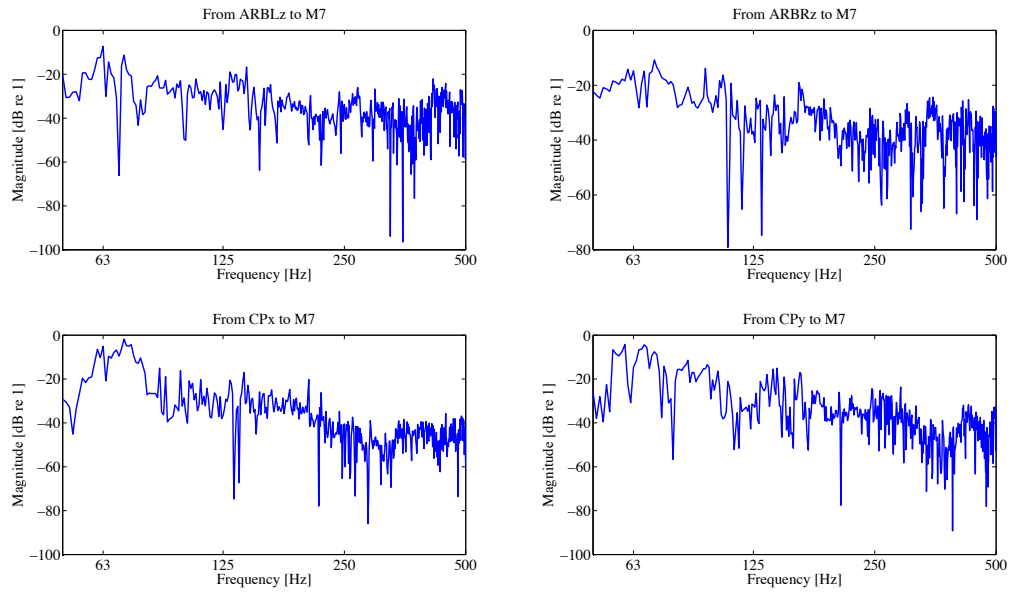


Figure B.8.: Transfer functions to microphone at right side, 0.5 m above floor(M7)

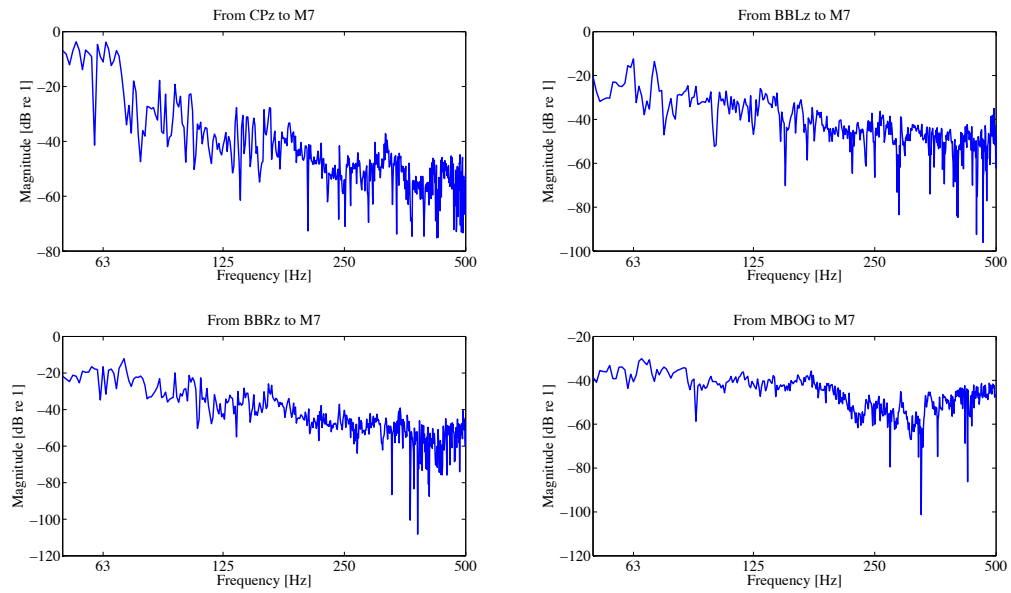


Figure B.9.: Transfer functions to microphone at right side, 0.5 m above floor (M7)

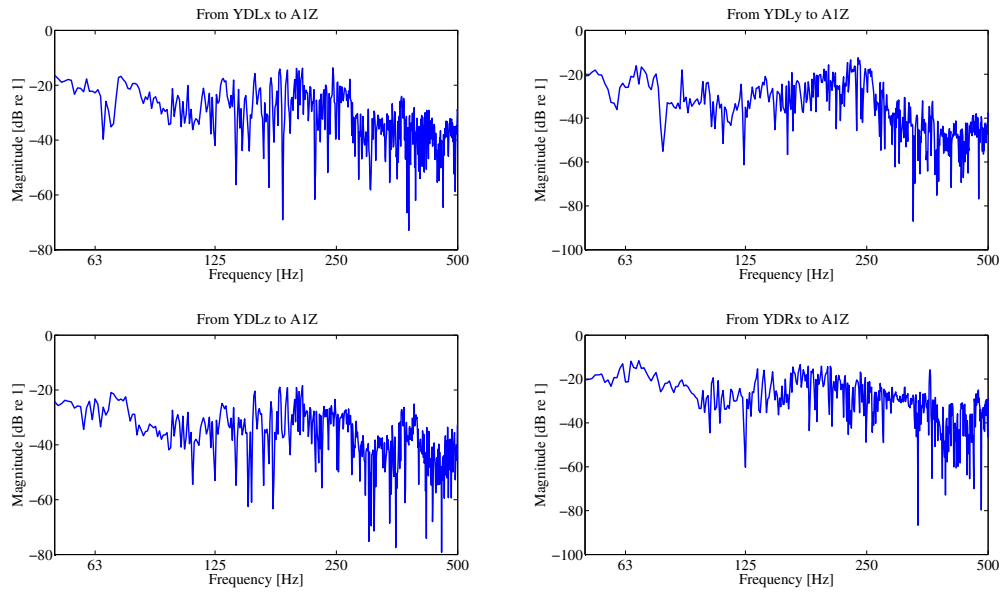


Figure B.10.: Transfer functions to accelerometer below driver's seat (A1z)

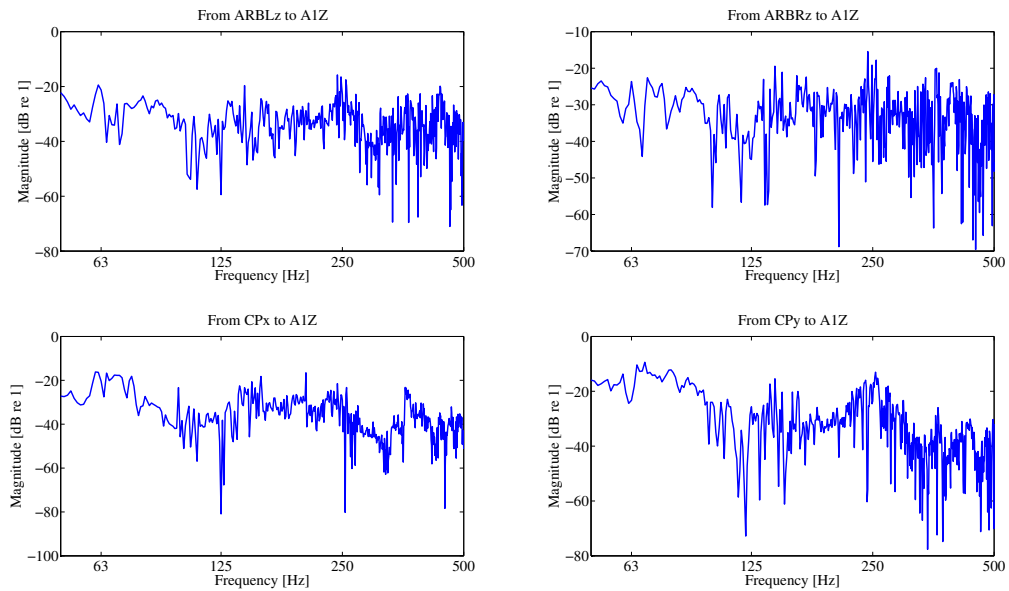


Figure B.11.: Transfer functions to accelerometer below driver's seat (A1z)

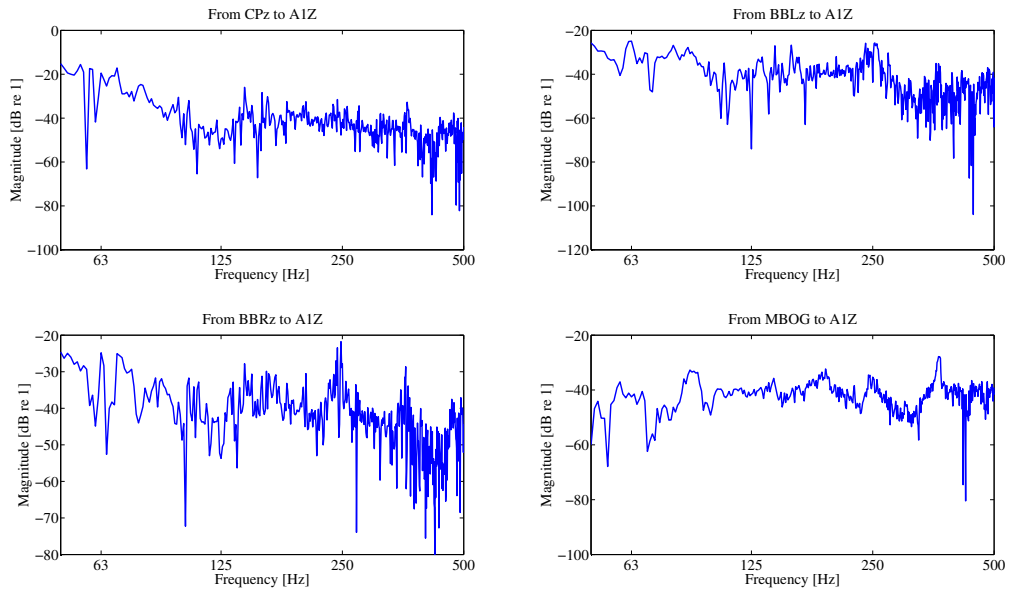


Figure B.12.: Transfer functions to accelerometer below driver's seat (A1z)

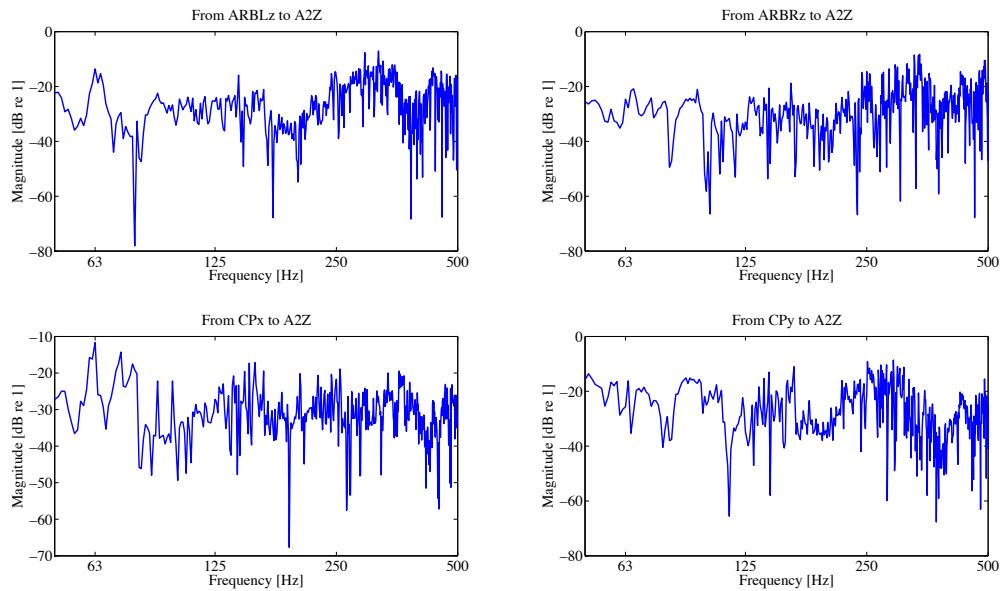


Figure B.13.: Transfer functions to accelerometer on driver's cabin floor, right side (A2z)

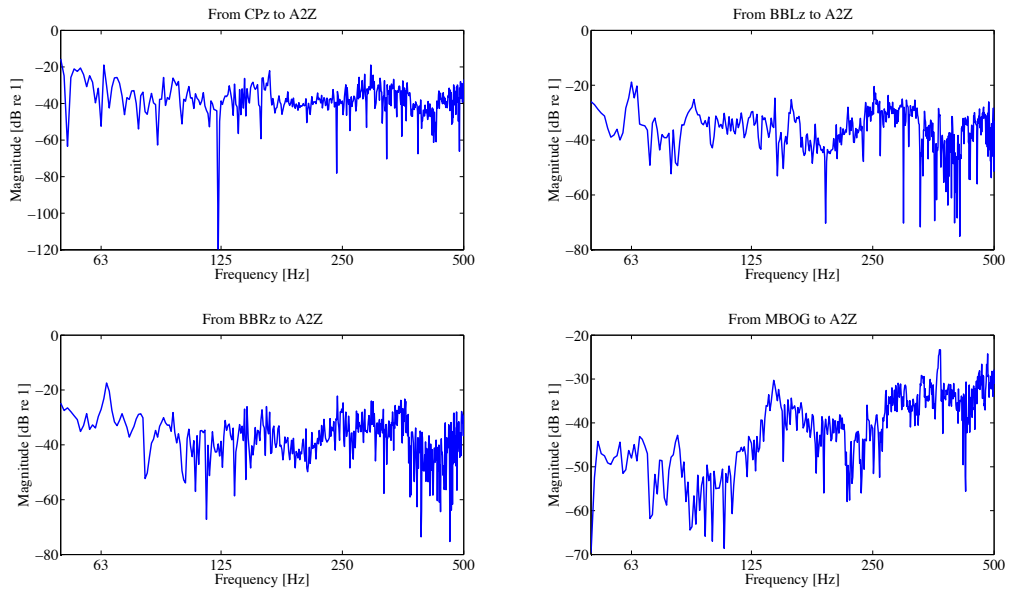


Figure B.14.: Transfer functions to accelerometer on driver's cabin floor, right side (A2z)

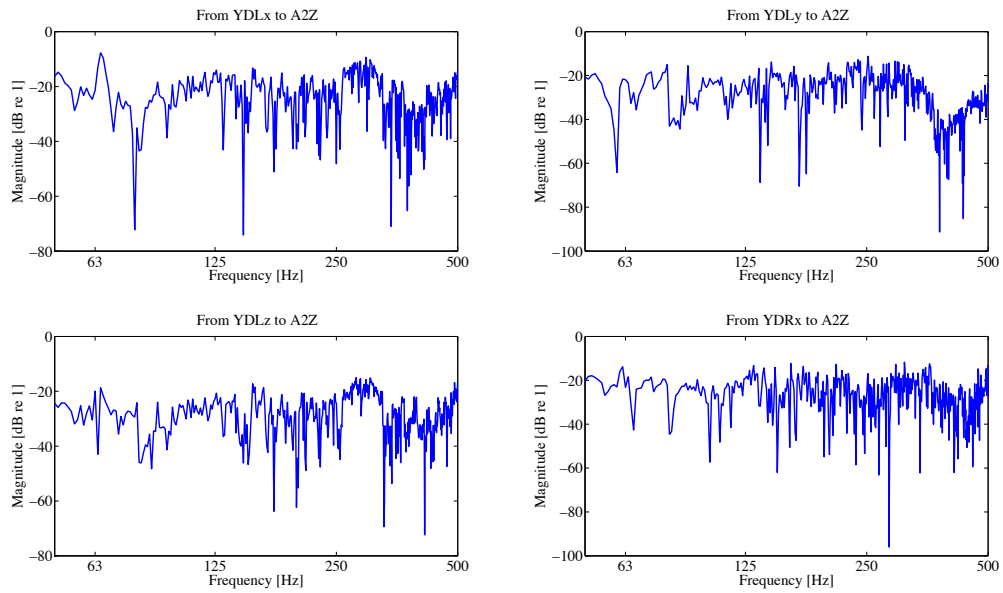


Figure B.15.: Transfer functions to accelerometer on driver's cabin floor, right side (A2z)

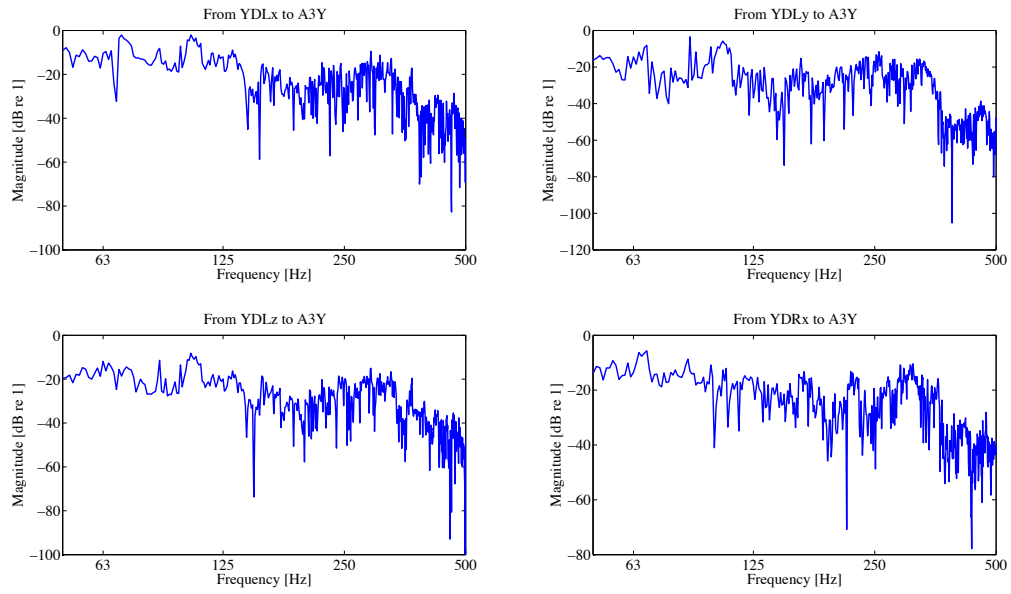


Figure B.16.: Transfer functions to accelerometer on lower sidewall in driver's cabin, right side (A3y)

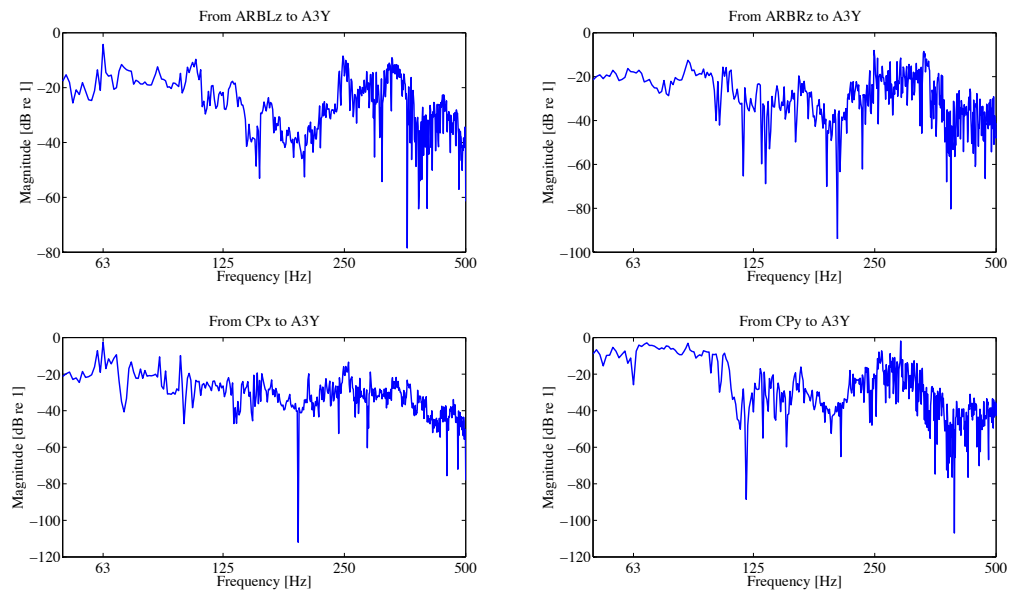


Figure B.17.: Transfer functions to accelerometer on lower sidewall in driver's cabin, right side (A3y)

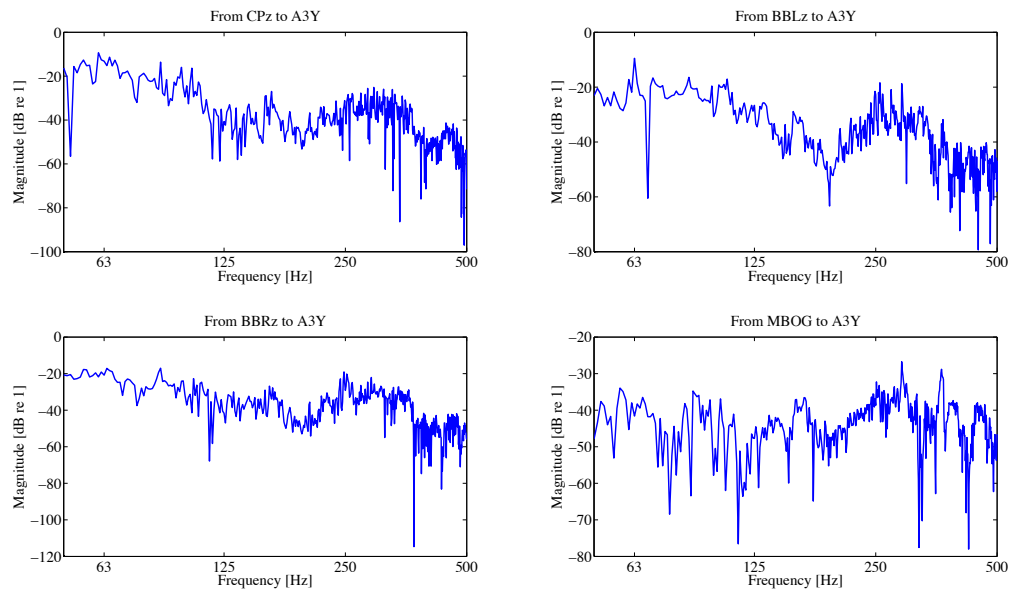


Figure B.18.: Transfer functions to accelerometer on lower sidewall in driver's cabin, right side (A3y)

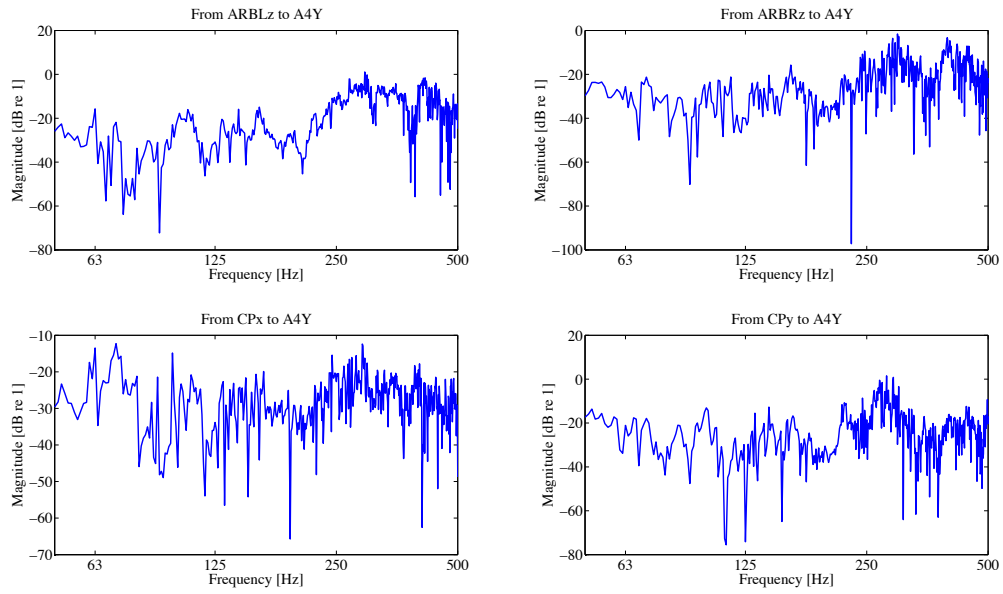


Figure B.19.: Transfer functions to accelerometer on higher sidewall in driver's cabin, right side (A4y)

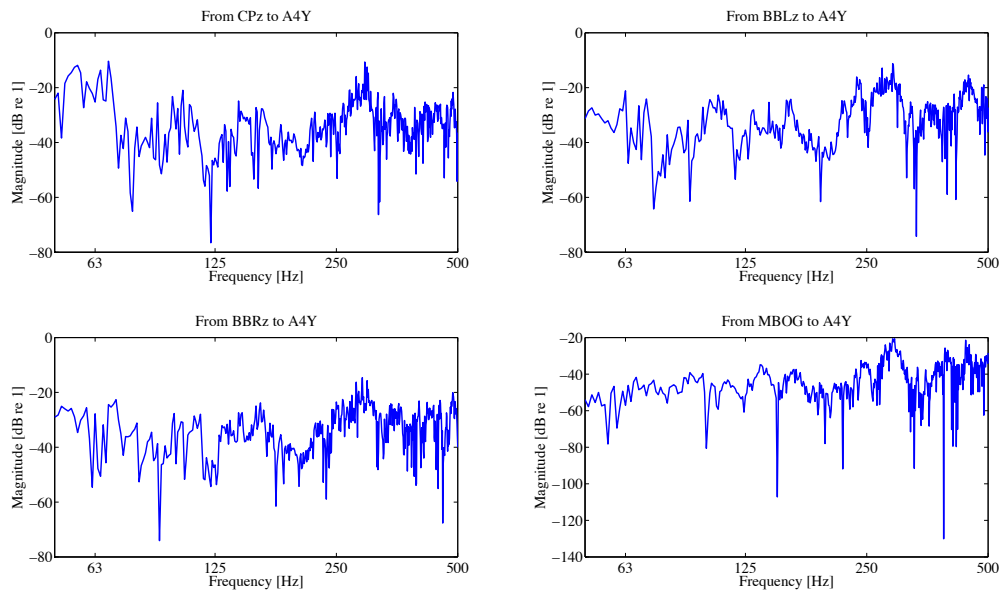


Figure B.20.: Transfer functions to accelerometer on higher sidewall in driver's cabin, right side (A4y)

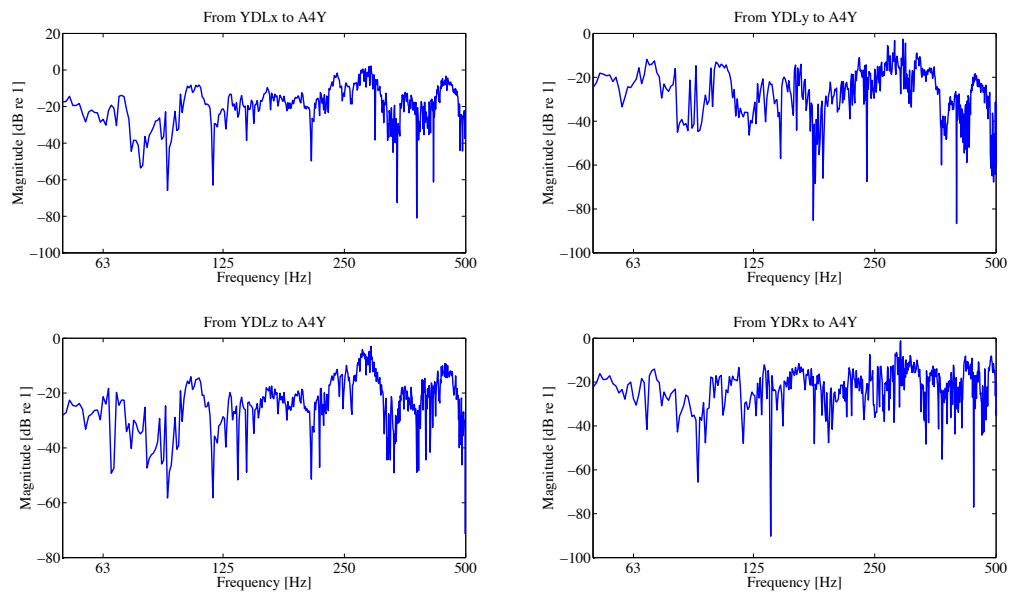


Figure B.21.: Transfer functions to accelerometer on higher sidewall in driver's cabin, right side (A4y)

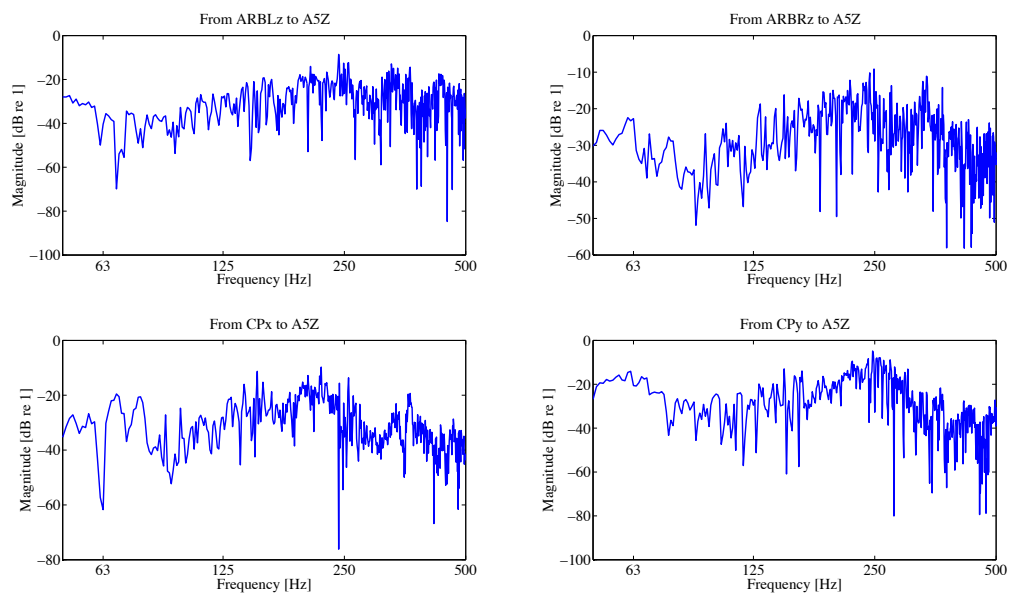


Figure B.22.: Transfer functions to accelerometer on driver's cabin floor, left side (A5z)

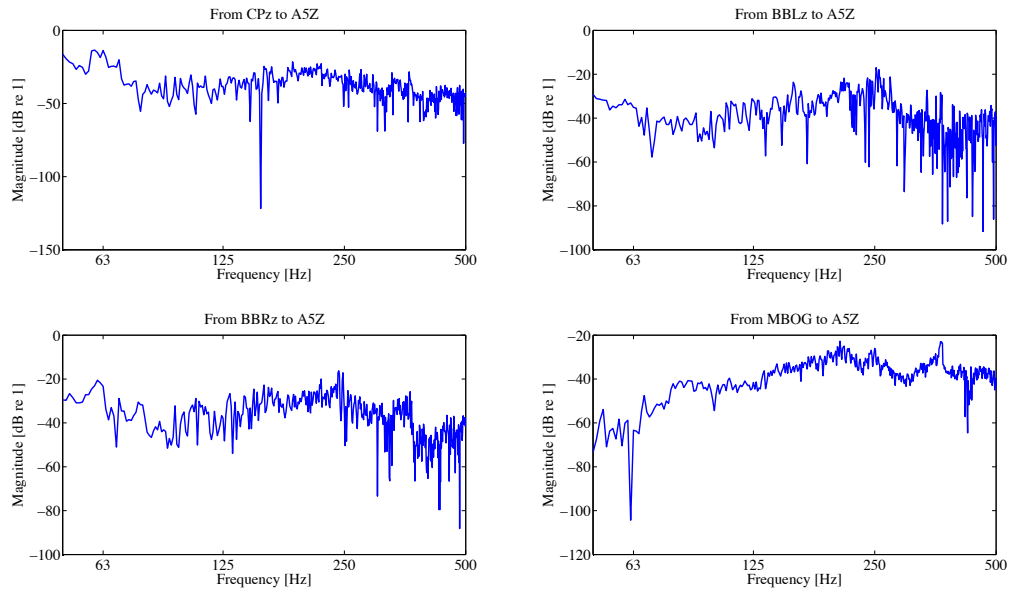


Figure B.23.: Transfer functions to accelerometer on driver's cabin floor, left side (A5z)

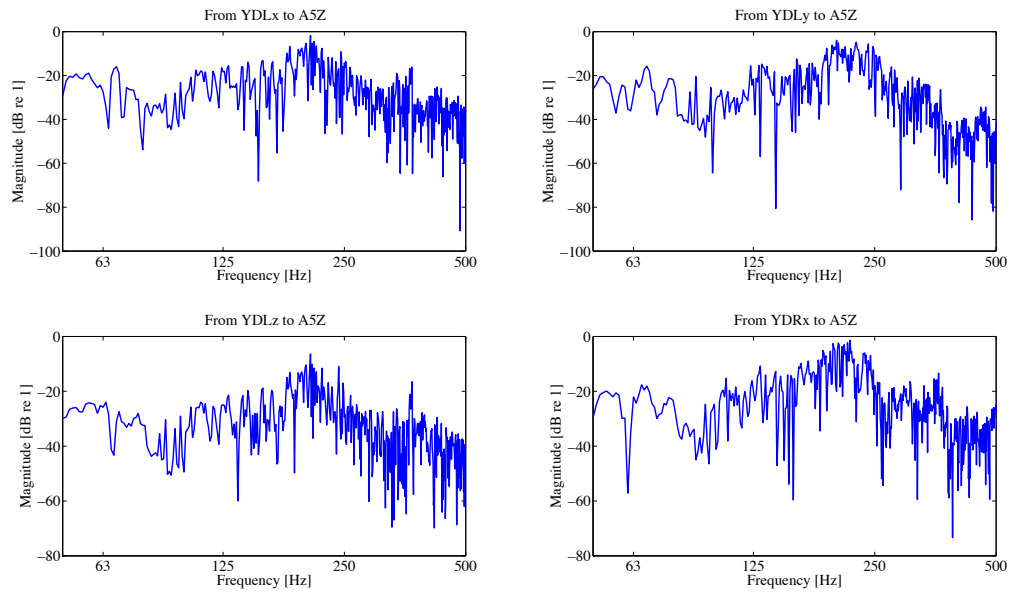


Figure B.24.: Transfer functions to accelerometer on driver's cabin floor, left side (A5z)